TRACE ELEMENT DISTRIBUTION IN SOILS OF THE PEMBINA ESCARPMENT, NORTH DAKOTA

A Thesis
Submitted to the Graduate Faculty
of the
North Dakota State University
of Agriculture and Applied Science

By

Vijaya Jyoti

In Partial Fulfillment of the Requirements
for the Degree of
MASTER OF SCIENCE

Major Program:
Environmental and Conservation Sciences

July 2010

Fargo, North Dakota

North Dakota State University
Graduate School

Title

Trace Element Distribution in Soils

of the Pembina Escarpment, North Dakota

By

Vijaya Jyoti

The Supervisory Committee certifies that this ***disquisition*** complies with North Dakota State University's regulations and meets the accepted standards for the degree of

MASTER OF SCIENCE

ABSTRACT

Jyoti, Vijaya, M.S., Environmental and Conservation Sciences Program, College of Graduate and Interdisciplinary Studies, North Dakota State University, July 2010. Trace Element Distribution in Soils of The Pembina Escarpment, North Dakota. Major Professors: Dr. Bernhardt Saini-Eidukat and Dr. David Hopkins.

Association of element concentrations for soils of northeastern North Dakota formed from different sources of parent materials were determined based on geochemical data. These soils overlie the Cretaceous Pierre Formation and parent materials consist of shale rich glacial till, residual shale, and colluvial materials. Surface and core sampling locations included a cropped field, Conservation Reserve Program land, and grassland fields in a North Dakota State Wildlife Management Area. Samples were analyzed for cadmium and other trace elements using a nitric acid digestion followed by optical emission spectroscopy. Results of a preliminary study in cropped and CRP fields showed elevated concentrations of cadmium. Later comprehensive field work in a Wildlife Management Area was carried out to examine the landscape scale variation for a suite of elements. Morphologic and laboratory analysis of soil cores indicate high clay content with mixed clay mineralogy, indicative of the influence of shale residuum on the parent materials of the escarpment soils. Chemical properties of the escarpment soils revealed high levels of organic matter (2.62-13.30 %), ultra acidic to slightly alkaline pH range, and low electrical conductivity for the soils. Average cadmium concentration of 0.28 mg/kg was reported for the samples from eight cores while 16.4 mg/kg cadmium was found in the CRP field sample. Correlations of different analytes with cadmium showed significance with shale and argillic horizons. Principal Component Analysis revealed that elevated trace element concentrations for the soils in northeastern North Dakota are linked to a variety of

factors including organic matter content, clay mineralogy, pH, elevation, and electrical conductivity. Results of this study suggest that lateral as well as vertical water movement of water could be an important factor leading to transport and elevated trace metal zones in these soils.

ACKNOWLEDGMENTS

A number of people contributed in sampling and conducting laboratory data for this project. I would like to thank Larry Swenson and Keith Jacobson of the Soil and Water Environmental Laboratory at NDSU for data collection. I would also like to acknowledge Angle Ugrinov for his instruction and advice with the X-Ray diffractometer. I am thankful to Ted Feit and Michael Ginsbach for their support in characterizing soil data. Acknowledgments are forwarded to ND EPSCoR for providing financial support in buying the geoprobe unit through NSF grant no. EPS-0447679.

I would like to thank my adviser, Dr. Bernhardt Saini-Eidukat, for his guidance and support for the successful completion of the project. I would also like to express sincere gratitude to Dr. David Hopkins for co-advising me and encouraging me throughout the project. I would like to acknowledge my committee, Dr. Thomas DeSutter, for providing GeoProbe for core sampling and guidance during field work, Dr. Donna Jacob, for her assistance in collection of multi-element data, and Dr. Ross Collins, for his unceasing support and insight. Acknowledgments are forwarded to the staff and faculty of the NDSU Department of Geosciences.

On a personal note, I would like to thank my husband, family and friends for their unconditional love and care, and for keeping my morale up.

TABLE OF CONTENTS

TABLE OF CONTENTS (Continued)

TABLE OF CONTENTS (Continued)

LIST OF TABLES

LIST OF FIGURES

LIST OF APPENDIX TABLES

LIST OF APPENDIX TABLES (Continued)

LIST OF APPENDIX TABLES (Continued)

LIST OF APPENDIX FIGURES

LIST OF APPENDIX FIGURES (Continued)

LIST OF APPENDIX FIGURES (Continued)

CHAPTER 1. INTRODUCTION

The degree and increasing number of heavy metal pollution sources have become a matter of grave concern for environmentalists all over the world. Cadmium (Cd) is a chalcophile element (i.e. it has an affinity for sulfur), found in close geochemical association with zinc (Zn) in the sulfide minerals in rocks (McBride, 1994). Cadmium is a trace metal with no known essential biological functions, and is highly toxic to plants and animals (Lindsay, 1979). The toxic effects of Cd on human health were reviewed by Grum (1990) and Tucker (2008). Low levels of Cd may result in respiratory disorders and hypertensive heart diseases in humans. A classic example of "Itai Itai" disease reported in Japan was caused by Cd toxicity which occurred due to consumption of rice that was irrigated with water containing heavy metals (Kjellstrom, 1986). Thus, Cd has ability to bioaccumulate. Cadmium has also been associated with the development of many human cancers (Siemiatycki *et al.*, 1994; Waalkes, 2000; Huff *et al.*, 2007).

1.1. Chemistry of Cadmium

The distribution of elements in soil is driven by combination of various factors of which climate and parent material stand out as critically important (Oertel, 1961; Kabata-Pendias, 2001). Determining natural backgrounds of elements in soils is necessary to provide a quantitative estimation of those elements that could have an effect on human health when concentrated through the food chain. Efforts have been made worldwide to report background values for various trace elements. Lindsay (1979), McBride (1994), and Alloway (2000) reported cadmium content in the lithosphere as 0.2 mg/kg (0.2 ppm) and

that the average for agricultural soils worldwide is within a range of 0.06 - 1.1 mg/kg. According to Holmgren *et al.* (1993), the average total Cd content of agricultural soils in United States is 0.27 mg/kg with Northern Great Plains (rich in Pierre Shale) having a mean of 0.36 mg/kg. A similar estimate was determined by Garrett (1994), who established a baseline value for Cd (0.3 mg/kg) for the topsoils in prairie provinces of Canada and adjoining states of the United States.

Page and Bingham (1973) suggest that soils derived from igneous rocks would have Cadmium contents of 0.1-0.3 mg/kg, while those from metamorphic rocks would contain 0.1-1.0 mg/kg and soils derived from sedimentary rocks generally possess the highest levels of cadmium (0.3-11 mg/kg). Most soils can be expected to contain less than 1 mg/kg total Cadmium, except those contaminated from anthropogenic sources or developed on parent materials with high Cd contents, such as black shales (Lund *et al.*, 1981; Alloway, 1990).

Several factors affect the proportion between Cd present in the soil solution and the amount adsorbed on the solid phase. These factors include the chemical nature of the metal species, soil pH, and geochemical stability of Cd complexes, the binding ability with functional groups on soil organic matter and clay minerals, and contending ions such as Calcium (Ca), Cobalt (Co), Chromium (Cr), Copper (Cu), Nickel (Ni), and Lead (Pb) and their ionic potential (Pickering, 1980; Gerritse and Driel 1984). Pulls and Bohn (1988) investigated the chemical characteristics of Cd and concluded its behavior can be described as that of a Lewis acid and thus it is more likely to react and form complexes with soft Lewis bases, for instance, chloride (Cl^-) and hydroxyl (OH^-) groups. Thus, Cd can form complexes with these ligands. Research by Norvell *et al.* (2000) in North Dakota soils

suggested association of Cd in the durum wheat with soluble Cl^- in the roots due to groundwater movement through capillary action.

1.1.1. Speciation of Cadmium

In order to understand the speciation of Cd, it is essential to know its various chemical forms and how they react in the soil solution. For most metals in soil, the amount available depends largely on the concentration of ligands present and the strength of ligand-metal complexes (Alloway, 1990). Cadmium has the ability to form several ion complexes such as $CdCl^+$, $CdOH^+$, $CdHCO_3^+$, and $CdCl_3^-$, but as a cationic species $Cd^{(+2)}$ has a greater tendency to be adsorbed by charged soil surfaces (Tills and Alloway, 1983). Mattigold and Sposito (1979) developed the GEOCHEM model for soils to determine various chemical species of metals using pH, organic carbon, and the concentration of cations and anions as various parameters. For Cd, species predicted by the model in decreasing order of abundance are: $Cd^{(2+)}$, $CdSO_4^{(0)}$ and $CdCl^{(+)}$ in acid soils, and $Cd^{(2+)}$, $CdCl^{(+)}$, $Cd\ SO_4^{(0)}$ and $CdHCO_3$ in alkaline soils.

1.1.2. Effect of pH and Organic Complexes

Research by Alloway *et al.* (1985) revealed that pH, along with organic matter and metal oxides, were among the main factors responsible for specific adsorption of Cd. Results by Garcia-Miraga and Page (1978) indicate soils having either high organic matter or hydrous iron oxides adsorbed more Cd when pH was between 6 and 7. The adsorption of Cd increases with increased pH due to the increase in net negative surface charge, i.e. pH dependent charge, as suggested by Naidu *et al.* (1994) for oxisols and fragiaqults. Cation

exchange in most of the clays is favorable when pH is $\geq$ 6 or 7 as below this pH cation exchange sites are occupied by either $Al(OH)^{2+}$ or Al^{3+} (Miller and Gardiner, 2000). The amount of Cd adsorbed from the soil solution varies with the formation of organometallic complexes with humic material and the soil's inherent cation exchange capacity. With increasing acidity the tendency to form organometallic complex decreases because H^{+} binding is dominant at low pH, thus anionic complexes formed by Cd with humic and fulvic acids are less stable at acidic pH (Duffy *et. al.*, 1988).

1.1.3. Soils and Processes causing Soil Enrichment

Climate, organisms, relief, parent material and time are the major factors leading to soil formation (Jenny, 1941; Schaetzl and Anderson, 2005). Collective effects of climate (physical and chemical weathering) and organisms (biological weathering) on residual and transported parent materials leading to addition, transformation, deletion and transport over time through water, air and ice lead to formation of different types of soil profiles with general soil horizons as O, A, E, B, C and R (Schaetzl and Anderson, 2005). Various pedogenic processes may include surface addition of material (profile thickening) or translocation of materials laterally and from upper horizons to the lower soil profile or vice versa. The upper horizons, like (A, E, B, collectively referred to as the solum) are more subject to alteration and can significantly differ from their parent material (Muckenhirn *et al.*, 1949; Schaetzl and Anderson, 2005). However, some properties of parent materials are retained over time and the soils formed from them (e.g. soils formed from sedimentary rocks like shale) will result in clayey soils (Yaalon, 1971; Schaetzl and Anderson, 2005). Morphological characteristics that help to differentiate soil from its parent regolith include

color, texture, structure, presence of roots, concretions of secondary minerals, and redoximorphic depletions and accumulations (Schoeneberger and Wysocki, 1998; Schaetzl and Anderson, 2005). New parent material rich in metals formed from weathering and erosion of the parent materials on the slope and cation exchange capacity affecting plant growth and degradation of organic matter are some of the significant chemical properties that can help in differentiating soil from its parent material. Other principal properties controlling the chemical behavior of metals in the soil include soil pH, soil organic matter, and clay mineral groups like kaolinites, smectites, and illites (Alloway *et al.*, 1990; Alloway, 1990; Sposito, 1983). Solubility of Cd can increase at higher pH due to the presence of dissolved organometallic complexes (Almas and Singh, 2001; Kirkham, 2006).

Soil formation in shale residuum occurs by means of both physical and chemical weathering. Lessivage is the major process which is associated with the formation of clay rich soils in which clay particles translocate from A and E horizons (eluviation) into B horizon, producing an (illuvial) clay rich B_t horizon (Schaetzl and Anderson, 2005). Neoformation of clays can also take place in B_t resulting in diagnostic argillic horizon. Because the B_t horizon is fine textured, the accumulation of major and trace elements is enhanced in this horizon. A horizons, which are rich in organic matter, can bind various elements forming organometallic complexes. Leaching facilitates major and trace element movement in lower B_t horizons from upper horizons. Thus the B horizon can act as a major accumulation or sink zone for trace elements. The availability of major and trace elements can be limited or enhanced by various processes in the soil profile including weathering intensity, sorption (cation/anion exchange), specific adsorption of anions by ligands, co-precipitation, organometallic complex formation, and pedogenic processes such as

leaching, salinization, calcification and eluviation/illuviation (Alloway, 1990). Research by Burau *et al.*, (1973) on agricultural soils developed from or near Monterey shale reported Cd mean level 1.24 mg/kg. Soils developed from shale residuum were found to have Cd mean level of 7.5 mg/kg (Lund *et al.*, 1981). Kim and Thornton (1993) showed elevated concentrations of trace elements (Cd- 6.3mg/kg; Mo-136mg/kg; Se-8.6 mg/kg) in Ordovician black shales. Lee *et al.*, (1998) reported trace elements in soils formed from black shales and slates. Soils derived from Ankang black shales have trace metal distribution (Fang *et al.*, 2002). Trace metal levels were investigated by Horckmans *et al.*, (2005) to report background levels in soils developed from bituminous shales and minette sandstone. Tuttle *et al.* (2003) reported trace element levels in Kentucky shales resulting from weathering. Trace element concentrations have been reported in Mancus shale (Tuttle *et al.*, 2007).

1.2. Regionalized Zones of Enriched Cadmium

Soil in the Red River Valley of North Dakota, Minnesota, and Canada is widely recognized as some of the most fertile soil in the world. However, this is not always the case as some studies in the state of North Dakota have revealed soils with elevated metal concentrations (Holmgren *et al.*, 1993; Li *et al.*, 1994). Hopkins *et al.* (1999) showed elevated Cd levels in topsoils on the Pembina Escarpment in northeastern North Dakota. Results by Franzen *et al.* (2006) revealed Cd concentrations in North Dakota varying from 0.01 to 0.31 mg/kg. Apart from these regional investigations, trace element surveys have been conducted at both national and international scales, and some of these sites are located in northeastern North Dakota. An early geochemical database for the conterminous United

States was conducted by the U.S. Geological Survey in the early 1960s and is referred to as the Shacklette dataset (Shacklette and Boerngen, 1984). The goal was to provide an estimate about the naturally occurring element availability in soils. This data set consisted of 1323 samples collected from fields having native vegetation. Smith *et al.* (2005) presented results of this survey revealing 0.5 mg/kg Cd in each A and O horizon and 0.4 mg/kg in C horizon soils of northeastern North Dakota. Another survey conducted in 2004, showed 0.1 mg/kg Cd in (0-5) cm soils for N-S and E-W transects in United States and Canada (Smith *et al.*, 2009; Woodruff *et al.*, 2009; Klassen, 2009). Garrett (1994) reported that the mean total Cd concentration of 1273 soils from the prairie provinces of Canada and adjoining areas in Montana, North Dakota, and Minnesota was 0.28 mg/kg, and he suggested an environmental baseline of 0.3 mg/kg. Another nationwide geochemical database was generated by the Natural Resources Conservation Service (Holmgren *et al.*, 1993) in 1978 sampling at 3045 different locations for soils and crops for determining Cd, Pb, Ni, Cu and zinc (Zn) levels. Results of this survey also showed elevated levels of Cd in the region of northeastern North Dakota with a mean of 0.36 mg/kg. Investigations by White *et al.* (1997) showed high Zn (> 55mg/kg) levels in soils of northern United States. Thus, these naturally occurring high levels of trace elements in soils could be likely because of Pierre shale (Tourtelot *et al.*, 1964; Holmgren *et al.*, 1993).

1.2.1. Crop Quality Concerns

All the previously mentioned trace element surveys in the region indicate a need to understand the link between trace elements, their availability and bioaccumulation in the agricultural crops. North Dakota ranks first of the top ten states in terms of principal crops

planted in 2009 (NASS, 2010). Major food crops produced by the state are sunflower, durum wheat, potatoes, sugar beets, flaxseed, and beans. Three crops are of concern in terms of cadmium. North Dakota produces 95 percent of nation's flaxseed, 56 percent of all durum wheat, and is the top producer of confectionary sunflower (NASS, 2010). All these crops are known to bioaccumulate Cd. Researchers all over the world have reported various crops that bioaccumulate Cd. Cadmium concentration within a range of 0.14-2.63 mg/kg was found by Onyedika and Nwosu (2008) in crops like cassava, yam, potato and cocoyam. High levels of Cd were found in durum wheat (grain) and flax in Saskatchewan soils (Ciesacutelinacuteski *et al.*, 1996). Elevated Cd levels in soils of North Dakota were reported by Norvell *et al.*, (2000). Low levels of Cd were found in enterprise durum wheat which is a hybrid wheat developed at the Semiarid Prairie Agricultural Research Centre in Saskatchewan (Singh *et al.*, 2010). It has been reported that Cd accumulates more easily in durum wheat as compared to all other cereals (Jansson, 2002; Perilli *et al.*, 2010). Maximum Cd levels upto 0.2 mg/kg (Rev.5, 2009) in durum wheat grains have been fixed by Codex General Standard for Contaminants and Toxins in Foods (CODEX STAN, 2009; Perilli *et al.*, 2010.) Research has shown that confectionary sunflower accumulates Cd from the soil and deposits it in the sunflower seeds (Li *et al.*, 1995). Cadmium and Zn can accumulate in soybean which can pose a threat to food safety (Shute and Macfie, 2006). Cadmium content is linked with a food quality concern nationally, it is essential to determine specific combinations of soils and crops that might result in questionable crop quality.

CHAPTER 2. GEOLOGIC AND PEDOLOGIC BACKGROUND

2.1. The Pierre Shale: Formation and Lithologic Significance

During the Late Cretaceous (about 99.6-65.5 million years ago), the North American continent was split into two large islands by an epicontinental sea known as Cretaceous Seaway. This shallow sea, which flooded the interior of North America, extended from Gulf of Mexico as far north as the Arctic sea. Sediments in the marine basins were dominantly derived from the west due to the rising of the Rocky Mountains during the Laramide Orogeny (Gill and Cobban, 1973). Organic black shales were deposited under anoxic water conditions as one of the sediments (Gill and Cobban, 1973). Brumsack (2006) suggested a conceptual model for the formation of Cretaceous black shales. Carbon dioxide (CO_2) has been considered as a vital factor in this model, and is derived from volcanic activity leading to warm temperatures that create reducing conditions in the ocean water. Black shale formation occurs under these reduced, slow sediment deposition conditions in association with sulfur bacteria on the inundated open shallow continental shelves (Arthur *et al.*, 1987; Brumsack, 2006).

Cretaceous black shales have been found to be rich in organic matter and trace metals (Brumsack, 1980; Schultz *et al.* 1980; Adriano, 1986; Warning and Brumsack 2000; Brumsack *et al.* 2003). Nijenhuis *et al.* (1999) characterized marine sediments from the eastern Mediterranean considered younger to cretaceous organic rich black shales with high contents of Fe and S leading to trace metal enrichment. Shales are enriched in trace elements due to adsorption by clays and organic matter (Krauskopf, 1979). Throughout the world, data has been reported by various workers concerning enriched values of trace

elements in black shales (Atkinson, 1967; Fletcher; 1968; Vine and Tourtelot, 1970; Armands, 1972; Coveney and Glascock, 1989; Kim, 1989). Lavergren and Bergbäck (2006) reported high levels of Cd, Ni and Zn in alum shale in Sweden. Trace metal enrichment in black shales can be linked to the depositional environment of these shales i.e., anoxic conditions (Wignall, 1994). For most of the trace metals, processes of enrichment could include precipitation as sulfides, incorporation as trace elements in pyrite and development of organic complexes that are resistant in anoxic settings (Wignall, 1994). Cadmium has a tendency to associate with sulfides, mainly pyrite, in many black shales (Raiswell and Plant, 1980). During marine shale formation under anoxic conditions, an intermediate sulfate reduction zone exists before methanogenesis during which sulfur bacteria degrade the organic matter and produce copious amounts of hydrogen sulfide (Wignall, 1994). Pyrite mineralization during this stage is capable of incorporating several trace elements forming sulfides of Fe, Cd, Mn and V while elements like Cr, Pb, Zn and Cu do not show significant rate of pyritization, which is controlled by availability of trace elements and organic matter content (Huerta-Diaz and Morse, 1992; Brumsack, 2006).

The Pierre Formation is a major and widely distributed sedimentary deposit of Late Cretaceous Period in north-south direction covering approx. 1609 km and outcrops and subcrops across much of South Dakota, North Dakota and Montana with correlative units in Canada (Gill and Cobban, 1965; Schultz *et al.*, 1980). The occurrence of the Pierre Formation in North Dakota was reported by Upham (1895) in his monograph on glacial Lake Agassiz. Most of the Pierre Formation is buried by glacial drift in eastern North Dakota but it is exposed in two specific areas near Valley City in the central southeastern part of the state and on the Pembina Escarpment along the international boundary in the

northeastern part of the state (Gill and Cobban, 1965). These areas include the north easternmost exposed outcrops of the Pierre Formation and thus provide important information about paleoenvironmental conditions of deposition in the Pierre basin (Gill and Cobban, 1965).

Pierre Shale deposits in North Dakota have been divided into four major stratigraphic units from oldest to youngest, 1) Pembina Member, 2) Gregory Member, 3) DeGrey Member and 4) Odanah Member (Gill and Cobban, 1965). These shale units are rich in bentonite beds and Fe and Mn concretions (Arndt, 1975). Bentonite is a porous clay material consisting mainly of the smectite group mineral montmorillonite which is formed by alteration of volcanic ash (Schultz *et al.*, 1980; Bluemle, 2000). Schultz *et al.* (1980) reported that one percent or less of the volume of the Pierre Formation and its equivalents contain bentonite and that smectite is the dominant mineral constituent of the bentonitic samples. Stratigraphic studies have shown that the bentonite beds in the Pembina member have resulted from the deposition from one or more ash falls due to explosive volcanism, likely in Montana (Gill and Cobban, 1965). Bentonite beds are highly absorbent and are abundant in the Pierre Formation near the Pembina Escarpment (Gill and Cobban, 1965). Schultz *et al.* (1980) found two bentonite samples with 11 mg/kg Cd in the Sharon Springs Member in South Dakota, which is a lithologic equivalent to the Pembina Member of the Pierre Formation.

2.2. Description of the Cavalier County

Cavalier County lies in the northeastern part of North Dakota (48° 40' 9" N, 98° 49' 56" W) and is within the physiographic division of the Drift Prairie with an elevation for

the county between 493.8 m in the western part to less than 365.8 m in the northeastern part covering 3911sq. km total area (Arndt, 1975; Simons and Moos, 1990). The extreme northeastern part of the county is covered by offshore sediments of Lake Agassiz (Arndt, 1975). The majority of Cavalier County is covered by glacial till, but the eastern part is a dissected upland, (Pembina Escarpment), which exposes Cretaceous shales ranging in age from the Carlisle to the Pierre Formations of Late Cretaceous about 72- 83 Ma (Gill and Cobban, 1965). Major soil series formed in the Cavalier County include the Barnes (Fine-loamy, mixed, superactive, frigid Calcic Hapludolls) and Svea (Fine-loamy, mixed, superactive, frigid Pachic Hapludolls) series, formed on unsorted glacial till, soils like Hegne (Fine, smectitic, frigid Typic Calciaquerts) and Glyndon (Coarse-silty, mixed, superactive, frigid Aeric Calciaquolls) have lacustrine parent material, soil series like Sioux (Sandy-skeletal, mixed, frigid Entic Hapludolls) and Fordville (Fine-loamy over sandy or sandy-skeletal, mixed, superactive, frigid Pachic Hapludolls) were formed in glacial outwash, some of the soils were formed in alluvium while some of them were formed partially in shale (Simons and Moos, 1990). Average annual mean temperature and precipitation of Cavalier County for the last 30 years (1971-2000) have been recorded as 2.2°C and 18.1" (NDAWN; NCDC). Soils in the County are best suited for cultivated crops, hay and pasture. (Simmons and Moos, 1990).

2.3. The Pembina Escarpment

The Pembina Escarpment (Fig. 2.1) is a 70-100 m high east-facing escarpment extending from near the town of Park River, North Dakota about 160 km (100 miles) to the north near the town of Treherne in southern Manitoba. It marks the northwestern edge of

the Red River Valley.

"The Pembina Escarpment was a less prominent feature before glaciation and its origin has been tentatively linked to the development of the Red River Valley" (Bluemle, 2000, p. 45). Erosion of soft shale and sandstone that covered granite and other igneous rocks of the Canadian Shield by the ancient Red River formed an east facing Escarpment which was steepened by the glacial ice (Bluemle, 2000). The Pembina Escarpment continues to the north, where it is referred to as the Manitoba Escarpment in southern Manitoba (Smith *et al.*, 1973).

Fig. 2.1. Location of the Pembina Escarpment in northeastern North Dakota. Circles show field sampling locations. Figs. 3.1 and 3.2 show individual sampling sites for these two sampling locations. Graphic from NASA Shuttle Radar Topography Mission (SRTM) North America Images, 2000.

2.3.1. Soil Types on the Pembina Escarpment

Weathering of rocks and the type of minerals present in the regolith are key factors that influence soil formation. The parent material for the soils of Cavalier County, North Dakota is predominantly glacial drift containing Cretaceous shale fragments as advancing glaciers modified landforms and comminuted the parent material during the course of the Quaternary (Arndt, 1975; Simons and Moos, 1990). Retreating glaciers led to the deposition of the material along with the ice melt from the glaciers.

Research conducted by Hopkins *et al.* (1999) on the Pembina Escarpment revealed locations with high concentrations of Cd and several other trace elements that might likely be linked to soils derived directly from or containing shales that have contrasting composition and geochemical properties compared to drift prairie soils. Soil at a site investigated by Hopkins *et al.*, (1999) had a total Cd concentration of 15.9 mg/kg. Crustal rocks have average Zn/Cd ratio of 250 (Adriano, 1986). Hopkins *et al.* (1999) gave Zn/Cd ratio of 85 for the collivium from shales of the Pembina Escarpment indicating high degree of Cd accumulation in this landscape. Research locations investigated on the Pembina Escarpment by Hopkins *et al.*, (1999) were associated with the soil series mapped as the Rolette series (Fine, smectitic, frigid Alfic Vertic Argiudolls) which is distributed in northern and northeastern North Dakota (Simons and Moos, 1990). The Rolette soil is a well drained soil formed in glaciolacustrine deposits and exhibits silty clay to silty clay loam textures with typical horizons A, B/E, B_t and C (Simmons and Moos, 1990). Soils in Canada formed on normal glacial tills and other glacial materials have a mean Cd of 0.07 mg/kg; alluvial soil developed from a variety of parent materials had Cd levels of 1.5 mg/kg (Adraino, 1986). Soils found on the Pembina Escarpment include a variety of

parent materials as evident from a variety of soil series like Olga (Fine, smectitic, frigid Alfic Vertic Argiudolls) found in colluvium from shale as bedrock, Miranda (Fine, smectitic, frigid Leptic Natrustolls) and Cavour (Fine, smectitic, frigid Calcic Natrudolls) formed in till plains, shale rich Walsh (Fine-loamy, mixed, superactive, frigid Pachic Hapludolls) which were formed from glacial alluvium derived from shale or glacial till and Vang (Fine-loamy over sandy or sandy-skeletal, mixed, superactive, frigid Pachic Hapludolls) found in glacial outwash plains, Cresbard (Fine, smectitic, frigid Glossic Natrudolls) formed in glacial and alluvial till mainly on footslopes (Simmons and Moos, 1990).

2.4. Rationale and Objectives

Based on the information available, it can be postulated that there is an interaction of several factors and processes that have resulted in high levels of Cd in certain soils of northeastern North Dakota. These factors include: glacial history, sub-surface lithology, geomorphic history and weathering history of bedrock, and geochemical regime. Research based on the analysis of physicochemical and mineralogical properties can provide significant information for comprehensive geochemical assessment of the processes that trace elements undergo in soils as they form from parent materials through various pedogenic stages. Such research can increase knowledge of trace element availability. Keeping these perspectives in mind, this geochemical survey was undertaken to improve understanding of metal enriched soils and their spatial variability on the Pembina Escarpment.

CHAPTER 3. MATERIALS AND METHODS

3.1. Field Methods

3.1.1. Sampling

Soils were sampled in Cavalier County in northeastern North Dakota in areas that were previously identified as sites with high concentrations of trace elements by Hopkins *et al.*, (1999). The first sampling session occurred in October 2007 in an agricultural field and an adjacent Conservation Reserve Program (CRP) field (Fig. 3.1). Geographic location details for the agricultural field are not listed in the interest of land owner. A total of 25 samples were collected by spade and auger at depth intervals of (0-15) cm, (30-50) cm and > 50 cm. In June 2008, a second set of samples were taken on former agricultural fields that are now grassland fields in a North Dakota State Wildlife Management Area (NDSWMA) (Fig. 3.2). Soils from surface and core samples were collected from different locations in the fields using six transects having sampling sites at a distance of 250 ft. (approx. 76 m) from each other. Samples (n=139) were collected from 0-15 cm and 15-30 cm depths. Surface samples (n=5) at a distance of 50 ft. (15.24 m) were taken as a part of closed sampling grid. Cores 0-8 ft. (approx. 2.4 m) were taken using a percussive soil probe (Soil Sampler 9800E with 4″ diam. by Amity Technology) from 12 different sites (one site was cored to 12 feet (3.7 m)) on three transects in field three (Fig. 3.3.). Location of each sampling site was recorded using a sub-meter accuracy GPS. Soil samples from October sampling belong to Rolette soil series while samples from three fields belong to Rolette and Olga soil series having a similar taxonomic classification as previously

mentioned. All the samples (surface and core) analyzed for this study had an elevation range between 361.12-401.42 m. Township and Range numbers for three fields were 162° N and 57° W respectively, with SE quarter section 22 and NE quarter section 27 for the first field. Latitude and Longitude locations for three fields were within 48° 49′ 38.33″ N and 97° 59′ 37.96″ W to 48°50′ 08.73″ N and 98° 00′ 23.20″ W.

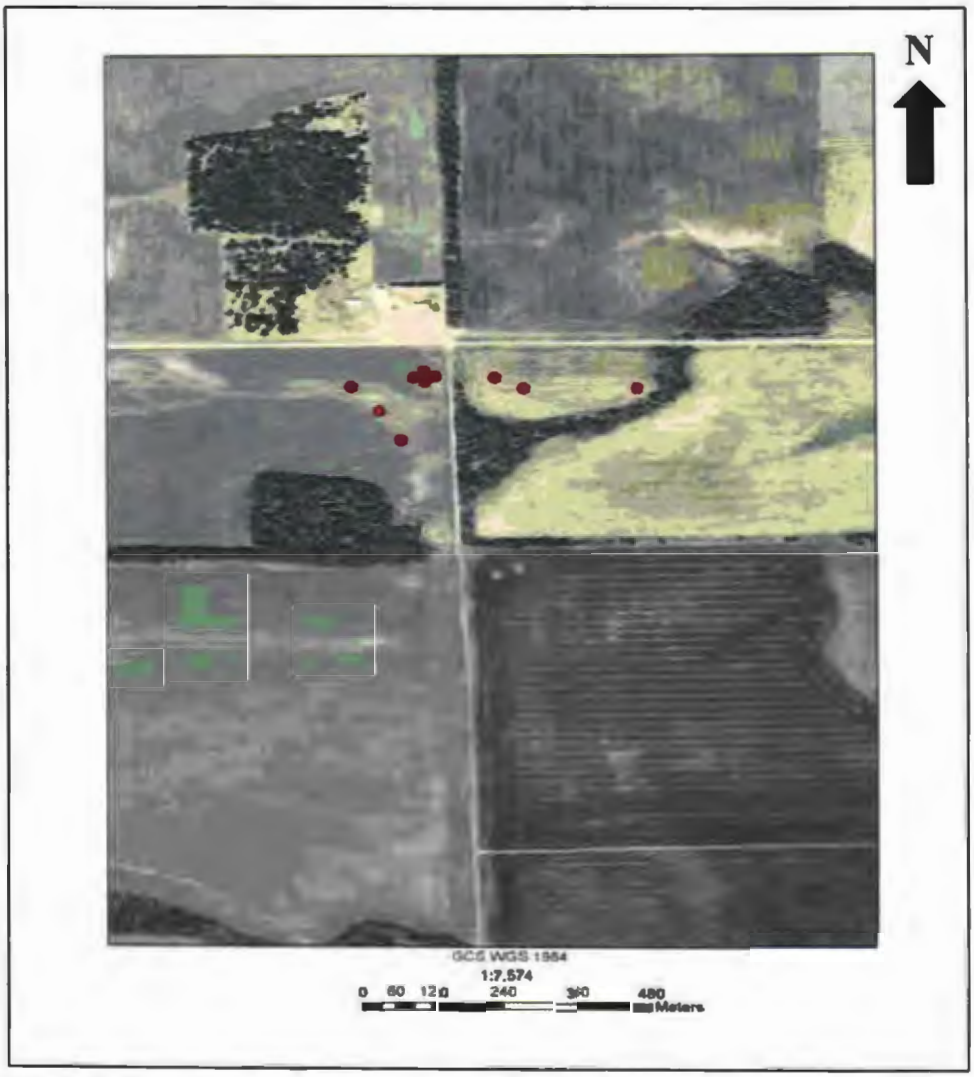

Fig. 3.1. Location of sampling sites in a Rolette soil map unit, Cavalier County, North Dakota. Cropland samples to the west of N/S field road, CRP samples to the east. Field location on the escarpment is shown in Fig. 2.1. Graphic from Aerial Photography Field Office (APFO). United States Department of Agriculture (USDA), 2007.

Fig. 3.2. Location of sampling sites in three former agricultural fields, Cavalier County, North Dakota. Black line shows baseline for six transects. Fig. 2.1 shows field locations on the escarpment. Graphic from APFO. USDA, 2007.

Fig.3.3. Encircled black dots denoting core sampling locations in field three in Cavalier County, North Dakota. Black line marks the baseline for six transect lines. Graphic from APFO. USDA, 2007.

3.2. Laboratory Methods

3.2.1.Core Description

All the cores were stored in a refrigerator at NDSU. Each core was thawed and cut with the help of saw cutter for detailed morphological description. Three of the most

important morphological properties used for the description of core soil profiles using the field guide book by Schoeneberger and Wysocki (1998) were texture, structure, and color (moist and dry). Additional observations were made with a 10 power hand lens and/or light microscope. Different horizons (with depths) like topsoils, argillic, eluvial, shale and bedrock were marked for all the 12 cores. Sub-samples of the cores were taken at 15 cm intervals for further chemical analysis. For graphical presentation of the cores, LogPlot 7 V.7.3.62.87 and Rockworks 6 by RockWare Incorporated software were used to create logs depicting lithology, soil properties and element concentrations for all the cores.

3.2.2. Particle Size Analysis

Particle size analysis was conducted using a modification of the Gee and Bauder (1986) method. Soil samples from October 2007 sampling season and 34 samples from 5 cores along transect 4 were analyzed for particle size distribution. See Appendix Table B.2. for sample identification. Soil samples were air dried in Al trays at room temperature. Soil was ground with mortar and pestle to break up chunks and loosen clods. A 2 mm mesh brass sieve was used to remove gravel. The soil sample was weighed and dried at 105°C overnight. The sample was cooled and 40 g were added to 100 mL of sodium hexametaphopshate (HMP) solution and allowed to equilibrate overnight. The slurry was transferred to a shaking bottle and was agitated at a medium speed overnight on a horizontal shaker. The mixture was then poured into a sedimentation cylinder and distilled water was added to bring the volume up to 1L. The mixture was stirred with plunger and a few drops of amyl alcohol were added to the sample if the surface of the suspension became foamy. After mixing was complete, the hydrometer (ASTM 152H) was gently

placed into the suspension. Readings were taken at 3, 10, 30, 60, 90, 120 and 1440 min. The hydrometer was removed and cleaned after each reading. Readings were recorded as (R) for each time interval. In another sedimentation cylinder, a blank solution was made by adding100 mL HMP solution and 900 mL distilled water. The solution was mixed with plunger and temperature was recorded and the reading was recorded as (R_l) for the blank solution. After 1440 min, sediment and suspension were transferred to a 53 μm brass sieve and were first washed using a wash bottle and a gentle stream of tapwater followed by deionized water. Sand from the sieve was transferred into a 500 mL beaker and oven dried overnight at 105°C and then cooled and quantified. Dried sand was then transferred to the nest of sieves arranged from top to bottom in the following order: 1000, 500, 250, 106, and 53 μm. Sands were shaken on a sieve shaker for 3 min and each sand fraction was determined.

The calculated value for B provided corrections for the density and viscosity variations of the HMP solution.

(1) $$B = 30\eta / [g (\rho_s - \rho_l)]$$

where

B= correction for HMP solution
η= fluid HMP solution viscosity (Eq.3) in poise, g/cm/s
g = gravitational constant, 980 cm/s^2
ρ_s = soil particle density, assumed standard 2.65 g/cm^3
ρ_l = HMP solution density (Eq.2), g/cm^3

(2) $$\rho_l = \rho^\circ(1+ 0.630\ C_s)$$

where

ρ_l = HMP solution density at temperature *t*, g/cm^3
ρ° = water density at temperature *t*, g/cm^3

At temp 20°C =0.998g/cm^3
At temp 25°C = 0.997g/cm^3
C_s = concentration of HMP, 0.05 g/cm^3

(3) $$\eta = \eta^\circ (1 + 4.25\ C_s)$$

where

η = HMP solution viscosity at temperature *t* in poise, g/cm/s
η° = water viscosity at temperature *t* in poise, g/cm/s
At temp 20°C = 0.01 g/cm/s
At temp 25°C = 0.0089 g/cm/s
Cs = concentration of HMP, 0.05 g/cm3

3.2.2.1. Particle Diameter (X) Calculation for each Time Interval

These calculations were used to determine particle diameter in solution at each time (t) interval.

(4) $$X = \theta / (t)^{-1/2}$$

where

X = mean particle diameter in suspension, μm at time t
θ = sedimentation parameter (Eq.5), μm min$^{1/2}$
t = time in minutes

(5) $$\theta = 1000(Bh')^{1/2}$$

where

h′ = effective hydrometer depth, cm

(6) $$h' = -0.164\ R + 16.3$$

where

R = uncorrected hydrometer reading, g/L

Summation Percentage (P) for each time interval

(7) $$P = C/C_0 \times 100$$

where

C = concentration of soil in suspension (Eq.8), g/L
C_0 = oven-dry weight of soil sample used for the test

(8) $$C = R - R_l$$

where

R_l = hydrometer reading of blank solution, g/L

3.2.3. X-Ray Diffraction

3.2.3.1. Slide Preparation

Soil suspensions (10 mL) after 1440 min from the particle size analysis for October samples (n=25) were taken with a hand pipette and placed in a (20 mL) storage cup. A 25 mm diameter cellulose acetate filter paper (0.45μm) supported by screens was placed on a flask and the funnel was attached to it. The suspension was shaken to redistribute particles and a small amount was poured into the funnel attached to a vacuum pump. The funnel was removed and the filter was placed upside down on a clean glass slide with a thin edge extending over the edge for removing the filter. The slide was gently rolled to remove air pockets and allowed to dry until the paper began to turn white. The filter paper was pulled off in one quick motion.

3.2.3.2. Clay Mineral Analysis

Clay slides were analyzed with Philips XPert MPD X-ray diffractometer in the Department of Chemistry and Biochemistry at North Dakota State University (NDSU) using CuKα radiation (40 kV, 30mA). Each sample was analyzed twice: (1) under air dry conditions (scanning from 2.01° to 39.99°); (2) after overnight exposure to ethylene glycol vapors (2.01° to 39.99°). Glycolation allows the smectite group minerals to be distinguished from chlorite or vermiculite group. After glycolation, the (001) reflection of smectite is shifted to 5.2°2θ (16.9Å) which in case of air dried condition is near 6° (15Å). See appendix B for details.

3.2.3.3. Peak Analysis

Identification of clay minerals was made by using the position of the (001) series of basal reflections. PANalytical X'Pert High Score software was used for computer aided pattern and peak identification for clay minerals by Search-Match application that identifies main peaks from the diffractogram and matches it to the peaks in its database. Diffraction graphs were plotted using Origin 6.0 software.

3.2.4. Inductively Coupled Plasma Spectroscopy

3.2.4.1. Microwave Digestion of Soil Samples

Surface samples from October 2007 were analyzed for Cd and arsenic (As) whereas June 2008 surface samples were analyzed for Cd only. Core samples were analyzed for multi-elements. A sample of 500 mg of soil (<2 mm) was placed in a Teflon vessel (55mL) and the procedure used was NDSU Wetland Ecosystem Research Group

(WERG) Soil 16 modified from EPA Method 3051 by Kingston (1997). Concentrated nitric acid was added twice (5 mL increments) into the vessel. The mixture was vortex mixed to insure thorough wetting of the soil. The suspension was set aside for 15 min. to allow sample pre-digestion. It was then subjected to treatment for 10 min. in a CEM MARS XPRESS Microwave digester (230 V, 60HZ) with Xpress Vessels (55mL PFA venting). Each set of digests consisted of 14 soil samples, a standard reference material and a reagent blank. After complete digestion, the vessels were allowed to cool and the contents were filtered with No.1 Whatman filter paper having diameter of 9 cm and particle retention up to 11μm to remove precipitates. Vessels were rinsed 3 times with 1 mL aliquots of distilled water and the filtrate was transferred into test tube.

3.2.4.2. Trace Element Analysis

Samples were analyzed at NDSU with a Spectro Genesis Inductively Coupled Plasma Optical Emission Spectroscope with cross flow nebulizer, using argon (Ar) gas. Smart Analyzer Vision V.3.013.0752 software was used for the interpretation. The instrument was calibrated using multi-element and individual standards with different concentrations. Instrument settings included plasma power: 1400 W; coolant flow: 13.5 L/min.; auxillary flow: 1.2 L/min.; nebulizer flow: 0.9 L/min. and were optimized for this instrument. Core samples were analyzed for the following elements : aluminum (Al), As, boron (B), beryllium (Be), Ca, Cd, Co, chromium (Cr), Cu, iron (Fe), mercury (Hg), potassium (K), lithium (Li), magnesium (Mg), manganese (Mn), molybdenum (Mo), sodium (Na), Ni, phosphorus (P), lead (Pb), sulfur (S), antimony (Sb), selenium (Se), silicon (Si), tin (Sn), strontium (Sr), titanium (Ti), Thallium (Tl), vanadium (V), and zinc

(Zn). The results were recorded as mean concentrations of three measurements of elements from the same sample in g/L. Values for respective elements were then calculated in mg/kg. Solid Standards used for multi-element analyses were Natural Matrix Certified Reference Materials (CRM026-050, CRM022-020, CRM028-050, and CRM200) purchased from RTC, Wyoming. Montana Soil Standard 2711 was also used for trace element analysis.

Element concentration (mg/kg) was calculated by

(9) $\{E = \text{Dilution} \times \text{Vol. of extract} \times \text{mean conc} \times 1000\}/\text{wt. of soil}$

where

E= element concentration in mg/kg
Dilution = 1
Volume of extract = 0.013 L
Mean concentration of element (mg/L)
Weight of soil sample (g)

Method error was calculated after running a standard (CRM026-050) for 21 times giving an error of 6%.

3.2.5. Organic Matter Content

Organic matter content (OM) was determined after loss on ignition for all the core and surface samples from June 2008 sampling using the method outlined in Storer (1984). A 5 g sample was placed in ceramic crucible and heated for 2 hr at 105°C. After 2 hr samples were weighed and values recorded as sample wet weights. Samples were then placed in a preheated muffle furnace at 360°C for 2 hr. After ignition, samples were cooled for 10 min. and dry weight was recorded for each sample. The percent weight loss and OM were calculated according to the following formula:

(10) % wt. loss = ((wet wt. - dry wt.)/ (dry wt.))*100

(11) % OM = (0.94*% wt. loss)

Method error was calculated after running 20 check standards and error was found to be 0.25%.

3.2.6. Soil pH and Electrical Conductivity

Surface and core samples from June 2008 were analyzed for soil pH and electrical conductivity. Ten grams of sample was used to determine pH and electrical conductivity (EC). The samples were placed in small 20 mL cups using 10 mL of deionized water to make a 1:1 soil/water ratio. The samples were stirred for a min. and allowed to equilibrate for 10 min. A Corning pH/ conductivity meter was calibrated with a standard solution having EC as 1.413 dS/m. The electrode was then placed in check soil and samples and then readings were recorded for EC.

A similar procedure was used for sample pH using an Orion research microprocessor Ion-analyzer/901. Two buffer solutions (pH 7 and 10) were used to calibrate the instrument. All the samples were run for pH and EC in Soil and Water Environmental Laboratory at NDSU.

3.2.7. Statistical Methods

Descriptive statistics such as average, median, minimum and maximum values were calculated for all the 12 cores taken in field three during June sampling 2008. Pearson correlation coefficients were used to test the linear relationship between all the elements and selected soil characteristics such as pH, electrical conductivity and organic matter

content with different types of lithologies such as topsoil, shale, silt and sand, argillic and carbonate horizons present in the core samples using SAS 9.1. system at NDSU.

Principal Component Analysis (PCA) was performed using R (V.2.11.0) and Matlab (V. 2006b) software on data matrices for different soil horizons described during core descriptions consisting of elements and soil characteristics for samples from 8 cores taken on transect 4. A correlation matrix was calculated to highlight elemental relations with each other and with different soil properties. The data were normalized with zero mean and variance was set to unity. Principal Components having eigenvalue > 1 were retained according to Kaiser's rule. Varimax rotation was applid to Principal Components and the resulting PC loadings having value 0.6 or greater which are considered stronger were retained for data interpretation (Nowak, 1998; Garcia *et al.*, 2004; Cheng *et al.*, 2009).

CHAPTER 4. RESULTS

4.1. Preliminary (October Sampling) Results

4.1.1. Particle Size Distribution

Samples from both fields in 2007 (Table 4.1.) are clay rich (46.2 to 66.5% clay), followed by silt (33.0 to 42.3%) and are low to very low in sand (2.5 to 28.7%). Soil samples from both fields have comparatively higher clay content in the deeper sampling interval (30-50 cm), which likely indicates the presence of subsurface argillic horizons. See Appendix B for the sample codes and relative percentages for all the samples.

Table 4.1. Results of particle size analysis for agricultural and CRP fields at depth intervals of (0-15) cm and (30-50) cm.

Agricultural Field					CRP field				
Sample Name	**Sampling depth (cm)**	**Sand %**	**Silt %**	**Clay %**	**Sample Name**	**Sampling depth (cm)**	**Sand %**	**Silt %**	**Clay %**
PE	(0-15)	18.3	33.5	48.2	CRP1	(0-15)	17.1	36.8	46.2
PW	(0-15)	16.2	34.3	49.5	CRP2	(0-15)	12.7	35.2	52.1
PN	(0-15)	17.0	36.5	46.4	CRP3	(0-15)	15.1	36.4	48.5
PS	(0-15)	15.5	36.1	48.4	CRP1	(30-50)	16.2	33.5	50.3
PC	(0-15)	15.6	33.0	51.4	CRP2	(30-50)	17.7	34.3	48.0
PD1	(0-15)	17.1	35.7	47.2	CRP3	(30-50)	7.2	26.3	66.5
PD2	(0-15)	13.3	38.0	48.7					
PD3	(0-15)	28.7	33.6	37.7					
PE	(30-50)	2.5	42.3	55.2					
PW	(30-50)	6.5	37.5	56.0					
PN	(30-50)	16.3	34.3	49.5					
PS	(30-50)	3.3	32.7	64.0					
PC	(30-50)	7.6	36.9	55.5					

PE:East; PW:West; PN:North; PS:South; PC:Center; PD:Depression

4.1.2. Clay Mineral Analysis

X-Ray Diffraction (XRD) analyses of the 25 samples (both A and B horizon) suggest that their fine clay fractions are composed of illite, smectite, chlorite, vermiculite and kaolinite clay minerals (See Appendix C for detailed description of all diffractograms). In addition to these clay minerals, other dominant minerals present were quartz and calcite. Criteria used to identify subsurface argillic horizons include hand texturing, observations of structural grade, and other properties noted in Table 4.2.

Table 4.2. Identification of clay minerals according to peak positions (°2θ) and d-spacing (Å) by Moore and Reynolds (1989).

Air Dried (d,°2θ)	Glycolated (d, °2θ)	Mineral (hkl)
10.1, 8.8	10.1, 8.8	Illite (001)
12-15, 5.9-7.2	16.9, 5.2	Smectite (001)
14.5, 5.9-7.2	14, 6.3	Vermiculite (001)
14.2, 6.2	14, 6.3	Chlorite (001)
7.2, 12.4	7.2, 12.4	Kaolinite (001)
5, 17.7	5, 17.7	Illite (002)
7.2, 12.4	7.2, 12.4	Chlorite (002)
3.58, 24.9	3.58, 24.9	Kaolinite (002)
4.74, 18.8	4.74, 18.8	Chlorite (003)
3.38, 26.7	3.38, 26.7	Illite (003)
3.55, 25.1	3.55, 25.1	Chlorite (004)

Figure 4.1. shows the diffraction patterns obtained for air dried and glycolated B horizon sample 20. See Appendix Table C.1. for sample identification. The mineral smectite is easily identified by comparing diffraction patterns of air-dried and ethylene glycol sample preparations. After glycolation, d-spacings change because of greater separation between the cations and the negative layer charge which produces weaker electrostatic attraction between the clay and interlayer cations. This allows more water molecules to enter the interlayer space, which in turn enables greater swelling between clay layers. Thus, there is a shift in smectite peak for the glycolated diffraction pattern as shown

in Fig.4.1.

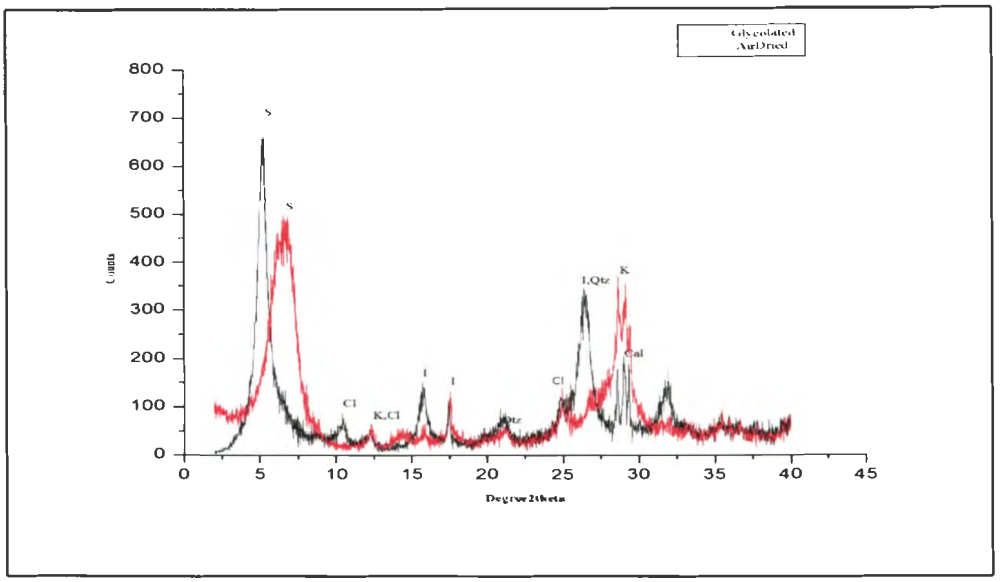

Fig. 4.1. X-Ray diffraction patterns for major clay and other minerals for air dried and glycolated B horizon sample 20. S: Smectite, K: Kaolinite, I: Illite, Qtz: Quartz, Cal: Calcite, Cl: Chlorite.

In kaolinites, the d-spacing is not affected by its exposure to glycerol vapors as they have no isomorphous substitution and lack interlayer cations, which can affect the d-spacing. Kaolinite and chlorite minerals are difficult to identify when they exist as a mixed system. Kaolinite has reflections based on a 7.1 Å structure, whereas chlorite has a basal series of peaks of first order on 14.2 Å structure. These peaks were identified by looking for the (004) peak reflection for chlorite at 25.1 °2θ. For quartz, peaks were identified at 20.9 °2θ, (4.25 Å) for (100), 26.7 °2θ, (3.33 Å) for (101), 36.5 °2θ, (2.46 Å) and 39.4 °2θ, (2.28 Å). Calcite peaks were found to be at 29.29 °2θ, (3.05 Å), 35.96 °2θ, (2.50 Å) and 39.34 °2θ, (2.29 Å). Presence of kaolinite, smectite and illite was observed in all the clay samples except sample 20 in which chlorite was also observed. The proportion of each clay mineral was not quantified for this study.

4.1.3. Element Analysis

Very high Cd concentrations were found in all the samples from the preliminary study in both CRP and agricultural fields (Table 4.3.).

Table 4.3. Results of elements analyzed for surface samples through ICP-OES.

Sample ID	Sample Name	Cd (mg/kg)	As (mg/kg)
1	PE (0-15)	4.79	1.87
2	PC (0-15)	6.63	2.21
3	PS (0-15)	4.47	1.53
4	PS (30-50)	8.14	2.58
5	PW (30-50)	6.33	1.80
6	PN (30-50)	3.15	2.00
7	PE (30-50)	3.02	2.16
8	PC (15-30)	5.12	1.92
9	PC (30-50)	4.66	2.16
10	PD1(0-15)	3.82	1.64
11	PD3 (0-15)	8.18	1.95
12	CRP1 (30-50)	8.24	1.51
13	PW (0-15)	8.87	1.82
14	PD2 (0-15)	3.49	1.33
15	PN (0- 15)	4.11	1.59
16	CRP1 (0-15)	5.40	1.25
17	CRP1 (114-130)	9.47	2.94
18	CRP2 (0-15)	10.59	2.27
19	CRP2 (30-50)	5.91	1.20
20	CRP2 (10" to auger handle)	11.58	5.49
21	CRP2 (Brown oxides)	12.37	2.71
22	CRP2 (7cm to handle)	16.39	4.12
23	CRP3 (0-15)	4.48	0.73
24	CRP3 (30-50)	6.83	1.20
25	CRP3 (5'Lime layer)	7.42	1.59

PE:East; PW:West; PN:North; PS:South; PC:Center; PD:Depression

Cadmium concentration of 16.39 mg/kg was reported as the highest (CRP field) and 3.02 mg/kg as the lowest (agricultural field) with an average of 6.9 mg/kg. Both surface (0-15 cm) and sub-surface (30-50 cm) average Cd concentration for the agricultural field was found to be 5.08 mg/kg whereas average surface Cd concentration for CRP field was 6.82

mg/kg and sub-surface value was found as 7.0 mg/kg. Arsenic concentrations found in both the fields were in a range of 0.73-5.49 mg/kg.

4.2. June Sampling Results

4.2.1. Core Description

Based on morphological and graphical descriptions of 12 cores (see Appendix A; for core identification see Table 4.4.), the typical master soil horizons present in the cores were dark colored topsoil (A horizons), formed by the degradation and accumulation of organic matter, underlain by an eluvial horizon (E) (Cores 2, 4, 5, 6, 11, and12), which is light colored due to leaching and loss of dark colored organic pigments and ferric oxyhydroxides.

Table 4.4. Identification of twelve cores taken in field three in Cavalier County, North Dakota.

Core No.	Core ID.	Elevation (m)
1	1500N, 0W	376.1
2	1900N, 1250W	394.4
3	1900N, 1500W	397.2
4	1500N, 250W	381.6
5	1500N, 500W	383.4
6	1500N, 750W	387.1
7	1500N, 1000W	389.2
8	1500N, 1250W	392.3
9	1500N, 1500W	396.5
10	1500N, 1750W	399.0
11	1700N, 1250W	392.9
12	1700N, 1500W	397.5

For the purpose of detailed description, subordinate distinctions included for these cores were B_t in which clay has accumulated and B_k (Core7) in which carbonates have

accumulated. Transition horizons (Cores 1, 2, 4, 6, 10 and11) are designated through the use of both horizon designations with the horizon having the more prominent features appearing first, as a BC horizon, would indicate a horizon that has a transition more like a B than a C horizon.

4.2.1.1. Texture

The texture for A, E and B horizons was restricted to fine textural classes and ranged between silty clay loam and silty clay. Clayey textures for these horizons indicate their origin from shale parent material. Thick E horizons appeared for the cores in upslope landscape settings indicating extensive weathering of these soils due to lateral and vertical flow of water. Occurrence of thick clay films on the peds in the illuvial horizons (B_t) reveal increased soil development in the profile. Very fine to medium (0.05-0.5) mm sand grains were observed in E and B horizons over the ped faces with the help of a hand lens.

4.2.1.2. Structure

Various types of structures were observed for different horizons in the soil profiles. Fine-medium granular to medium subangular blocky structures were characteristic for the A horizons. The E horizons had weak, fine prismatic to medium subangular blocky structures instead of the anticipated platy structures. Well defined prismatic structure was found in B horizon. Apart from these conventional structural types, small black charcoal lenses were reported in E and B horizons. These could be the weathering byproducts of shale. Redoximorphic features included Fe and Mn concentrations indicating water

movement within the soil profile. Root masses were observed in A and B horizons, and for some cores even in deeper C horizons as well. Very thick roots (>2cm in diam.) observed in core 6 and occurrence of several organic matter zones in cores 7, 11 and 12 indicate remnants of forests that once existed in this landscape. Minerals that were readily observed in the soil cores were jarosite, gypsum, calcite, and quartz.

4.2.1.3 Color

Dark grayish brown (10YR 3/1) dry to black (10YR 2/1) moist color of the topsoils indicated accumulation of OM in the A horizon. Presence of brownish yellow (10YR 6/6) dry, strong brown (7.5YR 5/6) dry and dark yellowish brown (10YR 4/6) dry color in the form of redoximorphic concentrations in the subsurface horizons is a result of the occurrence of oxides of Fe and Mn, indicating poor to moderately drained soils. The pale yellow (2.5Y 7/2) moist to (2.5Y 4/2) dry color in E horizon confirmed a leached zone in which only the resistant silicate minerals have remained. In some cases this light color might also be due to the presence of volcanic ash and bleached quartz grains in the soil profiles. Dark grayish brown (10YR 3/2) moist and brown (10YR 5/3) dry colors were observed in B_{t1} horizons for the majority of cores. Very dark gray (2.5Y 3/1) moist to light yellowish brown (2.5Y 6/3) dry colors were generally found in B_{t2} horizons. Grayish brown colors for B_{t2} horizons indicate mixing of parent material in these horizons overlying shale rich C horizons. Very dark grayish brown (2.5Y 3/2) moist to gray (2.5Y 5/1) dry colors marked C horizons.

The entire soil profile was leached of carbonates for all cores except core 7. Shale fragments were observed close to the surface in some profiles indicating rather shallow

depths to shale bedrock or colluvial materials derived from shale. Occurrence of ash layers in cores (2, 3, 5, 8 and 12) indicate the presence of bentonite layers as reported for the lithology of this area in literature. Other characteristic features observed in the cores were grayish white coatings or silans or skeletans over ped faces in E and B horizons in core 4 indicating glossic horizon in which E horizon material extends irregularly into the argillic horizon. Anomalous fine grained sedimentary zones having shale fragments were also observed in cores 6, 11, and 12, which might be due to the formation of secondary structures in the lower soil profile resulting from weathering of parent shale material. Black, fine grained lentil-shaped bodies were observed embedded in clay matrix or between fissures in ped faces in majority of the cores in B horizons. These could be OM or secondary iron minerals. Stratifications resulting from the original clay deposition were frequently observed in shales.

Figure 4.2. shows cross section AA' for 8 cores taken along transect 4 during June, 2008 sampling in field three. Different types of lithologies, redoximorphic features, minerals like jarosite and gypsum, zones rich in carbonate, organic matter and charcoal lenses along with other features like ash layers as depth function are shown for all the 8 cores. For instance, for core 9, topsoil is shown with a blue color followed by a small olive colored argillic horizon having silans (white and black small boxes) and organic matter (solid brown) which is followed by white colored ash layer in the bedrock having yellow colored jarosite mineral. The dark thick solid line over the top of all cores marks the surface of the field. See legend for color codes, symbols and corresponding lithologies present in these 8 cores. It can be seen from the graphic that argillic horizon comes out as a thick lithologic horizon in all the cores.

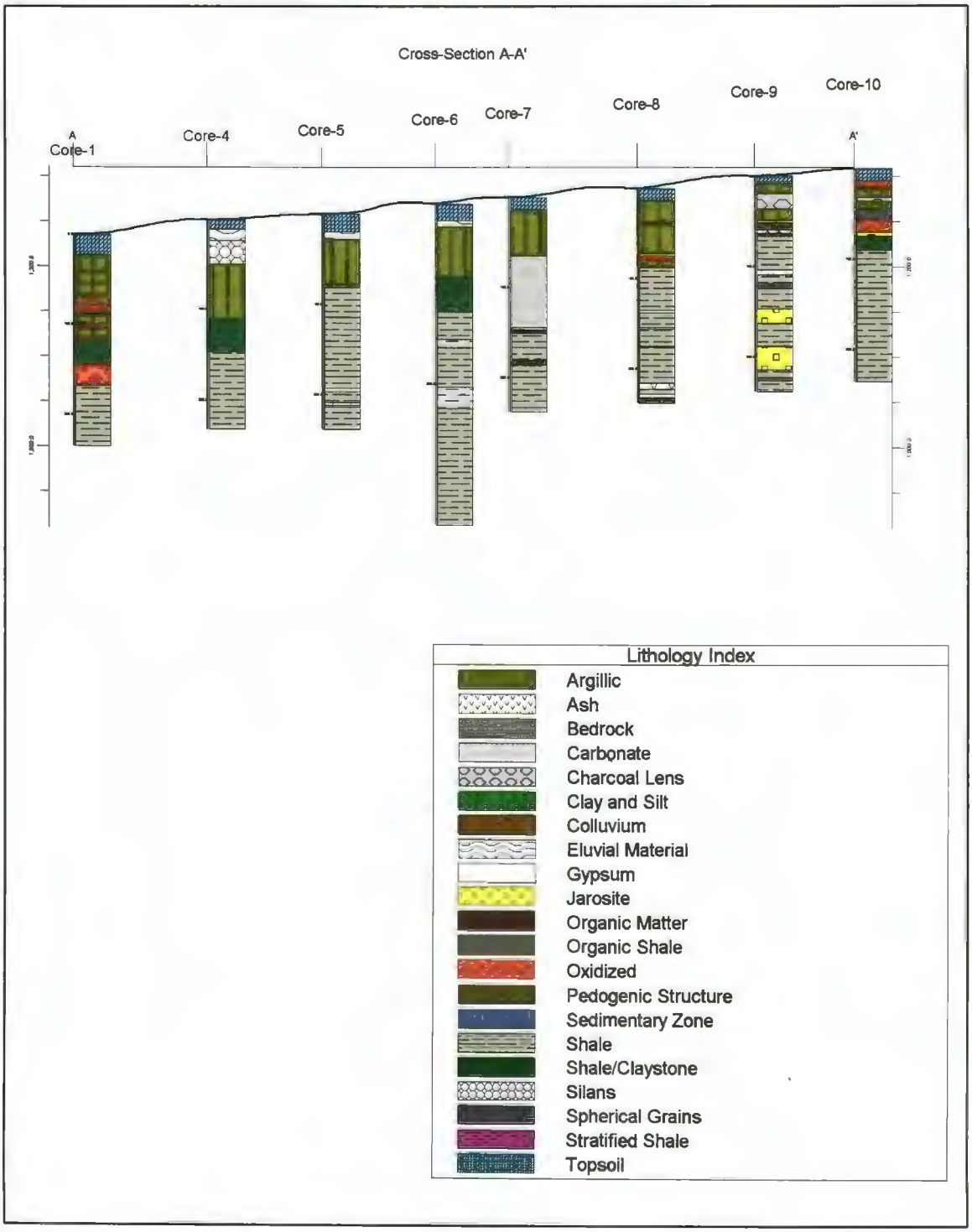

Fig.4.2. Cross section of 8 cores taken along transect 4 in field three showing lithology and other morphological features.

4.2.2. Soil Chemical Properties

4.2.2.1. Organic Matter

Figure 4.3. shows results of variation along elevation in organic matter content found in the surface and sub-surface samples from June, 2008. A wide range of organic matter (2.62-13.3%) was found in topsoils. As commonly expected, organic matter content in the surface (0-15 cm) layer was higher than that of subsurface (15-30 cm) samples.

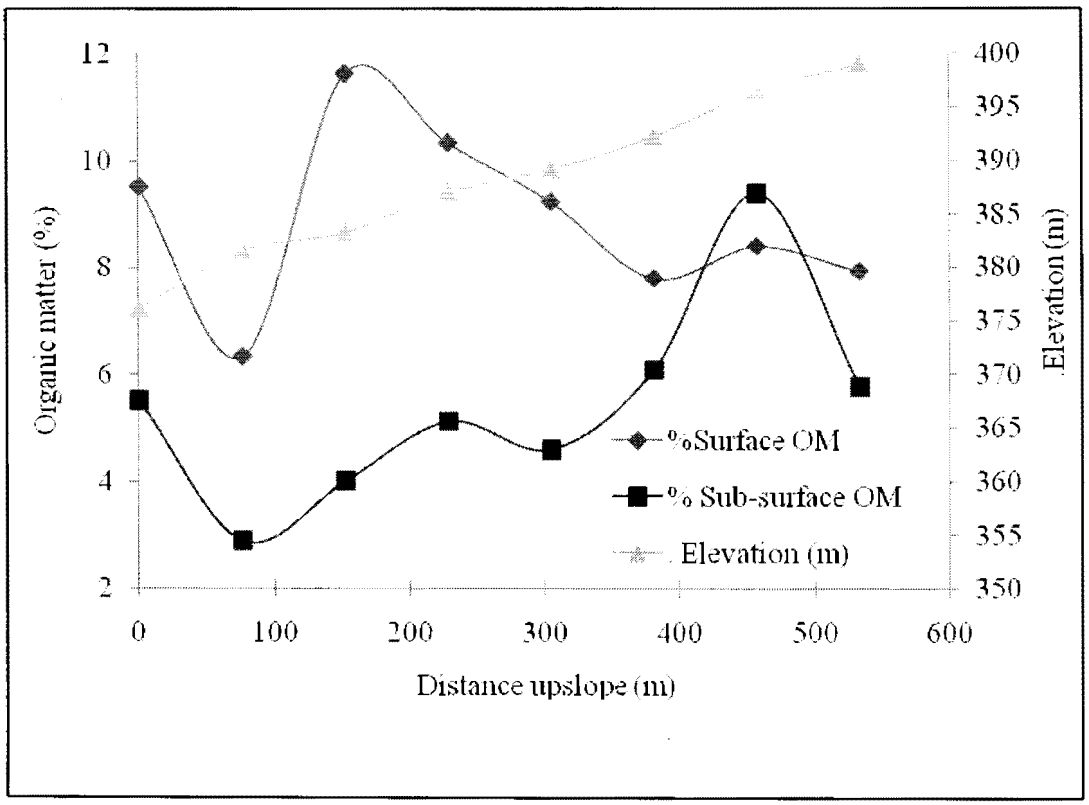

Fig. 4.3. Organic matter distribution in surface and sub-surface samples along transect 4. Distance measured west from baseline.

Results of the surface samples from 8 cores taken along transect 4 indicate that organic matter was high for the samples taken near the base line i.e. at the point of origin (0

m) and down the slope in comparison to the results of the samples from upslope. Sub-surface samples on the other hand show a different trend with upslope samples containing slightly higher organic matter than the samples near the baseline. Reduced organic matter in the samples from upslope could reflect the erosion of topsoil by wind and water and thus its accumulation near the base. The maximum organic matter present in the A horizon of core samples was 20.1% for core 3 (upslope) near the forested area and the minimum was 2.8% core 4 (downslope). See Appendix D. Core descriptions also revealed occurrence of roots and root channels along with charcoal lenses which can attribute to high organic matter found in core 3.

4.2.2.2. pH and Electrical Conductivity (EC)

Soil samples ranged from being ultra acidic (pH = 3.2) to slightly alkaline (pH = 7.8) defined by Natural Resources Conservation Service (NRCS), and clearly reflect the presence of relatively unweathered shale (and its component sulfides). The electrical conductivity of the samples was between 0.2 to 4.0 μS/cm. pH and EC values were plotted against distance covered at regular intervals of 76.2 meters.

The pH values for surface and sub-surface samples from June, 2008 taken on transect 2 in field one are shown in Fig. 4.4. Surface (0-15) cm samples are marked by rectangles and sub-surface (15-30) cm samples are marked by triangles. Both surface and sub-surface samples show a similar trend for pH values except the last two samples taken upslope. The pH of the samples first is stabilized near the base (0 meters) followed by a decrease upslope which in the case of sub-surface samples shows first a decrease and then an increase in value.

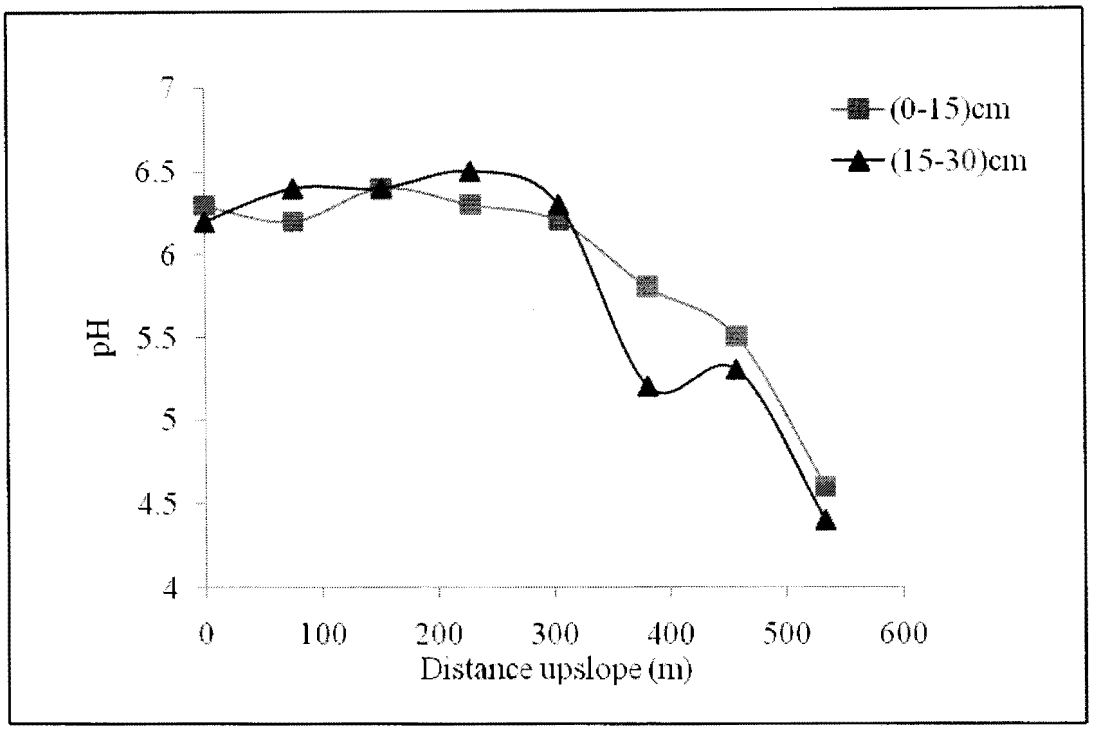

Fig. 4.4. pH values for the surface and sub-surface samples taken on transect 2 with distance measured upslope in meters.

Marked difference in the trend for pH values due to slope position is shown for cores 1, 7 and 10, which were sampled at the base, middle and upslope positions respectively, in field three (Fig.4.5.). Core 1 is marked by rectangles, core 7 is marked bytileted rectangles and core 10 is marked by triangles in Fig. 4.5. Core 7 exhibits alkaline pH after 50 cm depth interval due to a carbonate zone between (65-144) cm. The pH range for core 1 varies from being moderately acidic to slightly alkaline. This can be due to its position on the base due to which weatherd shale material has been translocated in the upper horizons of the soil profile making pH acidic. Highly acidic pH is shown by the core 10 due to high clay content and shallow contact to the C_r horizon having acidic shale parent material. Occurrence of weathered shale fragments and charcoal lenses in the soil profile could also be responsible for the acidic pH.

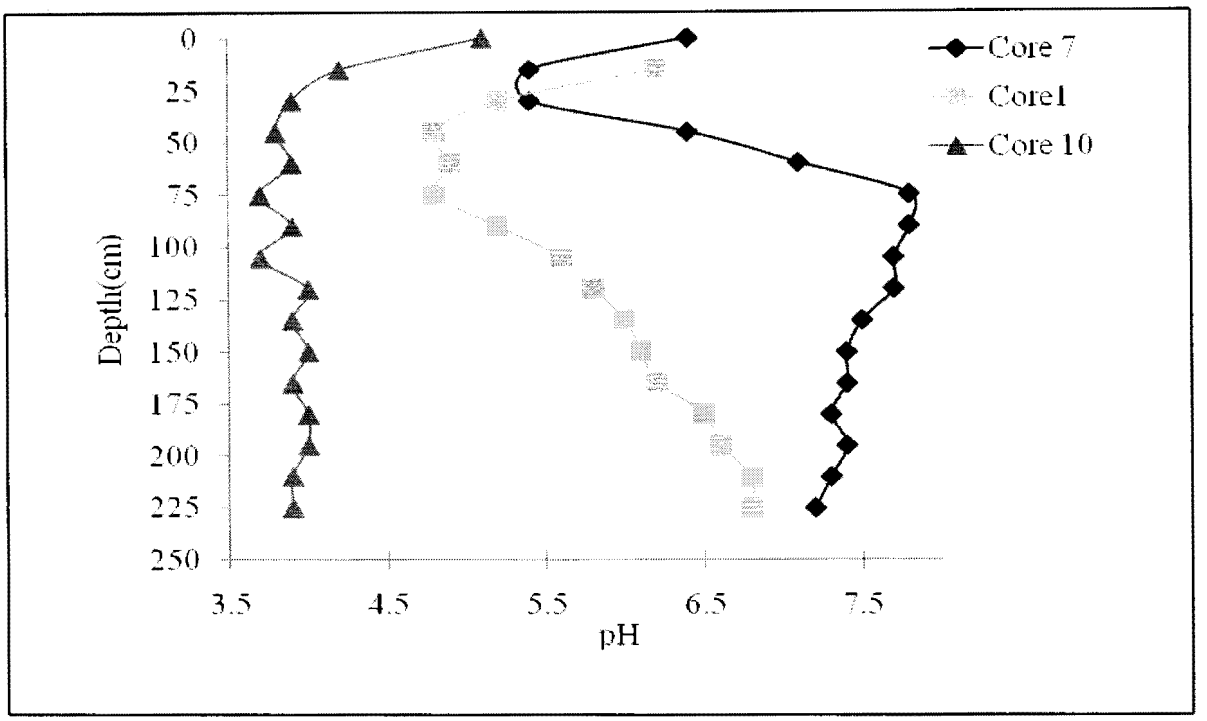

Fig.4.5. pH depth funtions for cores 1, 7 and 10.

In general, electrical conductivity observed for core soil samples is relatively low (Fig.4.6.). Core 1 is marked by rectangles, core 7 is marked by tilted rectangles and core 10 is marked by triangles. Higher electrical conductivity values for core 7 could be due to the presence of certain minerals in the profile, such as gypsum or other sulfate salts which were observed during core description. Electrical conductivity values for surface (0-15) cm and sub-surface (15-30) cm samples taken along transect 2 in field two during June, 2008 are shown in Fig. 4.7. Surface samples show more steady values near the base except for a sharp decrease near the middle of the slope and an increase in electrical conductivity for samples taken in upslope positions. Sub-surface samples, on the other hand, depict stability in electtrical conductivity for the first 3 samples and then a sinusoidal pattern of decrease and increase for the samples at upslope positions.

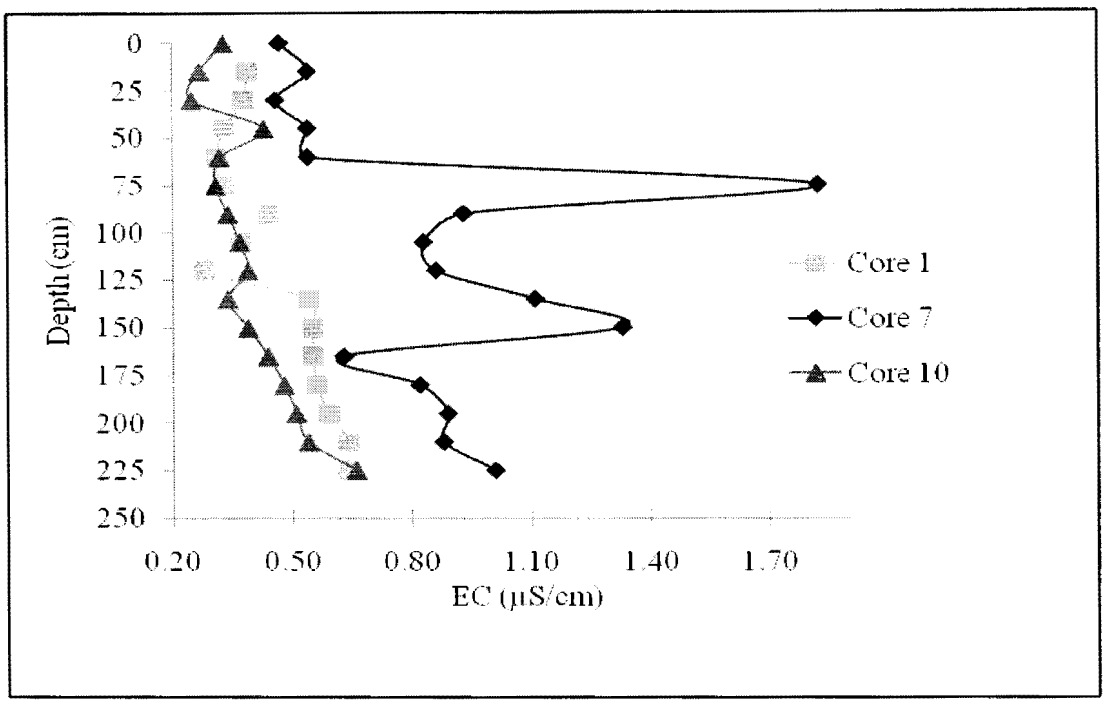

Fig. 4.6. Electrical conductivity depth functions for cores 1, 7 and 10.

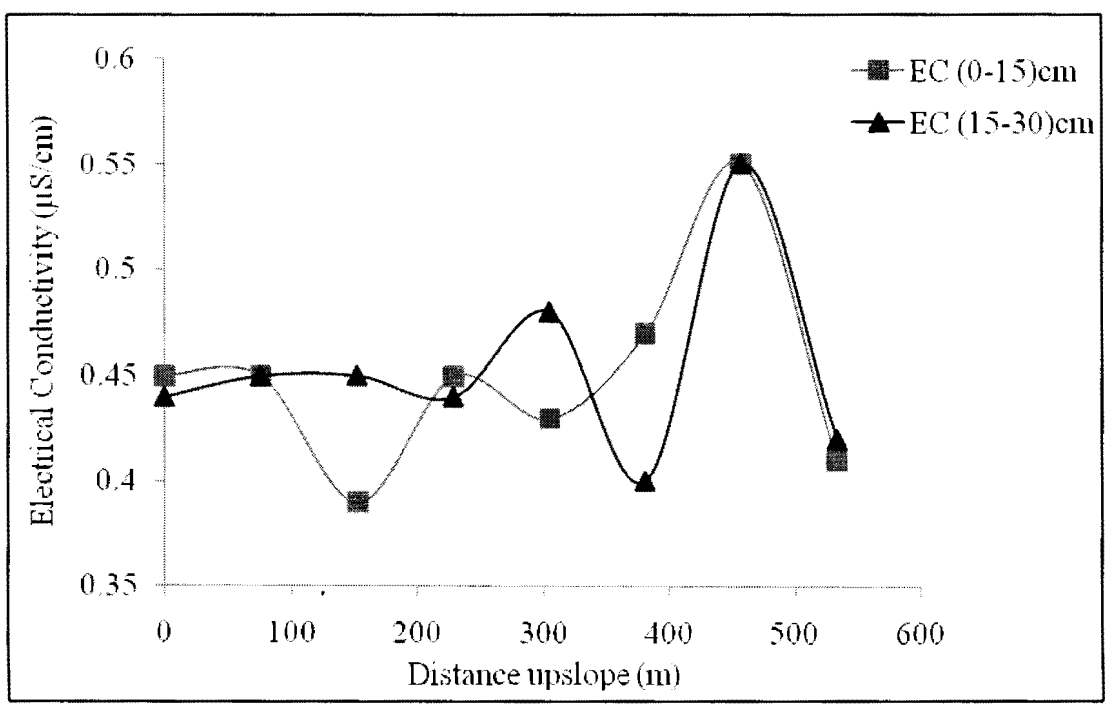

Fig.4.7. Electrical conductivity surface and sub-surface values for transect 2 in field two with distance measured upslope in meters.

4.2.3. Particle Size Analysis

The striking contrast between residual and transported soils is shown by the steady increase in clay content from the lower slope position to the west along transect 4 (Table 4.5.).

Table 4.5. Results of particle size analysis for A horizon samples (June, 2008) from cores along with their elevations taken along transect 4. Samples are arranged to show upslope gradient.

Core No.	A horizon with sampling depth	Elevation (m)	Sand%	Silt%	Clay%
1	1500N, 0W (0-24)	376.1	8.2	48.0	43.8
4	1500N, 250W (0-11)	381.6	7.4	55.8	36.8
7	1500N, 1000W (0-15)	389.2	7.0	55.4	37.6
9	1500N, 1500W (0-9)	396.5	2.8	45.7	51.5
10	1500N, 1750W (0-14)	399.0	4.8	35.2	60.0

Results of this analysis indicate that A horizon clay content obtained from cores at higher elevations is greater than from cores down the slope. Conversely, the percentage of silt particles is higher for samples near the base of the slope in comparison to the samples obtained from the cores up the slope. High silt content near the base of the slope can be attributed to the transport of silt and very fine sand fractions by slopewash as these particles are more easily entrained by flowing water than are clays (Schaetzl and Anderson, 2005).

4.2.4. Multi-Element Analysis

Tables E.1 and E.2 (Appendix E) show the results of element analysis for both surface and core samples respectively. Cadmium levels in the surface (0-15 cm) samples from three fields were found within a range of 0.65-7.43 mg/kg with an average of 1.35

mg/kg and for sub-surface (15-30 cm) samples had a range of 0.26-0.93 mg/kg and an average of 1.09 mg/kg. High concentrations of Al (an important clay mineral constitutent) was found for all the core samples with a maximum value reported for Core 2 as 3.12 mg/kg. Iron was found in widely varying amounts having a range of 0.60-27350 mg/kg. The average Cd concentration for eight cores covered in transect 4 was found to be 0.28 mg/kg. This concentration is approximately equal to the baseline value of 0.3 ppm reported by Garret (1994) for the Northern Prairies region. However, the highest concentration of Cd was found in Core 2 at a depth interval of 210-225 cm with 1.85 mg/kg. Other elements like Cu, Cr and Ni tend to predominate. Zinc levels were reported high for all the core samples (11.7 - 140.4 mg/kg).

Table E.3. (Appendix E) shows descriptive statistics reported for all the 12 cores. For correlation analysis results (Table 4.6.), among different lithologic units, shale and bedrock showed maximum significant correlations of Cd with other analytes. This could be due to the parent materials for these soils being Cretaceous shale which is a rich source of trace elements. Cadmium and Mn shared negative correlation in argillic horizon whereas the same pair had a very strong positive correlation in bedrock. This could be associated with the presence of Mn oxides in these soil horizons. Significant correlations of Cd with OM for different analytes could be due to organometallic complexes formed. Zinc and Cd shared a strong correlation in carbonate and argillic units as they have a tendency of common geochemical association.

4.2.4.1. Principal Components Analysis (PCA)

The correlation matrix obtained for samples from the shale horizons only for 8

cores taken along transect 4 in field three (a subset of the data analyzed for multielements) is given in Table 4.7. Values in bold indicate significance at $p \leq 0.05$. Beryllium showed significant correlations with Al and As. Calcium correlated negatively with As and Be. Significant correlations for Cu were obtained for all the elements except Al, Mo and Cd. Correlations of Cr with Al, As and Be were found to be positive and significant whereas with Ca and Co, they were negative but significant. Nickel showed negative significant correlations with Be, As, Cr and Cu. Highly significant ($p \leq 0.05$) negative correlation was obtained for Cu with pH. Copper showed a very significant correlation (0.89) with Cr. Molybdenum correlated significantly with Al, Be, and Cd. Zinc metal showed correlations with Al, Be, Co, Cr and Cu. Cadmium correlated significantly with As, Be and Mo in a positive manner but negatively with Co and Ni. Soil pH was found to have negative correlations with most of the elements. Majority of the elements showed significant correlations with organic matter content. Electrical conductivity correlations were found to be negative with most of the elements.

According to PCA results in Table 4.8, the first 4 principal components account for approximately 79% of the total variance in the data for the shale horizon. PC1 corresponds to 43% of data variation with an eigenvalue of 6.06. Eigenvalue of PC2 and PC3 is 2.18 and 1.69 respectively which acounts for 59% and 71% of cumulative variance. PC4 has the lowest eigenvalue of 1.14. The shale horizon exhibits strong loadings for As, Be, Cr, Cu and OM for PC1. A linear relationship between pH and Ni is shown in Table 4.7 but it correlates negatively in PC1. PC2 has a correlation with Al and Mo only, whereas Cd and Mo are heavily correlated in PC3. Only Zn correlates strongly in PC4 explaining 79% accumulative variation.

Table 4.6. Correlations of Cd with other analytes in soil horizons and lithologic units of 12 cores taken (June, 2008) from formerly cropped fields on the Pembina Escarpment in eastern Cavalier County, North Dakota. Top value: Pearson correlation coefficients; second value: Prob > |r| under H0: Rho=0. Analyte pairs with $p \leq 0.05$ are in bold. EC: Electrical Conductivity; OM: Organic Matter.

	Topsoil	Argillic	Shale/ Claystone Contact	Shale	Sand and Silt	Bedrock	Carbonate
Al	0.52234 0.0671	-0.00243 0.9872	-0.03326 0.9273	-0.02697 0.8076	-0.45209 0.1401	0.29024 0.5769	-0.79482 0.0588
As	0.44616 0.1265	0.00289 0.9848	-0.34887 0.3231	**0.22476** **0.0398**	**0.84432** **0.0006**	0.29695 0.5677	-0.53380 0.2754
Be	-0.37236 0.2102	-0.13627 0.3665	-0.32336 0.3621	-0.05466 0.6214	-0.27637 0.3845	0.19765 0.7074	-0.46877 0.3483
Ca	**-0.70712** **0.0069**	-0.05960 0.6940	0.22935 0.5239	-0.11513 0.2970	-0.05591 0.8630	**0.93263** **0.0067**	0.65245 0.1602
Co	-0.03474 0.9103	-0.02324 0.8781	-0.01428 0.9688	**-0.27621** **0.0110**	-0.40207 0.1951	0.41097 0.4183	-0.23005 0.6610
Cr	-0.48663 0.0917	-0.05368 0.7231	-0.15522 0.6685	-0.00363 0.9739	0.31109 0.3250	-0.59164 0.2161	**-0.84841** **0.0327**
Cu	-0.51459 0.0720	0.15721 0.2968	-0.22170 0.5382	0.14111 0.2004	**0.58723** **0.0447**	0.56231 0.2454	-0.68467 0.1335
Fe	0.01300 0.9664	0.06768 0.6549	-0.22250 0.5367	**0.29714** **0.0061**	-0.06416 0.8430	**0.95419** **0.0031**	**-0.88449** **0.0192**
Mn	-0.50237 0.0802	**-0.38380** **0.0085**	0.09720 0.7894	**-0.30303** **0.0051**	-0.34785 0.2679	**0.97235** **0.0011**	0.32746 0.5264
Mo	0.03232 0.9165	0.18080 0.2292	-0.26039 0.4675	0.05647 0.6099	**0.79068** **0.0022**	0.25432 0.6267	-0.54483 0.2636
Ni	-0.44271 0.1298	0.03115 0.8372	0.21408 0.5526	**-0.32009** **0.0030**	-0.31632 0.3165	0.74456 0.0895	-0.54483 0.2636
Zn	-0.33966 0.2562	**0.54407** **<.0001**	-0.08486 0.8157	-0.01583 0.8863	-0.26768 0.4003	0.44356 0.3783	-0.92077 0.0092
OM	0.33614 0.2615	**0.42438** **0.0033**	0.13459 0.7109	**0.37238** **0.0005**	0.43671 0.1558	**0.89186** **0.0169**	**-0.94494** **0.0045**
pH	-0.49324 0.1231	0.02249 0.8876	0.55652 0.0948	-0.16757 0.1324	-0.49948 0.1177	-0.99575 0.0587	**0.90687** **0.0126**
EC	**-0.78821** **0.0040**	-0.25248 0.1067	0.20024 0.5791	-0.21524 0.0521	0.46377 0.1508	**0.99760** **0.044**	0.47590 0.3400
n*	13	46	10	84	12	6	6

*n for pH and EC in: Topsoil = 11;Argillic = 42;Shale = 82;Sand and Silt = 11;Bedrock = 3

Table 4.7. Correlation table for different analytes in the shale horizons of 8 cores.

	Al	**As**	**Be**	**Ca**	**Co**	**Cr**	**Cu**	**Mo**	**Ni**	**Zn**	**Cd**	**OM**	**pH**	**EC**
Al	1.00													
As	0.06	1.00												
Be	**0.44**	**0.69**	1.00											
Ca	0.22	**-0.32**	**-0.25**	1.00										
Co	0.20	**-0.31**	-0.16	**0.34**	1.00									
Cr	**0.43**	**0.73**	**0.79**	**-0.34**	**-0.38**	1.00								
Cu	0.19	**0.81**	**0.75**	**-0.46**	**-0.43**	**0.89**	1.00							
Mo	**0.31**	-0.02	**0.43**	0.22	0.17	0.07	-0.13	1.00						
Ni	-0.06	**-0.61**	**-0.57**	**0.49**	**0.78**	**-0.69**	**-0.73**	0.02	1.00					
Zn	**0.29**	0.14	**0.33**	-0.14	**0.33**	**0.22**	**0.28**	0.01	0.11	1.00				
Cd	-0.09	**0.32**	**0.32**	-0.01	**-0.24**	0.15	0.22	**0.28**	**-0.35**	-0.02	1.00			
OM	**0.32**	**0.56**	**0.64**	-0.10	**-0.49**	**0.63**	**0.65**	**0.33**	**-0.66**	0.09	**0.36**	1.00		
pH	-0.13	**-0.78**	**-0.64**	**0.48**	**0.41**	**-0.76**	**-0.90**	**0.27**	**0.70**	-0.14	-0.07	**-0.53**	1.00	
EC	0.14	-0.20	**-0.26**	**0.37**	**0.42**	**-0.30**	**-0.35**	-0.14	**0.48**	-0.11	**-0.30**	**-0.31**	0.18	1.00

Values in bold are significant at $p \leq 0.05$

Table 4.8. Varimax rotated PC loadings for shale horizons (n=74).

	PC1	PC2	PC3	PC4
Al	0.22	**0.76**	-0.11	0.26
As	**0.82**	0.03	-0.13	0.06
Be	**0.82**	0.46	0.05	-0.07
Ca	-0.48	0.45	0.27	0.42
Co	-0.56	0.59	-0.31	-0.24
Cr	**0.90**	0.19	-0.16	0.11
Cu	**0.94**	0.00	-0.25	-0.01
Mo	0.06	**0.61**	**0.64**	-0.12
Ni	**-0.87**	0.30	-0.19	-0.12
Zn	0.18	0.48	-0.43	**-0.61**
Cd	0.35	0.02	**0.62**	-0.21
OM	**0.77**	0.21	0.31	0.18
pH	**-0.85**	0.12	0.38	-0.15
EC	-0.45	0.25	-0.37	0.56
Eigenvalue	6.06	2.18	1.69	1.14
% Variation	43	16	12	8
% AccumulativeVariation	43	59	71	79

Values in bold indicate strong loading i.e. > 0.6

The first two PC loadings for the shale horizon are plotted against each other in Fig.4.8. Horizontal axis represents values for PC 1 whereas PC 2 values are shown on the vertical axis. Correlation between OM, Cu, As, Be and Cr is significant for first two loadings. Cu, Cd and As behave similarly for PC2 (close to 0). Thus, there is no need to measure this group for further classification. Molybdenum showed very weak significance for PC loading 1. Aluminum also revealed similar information about its correlation for PC loading 2. Very strong negative correlation is shown by Ni and pH for PC1. This group does not show any significant correlation for further loadings.

For PC3 (Table 4.8.), Mo again shows a significant correlation, thus it cannot be eliminated from the data. Cadmium comes out as an outlier in the data showing significant correlation for PC3. Strong correlation of Zn in PC1 marks it a significant element for analysis. Tables 4.9. and 4.10. are constructed from a subset of topsoil multi-element data;

only those samples from the core transect are included in this analysis.

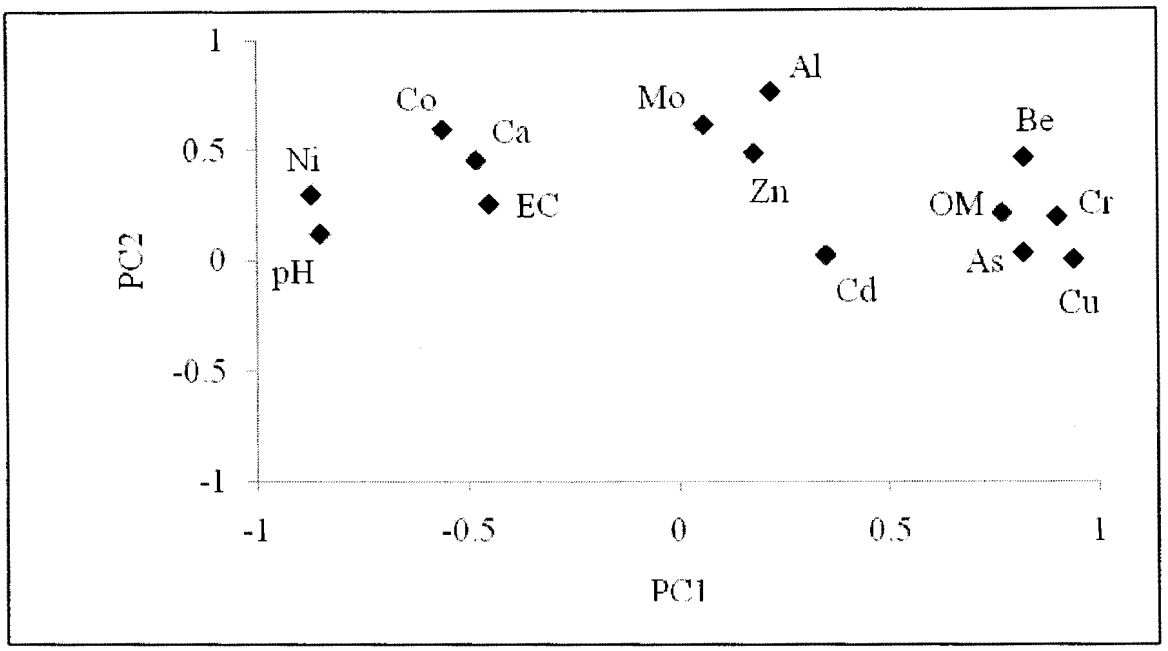

Fig.4.8. Varimax principal component loadings. PC1 vs. PC2 for shale horizons.

Cobalt showed significant correlations with Al, As and Be. Copper metal also showed significant correlations with other elements in the topsoil samples. Negative correlations were shown by Cd with majority of elements. Arsenic had significant correlations with Be, Co and Cu. Both Ni and Zn correlated significantly with (0.71) with Ca. No significant correlations were shown by pH in the topsoil samples. Highly negative correlation (-0.84) was observed between EC and Cd. Elevation also played a vital role in showing significant correlations with elements like Al, As, Be, Co and Cu.

In the top horizon samples (Table 4.10.), the four PC loadings correspond to90 % variation. All elements except Mo and Ni are strongly loaded in PC1corresponding to 47% accumulative variation for the data. Soil properties like OM, EC and pH do not correlate

Table 4.9. Correlation table for different analytes (plus elevation) in topsoils of 8 cores.

	Al	**As**	**Be**	**Ca**	**Co**	**Cr**	**Cu**	**Mo**	**Ni**	**Zn**	**Cd**	**OM**	**pH**	**EC**	**EL**
Al	1.00														
As	**0.87**	1.00													
Be	**0.87**	**0.96**	1.00												
Ca	0.52	0.36	0.25	1.00											
Co	**0.74**	**0.82**	**0.77**	0.28	1.00										
Cr	**0.66**	0.65	0.52	0.65	0.51	1.00									
Cu	**0.90**	**0.92**	**0.84**	0.55	**0.76**	**0.87**	1.00								
Mo	0.24	0.31	0.50	-0.09	0.11	0.17	0.23	1.00							
Ni	0.11	0.05	-0.13	**0.71**	0.32	0.46	0.23	-0.42	1.00						
Zn	0.45	0.47	0.30	**0.71**	0.53	0.48	0.50	-0.44	**0.74**	1.00					
Cd	-0.41	-0.33	-0.16	**-0.81**	-0.11	**-0.69**	-0.57	0.17	-0.48	-0.47	1.00				
OM	0.47	0.09	0.14	**0.66**	0.02	0.41	0.32	0.04	0.26	0.31	-0.42	1.00			
pH	0.33	0.45	0.38	0.38	0.36	0.34	0.48	0.20	0.14	0.08	-0.62	-0.11	1.00		
EC	0.29	0.13	0.04	**0.75**	0.03	0.44	0.37	-0.18	0.41	0.39	**-0.84**	0.63	0.53	1.00	
EL*	**0.85**	**0.88**	**0.94**	0.06	**0.78**	0.35	**0.74**	0.30	-0.24	0.25	0.00	0.09	0.24	-0.07	1.00

EL*= Elevation

Values in bold are significant at $p \leq 0.05$.

Table 4.10. Varimax rotated PC loadings for topsoils (n=9).

	PC1	PC2	PC3	PC4
Al	**0.91**	0.26	0.00	0.23
As	**0.88**	0.43	0.08	-0.10
Be	**0.80**	0.58	-0.03	0.05
Ca	**0.72**	**-0.61**	-0.07	0.12
Co	**0.76**	0.35	0.40	-0.17
Cr	**0.83**	-0.16	-0.08	0.05
Cu	**0.96**	0.16	-0.03	-0.02
Mo	0.15	0.57	-0.57	0.16
Ni	0.39	**-0.69**	0.43	-0.14
Zn	**0.64**	-0.41	0.58	0.01
Cd	**-0.65**	**0.60**	0.33	0.20
OM	0.43	-0.42	-0.21	**0.74**
pH	0.52	-0.05	-0.46	**-0.68**
EC	0.51	**-0.67**	-0.40	-0.02
EL*	**0.68**	**0.66**	0.12	0.09
Eigenvalue	7.12	3.54	1.57	1.21
% Variation	47	24	10	8
% Accumulative Variation	47	71	82	90

*EL = elevation

Values in bold indicate strong loading i.e. > 0.6

significantly in PC1. Elevation is strongly loaded in PC1. PC2 shows EC, Ca and Ni as negatively correlated with Cd .No significant correlations were observed in PC3. Organic matter is correlated positively and pH negatively in PC4.

The first two PC loadings for different analytes in topsoils are shown in Fig. 4.9. As expected, topsoil shows significant correlations among groups of elements for the first loading. Aluminum, As, Be, Ca, Co, Cr, Zn and Cu show heavy loadings in PC1 and thus form a group. However, Cd, Ca and elevation appear as correlated significantly in PC2 as well. Thus, this group has to be retained for further interpretation. Nickel also shows significance for PC loading 2. Molybdenum can be excluded from further interpretation as it fails to show any correlation for the four loadings and appear as an outlier in the data.

Organic matter, which plays an important role in holding trace elements, cannot be ignored as it shows significance for PC4. pH, which fails to show significance in the first two PC loadings cannot be neglected as it has a strong loading for PC4 (-0.68). This also fits with the well known variation of elements with the soil chemical properties. It looks as if OM,

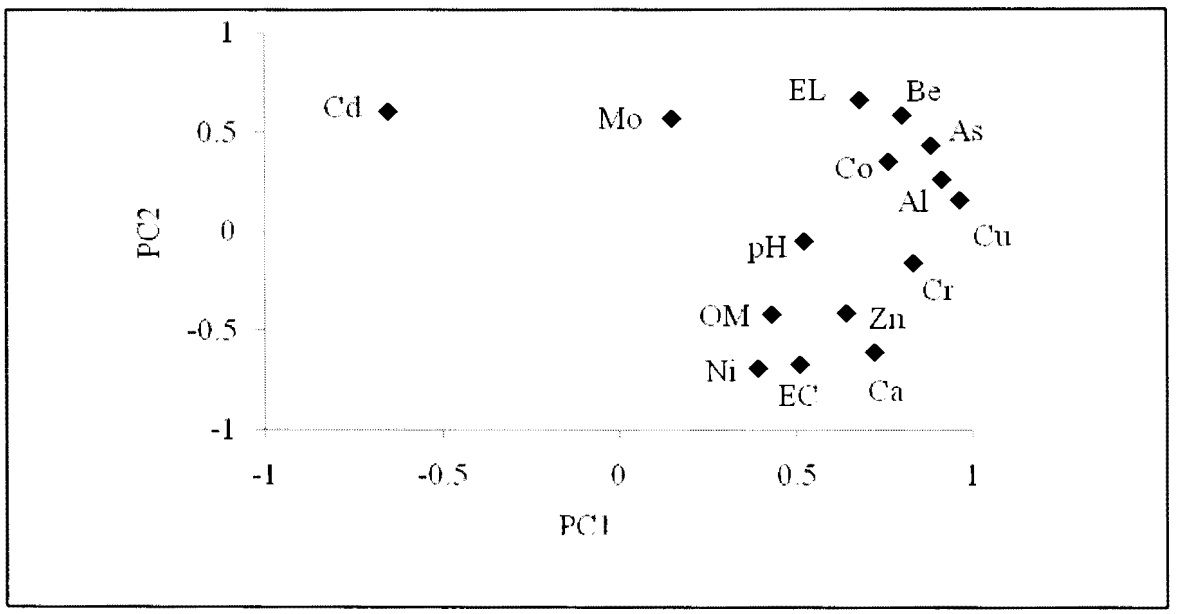

Fig. 4.9. Varimax principal component loadings. PC1 vs. PC2 for topsoils.

Ni, Zn, Ca and EC form a separate group. pH seems to have some correlation with this group as it lies in the vicinity of this group. Thus, by looking at the figure, OM appears to be the key factor holding the elements in the topsoils and thus responsible for showing significance for the first two loadings.

CHAPTER 5. DISCUSSION

5.1. Cores as a Guide to Soil Parent Material

The soil parent materials for Pembina Escarpment are Cretaceous shale and glacial till which itself contains remobilized shale material. The Escarpment soils of the backslope and shoulder landscape settings are shallow soils having a shale horizon high in the profile, at a depth averaging 70 cm. These soils are thus enriched with clay, as is also shown in Tables 4.1. and 4.5.

Key observations of the cores point to the process of slopewash as having been significant in the formation of these soils. First, soils of the footslope landscape were found to be rich in organic matter (0-15 cm) and silt content. These soils were porous and well structured deep soils. In addition, fine grained material over the ped faces in the lower soil profile indicates slopewash over shale regolith for these soils.

Highly oxidized zones in the soil profile occur due to leaching and translocation of minerals from the upper horizons to the lower by the vertical and lateral water flow in the soils. Presence of charcoal lenses, fungal hyphae and thick roots indicate high organic matter content in these soils which supports the fact that these soils have their origin from organic rich shale and that these parent materials were modified by pre-existing forests in this area. Volcanic ash layers found in the lower soil horizons indicate occurrence of bentonitic layers in Pierre Formation shale of this region.

The colluvial/alluvial nature of soils is also morphologically supported by the occurrence of stratifications in shale. Fine (1-2 cm) shale fragments in B and C horizons indicate residual shale. The general textural class of the escarpment soils ranged from silty clay loam to silty clay supports the formation of these fine textured soils from shale.

Occurrence of thick E horizons over B_t horizons for some cores might be due to enhanced eluviation (gain in E horizon thickness) and degradation of the B_t. Iron and Mn concretions due to redox conditions occurring in E with degraded B_t support this fact. The dominant secondary minerals observed in this study, e.g. ferric-oxyhydroxides, sulfur-bearing minerals like jarosite, clay minerals, gypsum and quartz, are consistent with fine textured shale and shale regolith as the parent material for these escarpment soils.

5.2. Grain Size and Mineralogy

The development of Pembina Escarpment soils from shale and till parent material led to the formation of fine textured silt and clay particle size fractions in the soils. Soil samples collected from the preliminary study in the cropped and CRP fields as well as from the three fields were found to have very high silt and clay content.

In general, the sand and silt fractions are composed of primary minerals, while the clay size fractions (<0.002 mm) are composed of phyllosilicate minerals (secondary clay minerals) along with some primary minerals like quartz (Schaetzl and Anderson, 2005). These fine-grained fractions (clays) are the ones that have higher capacity to accumulate trace elements (Miller and Gardiner, 2000; Schaetzl and Anderson, 2005; Klassen, 2009). Soil samples from the 2007 samples rich in clay content (>55%) were also found to have high concentrations of cadmium (Table 5.1.) See Tables B.1 in Appendix B and 4.3. for details.

Mineralogical profiles (Appendix C) for samples obtained from the cropped and CRP fields confirm the presence of a variety of clay mineral fractions. These include secondary mineral groups like illite, kaolinite and smectite groups found in majority of the

samples with chlorite group found as a minor constituent of the clay mineral fraction. Research by Schultz *et al.* (1980) in Northern Great Plains confirms mixed-layer clay mineralogy in the Pierre Shale and its equivalent rocks with illite and smectite groups as major and kaolinite and chlorite as minor clay mineral groups. Mixed layer clay minerals are dominant in the soils from North Dakota with smectite occupying the glacial deposits (Klassen 2009).

Table 5.1. Higher Cd concentration (mg/kg) in samples (October, 2007) rich in clay content.

Sample No.	Clay%	Cd (mg/kg)
2	64.0	6.6
4	55.2	8.1
7	56.0	3.0
10	55.5	3.3
17	56.0	9.5
20	64.1	11.6
21	70.7	12.4
22	57.2	16.4
24	66.5	6.9

High trace element content of the escarpment soils could be due to enriched clay content in these soils. Smectite due to its shrink and swell property can act as a host to trace elements. Cobalt in clay minerals is found in association with smectite (Sposito, 1989; Cornu *et al.*, 2009). Correlation between Al and Fe has been linked with clay minerals like smectite, chlorite and illite (Baize, 1997; Sterckeman *et al.*, 2006; Cornu *et al.*, 2009). Occurrence of ash layers in the soil profile of the escarpment soils support the smectite group clay mineralogy as these ash layers are thought to be equivalent to bentonite clay mineral (Schultz *et al.*, 1980). Trace element concentrations have been found in bentonite samples from Pierre shale by Schultz *et al.* (1980). Chlorite was also identified as one of

the clay mineral fractions in one of the samples. It belongs to (2:1) layer silicate chlorite and hydroxyl-interlayered clays group that is rich in Mg and Fe ions making cation exchange feasible in clays (Moore and Reynolds, 1989; Schaetzl and Anderson, 2005). Illite, another mineral identified in the clay samples is generally found in the soils formed from partial weathering (Schaetzl and Anderson, 2005). It could have been formed from the bedded shale that has not been altered by weathering.

Thus, clay minerals because of their large surface area and low porosity play a significant role in adsorption of trace elements in soil.

5.3. Soil Characterization

Soil properties like OM, pH, and EC are some of the key properties controlling the chemical composition of soil. Soil chemical properties are largely dependent on the colloids found in soil e.g. organic matter and clay minerals and thus, the chemical interactions are more determined by surface properties of these colloids (Miller and Gardiner, 2000).

Organic matter accumulation takes place in the surface layers of the upper soil horizon (A). Organic matter retains trace elements in the soil as it forms organometallic complexes with metals. Results of OM content revealed that surface layer (0-15 cm) contents of organic matter (avg. 8.2%) were higher as compared to the (15-30 cm) subsurface layer (avg. 5.2%) content of organic matter for all the samples from June, 2008 including cores. Cadmium concentration for surface samples was found to be higher (avg.1.24 mg/kg) as compared to the subsurface Cd levels (1.0 mg/kg) indicating affinity of Cd with OM. Results of PCA for topsoils (cores; Table 4.10.) show strong loading (0.74)

of OM in PC4. High Cd levels related to humus content in soils were found in Swedish topsoils (Andersson, 1977; Adriano, 1986). Results by Schultz *et al.* (1980) suggest association of Mo, Se, As and likely Cd and uranium (U) with marine OM signifying trace element enrichment of Pierre shale.

The pH of the soil reflects the acidity or basicity of the soil, and thus affects the mobility of elements within the soil profile. Acidic pH generally increases the mobility of the elements within the soil (Alloway, 1990; Miller and Gardiner, 2000). Most of the soil samples found from the Pembina escarpment have low pH values i.e. these soils are acidic in nature due to their genesis from acidic shale parent material. This is in accordance with high metal concentrations recorded for metals like Zn, Ni, Mn, Cd and Cu for these samples (See Appendix Tables E.1. and E.2.). Mean pH of the Pierre shale has been reported as 6.6 with its variation between two groups having pH ranges between 2-5 and 7-9 (Schultz *et al.*, 1980). Franzen *et al.* (2006) gave a pH range of 5.3 to 8.5 for soils found in the state of North Dakota. Weathering, prominently of pyrite minerals caused otherwise alkaline unweathered shale near the surface to result in acidic soils (Schultz *et al.*, 1980). Soil pH plays a significant role in adsorption of cations by controlling pH dependent H^+ sites in organic matter, clays and oxyhydroxides (Alloway *et al.*, 1985; Alloway, 1990; Miller and Gardiner, 2000). Exchange of H^+ ions at these sites with the cations of elements in the soil can have a marked effect in increasing element concentration (Miller and Gardiner, 2000). Strong principal component loadings for pH found in both shale horizon (-0.85) and topsoils (-0.68) in PCA also provide an evidence between correlation of elements and pH. A general trend of increase in pH with depth was observed for cores (Table 5.2).

Table 5.2. pH variation with depth in cores.

Core No.	Avg. pH (0-120 cm)	Avg. pH (120-225 cm)
1	5.2	6.4
2	3.9	3.4
3	4.1	3.6
4	4.9	5.1
5	5.2	5.8
6*	5.5	6.4
7	6.6	7.4
8	4.4	3.5
9	4.1	3.8
10	4.0	4.0
11	4.0	3.6
12	4.1	3.7

*core depth up to 350 cm.

Electrical conductivity of the soil quantifies the amount of charged ions that act as solutes in the aqueous soil solution. Low EC values reported for the Escarpment soils can be attributed to the presence of less soluble minerals like calcite found in these soils. However, some of the core samples (core 7) obtained at higher depths have high EC values. This can be attributed to subsurface accumulations of gypsum and other soluble sulfide minerals (pyrite) at these depths. Strong Correlation (-0.79) and PCA loading (-0.67) obtained for topsoils indicate EC as an important factor in element availability and mobility in the soil.

5.4. Multi-Element Distribution in Soils

For soil profiles, all surface samples were found to have high concentrations of elements like As, Cd, Cu and Zn. Occurrence of elements like Zn, Mn and Ni in high concentrations is consistent with formation of these soils from shale-like parent materials that are natural hosts to these elements (Schultz *et al.*, 1980; Alloway, 1990; Garrett, 2000).

High Fe and Al concentrations for these soils could be because of phyllosilicate and plagioclase minerals in Pierre shale (Schultz *et al.*, 1980; White, 1994; Horckmans *et al.*, 2005).

Elevated Cd observed in core samples in a zone between 60-75 cm suggests an association with clay that is a result of translocation within the soil profile. A sudden increase in concentration of Ni, Zn, Co, Cu and Mo is noticed in the majority of cores below 45 cm depth. Fine grain fractions at these depths could be resulting in high levels of trace elements (Cornelis *et al.*, 1993; Horckmans *et al.*, 2005). High levels of Cd were reported in North Dakota soils obtained from depressions which could be due to accumulation of organic matter at these landscape settings (Franzen *et al.*, 2006). Also, mobility of these elements within the soil profile and then an increase in pH (with depth as previously mentioned in table 5.2) causing their precipitation can lead to soil enrichment (Horckmans *et al.*, 2005). Weathering of the Escarpment during the early glacial periods causing loss of Cd^{2+} and SO_4^{2-} associated with pyrite in shales and then genesis of soils from these modified parent materials could be responsible for the incorporation of Cd in the Escarpment soils.

Cadmium and Zn, being geochemically correlated (Adraino, 1986; Alloway, 1990) behave similarly in these soils. Correlation results for Cd, Ni and Zn indicate its significance to OM, Mn and Fe hydroxides and clay content having abundant sites of cation exchange. Cadmium is more mobile in soils with such chemical properties (Schultz *et al.*, 1980; Adriano, 1986; Alloway, 1990). Adsorption on clay minerals and precipitation with sulfides and carbonates increase Zn and Cd concentration in mineralized zones, i.e., B horizons (Alloway, 1990). Strong correlation with pH favors increased Ni levels in soils

having alkaline pH (Alloway, 1990). Chromium and Cu showed great correlations with majority of elements in the shale horizon. These elements have a tendency to be associated with insoluble hydroxides and oxides which in our case of soils are Fe and Mn. Strong correlation with pH indicate their vulnerability with different oxidation states. Chromium can be found as one of the cations in clay minerals. Smectite group mineral (montmorillonite) has been reported to adsorb high amounts of Cr in the form of Cr^{2+} while Cu also behaves in a similar fashion (Griffin, 1977). Aluminum and Be belong to the same group of periodic table and share a common chemistry. Both are highly correlated with OM, Zn, Mo and Cr. Chemistry of Mo is related to colloids like organic matter surfaces and mineral surfaces as depicted by the correlation analysis (Wichard *et al.*, 2009). Trace elements Co, Ni, Zn, Cd, Cr, Cu, Mo, As have been reported to have their association with organic matter and sulfur (pyrite) in Pierre shales (Schultz *et al.*, 1980). Cobalt, Ni and Zn show great correlation with clay minerals (Schultz *et al.*, 1980) which is evident from strong correlation results (Table 4.6.).

Spatial variations for Cadmium, observed as mean surface (0-15 cm) Cd level for two transect lines 1500N and 1600N was 1.3 mg/kg whereas surface Cadmium level from 8 cores along transect 4 was 0.28 mg/kg. Spatial variations due to landscape positions and OM were reported for Cd, Cu and Zn in soils from North Dakota (Franzen *et al.*, 2006). Table 5.3. provides a summary of results for Cd among various types of fields sampled for this study. Cadmium levels from October, 2007 (CRP and agricultural fields) were very high. The three fields from June, 2008 sampling did not have similar elevated concentrations (avg. 1.35 mg/kg) yet, but a maximum of 7.43 mg/kg was obtained for one sample.

Table.5.3. Summary of Cd concentration (mg/kg) for A horizons (0-15) cm.

	Agr. field	**CRP field**	**NDWMA fields**	**Cores**
Min	4.11	4.48	0.65	0.12
Max.	8.24	10.59	7.43	1.05
Average	5.83	7.98	1.35	0.64

Thus, the overall criteria for enhanced element concentrations in the Escarpment soils can be attributed to adsorption by clay minerals and soil organic matter controlled by the effects of pH, EC and elevation gradient.

CHAPTER 6. CONCLUSIONS

Trace element distribution and characterization for the soils of the Pembina Escarpment have been reported in this study. In order to determine the distribution of the trace elements, multi-element analysis was performed on nitric acid digested soil samples using ICP-OES. Soil characterization data included pH, EC, particle size distribution, clay mineralogy and organic matter content for the soil samples.

Results of particle size distribution revealed that the soil samples are fine textured and are rich in clay and silt. The textural range of the soils was between silty clay loam–silty clay. X-Ray Diffraction patterns for clay minerals showed smectite and illite group minerals to be present in majority of the samples. Other minerals included kaolinite, chlorite, quartz and calcite.

The OM levels reported for surface samples in this study were within a range of 2.62-13.30 % with a standard deviation of 2.24. Surface samples were found to have high OM as compared to sub-surface samples. The highest pH reported for the soil samples was 7.8 and the lowest was 3.2. The pH ranged from soils classified as ultra acidic to slightly alkaline in nature. For the core samples, pH was found to be steady near the baseline whereas near the slope, it showed a spike. Electrical conductivity of the soil samples had a range between 0.2- 4.01 (μS/cm) with maximum samples having low EC values. Surface samples showed steady EC values near the base, a sudden spike in the middle and increased values near the slope. Sub-surface samples on the other hand had steady values along the transect except near the slope.

Results of multi-element analysis suggested average Cd concentration as 0.28 mg/kg for 8 cores taken along transect 4 analyzed in this study. Maximum concentrations

(mg/kg) of Zn (140.43), Ni (84.23) and Cu (73.74) were also found to be high in the core samples. The highest Cd concentration found in the agricultural and CRP field was 16.4 mg/kg. Surface samples from Wildlife Area fields range from 0.3 mg/kg to 7.0 mg/kg. Pearson Correlation Coefficient analysis done for these trace elements and other soil characters indicate a strong correlation between Cd, OM and soil horizons like shale, argillic, and topsoils. PCA highlighted pH, clay content, elevation, and soil organic matter as vital components responsible for trace metal concentrations in the Escarpment soils.

Based on the results from the current study, questions can be raised about the transport of metals as a result of soil formation, and the existence of zones with anomalously high Cd. Future studies should examine whether, in the cropped field, sub-surface samples with elevated Cd concentrations indicate sorption on illuvial clays at depth, or the loss of organic matter. The latter may be due to agricultural erosion that has removed the most common reservoir of Cd (the organic fraction in the A horizon).

For the Wildlife Area fields, soils near the forested areas can be critical in terms of trace element concentrations. Also, regions that mark the base of the escarpment can have high levels of metals due to transport and accumulation of material from upslope landscape settings. All the samples (surface and core) analyzed for this study had an elevation range between 361.12- 401.42 m. A critical elevation zone between (371- 376 m) was reported for the CRP field having elevated Cd levels.

Thus, it can be summarized that regions towards the south of the escarpment falling within the same elevation range can be assumed to have high trace element concentrations that can provide a guide for future studies.

REFERENCES CITED

Adriano, D.C. (1986). Trace elements in terrestrial environments: biogeochemistry, bioavailability and Risks of Metals.2nd ed. Springer-Verlag, New York.

Alloway, B.J., Tills, A.R., Morgan, H. (1985). The speciation and availability of cadmium and lead in polluted soils. In : Hemphill, D.D. (Hrsg). (Ed.). *Trace Substances in Environmental Health.* **(18)**:187-201.

Alloway, B.J. (1990). Heavy Metals in Soils.2nd ed., Blackey Academic and Professional. Chapman and Hall.

Alloway, B.J., Jackson, A., Morgan, H. (1990). The accumulation of cadmium by vegetables grown on soils contaminated from a variety of sources. *Trace Substances in Environmental Health.* **(18):**187-201.

Alloway, B.J. (2000). Bioavailability of elements in soil. In: Selinus, O., Centeno, J.A., Finkelman, R.B., Fuge, R., Lindh, U., Smedley, P. (Eds.), Essentials of Medical Geology. Impacts of the Natural Environment on Public Health. Elsevier's Academic Press. New York.

Alloway, B.J., Tills, A.R. and Morgan, H. (1985). The Speciation and availability of cadmium and lead in polluted soils. *Trace Substances in Environmental Health.* **(18):**187-201.

Almås Å., Singh B.R. (2001). Partitioning and reaction kinetics of Cd-109 and Zn-65 in an alum shale soil as influenced by organic matter at different temperatures. In: I.K. Iskandar and M.B. Kirkham, (eds). Trace Elements in Soil. Lewis Publishers, Boca Raton.

Andersson, A. (1977). Heavy metals in Swedish soils: on their retention, distribution and amounts. *Swedish J. Agric. Res.* **(7):** 7-20.

APFO. (2007). Aerial Photography Field Office. United States Department of Agriculture. Farm Service Agency.
http://www.fsa.usda.gov/FSA/apfoapp?area (accessed October, 2007).

Armands, G. (1972). Geochemical studies of uranium and vanadium in a Swedish alum shale. Stockholm Contrib. Geol. **(27)**:1–148.

Arndt, B.M. (1975). Geology of Cavalier and Pembina Counties. County Groundwater Studies Part 1. North Dakota Geological Survey, Bismarck.

Arthur, M.A., Schlanger, S.O., Jenkyns, H.C. (1987). The Cenomanian–Turonian oceanic anoxic event, II. Palaeoceanographic controls on organic-matter production and

preservation. In:Brooks, J., Fleet, A.J. (Eds.), *Marine Petroleum Source Rocks,Geol. Soc. Spec. Publ.* **(26):** 401–420.

Atkinson, W.J. (1967). Regional Geochemical Studies in County Limerick, Ireland with particular reference to Selenium and Molybdenum. Ph. D. Thesis, University of London.

Baize, D. (1977). *Teneurs totales en élèments traces metalliquès dans les sols.* I.N.R.A. (ed.). Paris, France.

Bluemle, J.P. (2000).The Face of North Dakota. 3rd (ed). North Dakota Geological Survey.

Brumsack, H.-J. (1980). Geochemistry of Cretaceous black shales from the Atlantic Ocean (DSDP Legs 11, 14, 36, 39 and 41) *Chem. Geol.* **(31):**1-25.

Brumsack, H.J., Lipinski, M. and Warning B.(2003). Trace metal signatures of Jurassic/Cretaceous black shales from the Norwegian shelf and the Barents Sea. *Palaeogeogr. Palaeoclimatol. Palaeoecol.***(190):** 459-475.

Brumsack, H-J. (2006). The trace metal content of recent organic carbon-rich sediments: Implications for Cretaceous black shale formation. *Palaeogeogr.Palaeoclimatol. Palaeoecol.***(232)**: 344-361.

Burau, R.G., Kalita, K.Y., Inouye, T.S., Miller, M. (1973). Chemical Analysis of Soil samples from the Salinis Valley, California for cadmium, Zinc and Phosphate. Report to State Water Resources Control Board. University of California, Davis.

Cheng, C.H., Jien, S.H., Tsai, H., Chang, Y.H., Chen, Y.C., Hseu, Z. Y. (2009). Geochemical Element Differentiation in serpentine Soils From the Oophilitic Complexes, Eastern Taiwan. *Soil Science.* 174 **(5)**:283-291.

Ciesacutelinacuteski, G., Van Rees, K. C. J., Huang, P. M., Kozak, L. M.,. Rostad, H. P. W., Knott, D. R. (1996). Cadmium uptake and bioaccumulation in selected cultivars of durum wheat and flax as affected by soil type. *Journal of Plant and Soil.* 182**(1):**115-124.

CODEX STAN. (2009). Codex General Standard for Contaminants and Toxins in Food. (193-1995, Rev. 5).

Cornelis, C., Geuzens, P., Corthouts, V., Van Den Broeck, H., (1993).Achtergrondgehalten van een aantal anorganische en organische verontreinigingen in Vlaamse bodems, Voorstel voor referentiewaarden. Deelrapport 3 MIE/DI/9327, VITO, Mol, Belgium.

Cornu, S., Chevalier, M., Hardy, M., Bourennane, H., Josière, O., Pernes, M., Jolivet, C., Boulonne, L., Arrouays, D. (2009). X-Ray Diffraction Determination of Minerals

carrying Trace Elements in Soil: Application to the French Soil Quality Monitoring Network. *Communications in Soil Science and Plant Analysis.* **(40)**: 1138-1147.

Coveney Jr., R.M. and Glascock, M.D. (1989). A review of the origins of metal-rich Pennsylvanian black shales, central U.S.A., with an inferred role for basinal brines. *Appl. Geochem.* **(4)**:347–367.

Duffy, S.J., Hay, G.W., Micklethwaite, R.K. and Van Loon, G.W. (1988). A method for determining metal species in soil pore water. *Science of Total Environment.* **(76)**:203-215.

Fang, W., Hu, R., Wu, P. (2002). Influence of Black Shale on Soils and Edible Plants in The Ankang Area, Shaanxi Province, P.R. of China. *Environmental Geochemistry and Health.* **(24)**:35-46.

Fletcher, W.K. (1968). Geochemical Reconnaissance in Relation to Copper Deficiency in Livestock in the Southern Pennines and Devon. Ph.D thesis, University of London.

Franzen, D.W., Nanna, T., Norvell, W.A. (2006). A Survey of Soil Attributes in North Dakota by Landscape Position. *Agronomy Journal.* 98**(4)**:1015-1022.

Garcı´a, J. H., W. W. Li, R. Arimoto, R. Okrasinski, J. Greenlee, J. Walton. (2004). Characterization and implication of potential fugitive dust sources in the Pasodel Norte region. *Sci. Total Environ.* **(325)**:95Y112.

Garcia-Miragaya, J. and Page, A. (1978). Sorption of trace quantities of cadmium by soils with different chemical and mineralogical composition. *Water, Air and Soil Pollution.* **(9)**:289-299.

Garrett, R.G. (1994). The distribution of cadmium in A horizon soils in the prairies of Canada and adjoining United States. Geological Survey of Canada. (B):73-82

Garrett, R.G. (2000). Natural Distribution and Abundance of Elements. In: Selinus, O., Centeno, J.A., Finkelman, R.B., Fuge, R., Lindh, U., Smedley, P. (Eds.), Essentials of Medical Geology. Impacts of the Natural Environment on Public Health. Elsevier's Academic Press. New York.

Gee, G.W. and J.W. Bauder. (1986). Particle-size Analysis. In: Klute, Arnold. (Eds.). Methods of Soil Analysis Part1, Physical and Mineral Methods Second Edition. American Society of Agronomy- Soil Science Society of America. Madison, WI.

Gerritse, R.G. and Van Driel, W. (1984). The relationship between adsorption of trace elements, organic matter, and pH in temperate soils. *J. Environ.Qual.* 13**(2)**: 197-204.

Gill, J. and Cobban, W.A. (1965). Stratigraphy of the Pierre Shale, Valley City and

Pembina Mountain areas North Dakota. USGS Prof. Paper #A392: 20.United States Government Printing Office, Washington D.C.

Gill, J. and Cobban, W.A. (1973). Stratigraphy and Geologic History of the Montana group and Equivalent Rocks, Montana, Wyoming and South Dakota. USGS Prof. Paper #776.

Griffin, R.A., Au, A.K. and Frost, R.R. (1977). Effect of pH on adsorption of chromium from landfill leachate by clay minerals. *Journal of Environmnental Sci. and Health, PartA.* **(12):** 431-449.

Grum, E.E. (1990). Cadmium toxicity, case studies in environmental medicine. U.S. Department of Health and Human Service. Agency for Toxic Substances and Disease Registry.

Holmgren, G.G., Meyer, M.W., Chaney, R.L. and Daniels, R.B. (1993). Cadmium, lead, zinc, copper, and nickel in agricultural soils of the United State of America. *J Environ Qual.* **(22):** 335-348.

Hopkins, D.G., Norvell, W.A. and Wu, J. (1999). Formation and distribution of trace-element-enriched soils near the Pembina Escarpment, Cavalier County, North Dakota. Proc. 91st ND Acad. Sci., Grand Forks, ND.

Horckmans, L., Swennen, R., Deckers, J., Maquil, R. (2005). Local background concentrations of trace elements in soils: a case study in the Grand Duchy of Luxembourg. *Catena.* **(59):** 279-304.

Huerta-Diaz, M.A. and Morse, J.W. (1992). Pyritization of trace metals in anoxic marine sediments. *Geochim. Cosmochim.Acta* **(56):** 2681-2702.

Huff, J., Lunn, R.M., Waalkes, M.P, Tomatis, L. and Infante, P.F. (2007). Cadmium-induced cancers in animals and in humans. *International Journal of Occupational and Environmental Health.* **(13):** 202-212.

Jansson, G. (2002). Cadmium in arable crops, the influence of soil factors and liming. Ph.D. Thesis. Department of Soil Sciences, Swedish University of Agricultural Sciences, Uppsala.

Jenny, H. (1941). Factors of soil formation. Mc-Graw Hill. New York.

Kabata- Pendias, A. (2001). Trace elements in soils and plants, 2nd ed., CRC Press. Boca Raton, Florida.

Kim, J.H. (1989). Geochemistry and genesis of the Guryongsan (Ogcheon) uraniferous black slates. *J. Korean Inst. Min. Geol.* **(22):**35–63.

Kim, K.W., Thornton, I. (1993). Influence of Ordovician Uraniferous black shales on the trace element composition of soils and food crops, Korea. *Applied Geochemistry.* 8(**2**):249-255.

Kingston, H.M. (1997) .Microwave assisted acid digestion of sediments, sludges, soils and oils. In : SW 846 Test Methods for Evaluating Solid Waste, Physical/Chemical Methods (2nd eds.); U.S. Environmental Protection Agency, Washington, D.C.

Kirkham, M.B. (2006). Cadmium in plants on polluted soils: Effects of soil factors hyperaccumulation, and amendments. *Geoderma.* **(137)**:19-32.

Kjellstrom, T. (1986) Itai-Itai disease. In, L. Frieberg, C.G. Elinder, T. Kjellstrom, and J.O. Nriagu (Eds.). Cadmium and health: a toxicological and epidemiological appraisal.II. Effects and response. (p. 257-290). CRC Press, Inc. Boca Raton, Florida.

Klassen, R.A. (2009). Geological controls on soil parent material geochemistry along a northern Manitoba-North Dakota transect. *Applied Geochemistry.* 24(**8**):1382-1393.

Krauskopf, K.B. (1979). Introduction to geochemistry. 2nd edition. McGraw Hill Book Co. NewYork.

Lavergren, U., Falk, H., Bergbäck, B. (2006). Metal mobility in alum shale from Öland, Sweden. *Journal of Geochemical Exploration.* (**90**):157-165.

Lee, J.S., Chon, H.T., Kim, K.W. (1998). Migration and dispersion of trace elements in the rock–soil–plant system in areas underlain by black shales and slates of the Okchon Zone, Korea. *Journal of Geochemical Exploration.*(**65**):61-78.

Li, Y.M., Stanislavova, L., Chaney, R.L. (1994). Determination of total cadmium in calcareous soils by extraction using Aliquat-336 and 3-heptan-one after *aqua regia* digestion. *Commun Soil Sci Plant Anal.* **(25)**:2029-2045.

Li, Y.M., Chaney, R.L. and Miller J.F. (1995). Genotypic variation in kernel cadmium concentrations in sunflower germplasm undervarying soil conditions. *Crop Sci.* **(35)**:137-141.

Lindsay, W.L. (1979). Chemical equilibria in Soils. New York: John Wiley and Sons.

Lund, L.J., Betty, E.E., Page, A.L. and Elliot, R.A. (1981). Occurrence of naturally high cadmium levels and its accumulation by vegetation. *J. Environ. Qual.* **(10)**:551-555.

Mattigold, S.V. and Sposito, G. (1979). In: Jenne, A. (Ed.) Chemical modeling in aqueous systems. American Chemical Society.Washington D.C.

McBride, M.B. (1994). Environmental Chemistry of Soils. Oxford University Press, New York.

Miller, R.W., Gardiner, D.T. (2000). Soils in our environment. 9th ed. Prentice Hall, New Jersey.

Moore, D. M. and R. C. Reynolds, Jr. (1989). X-ray diffraction and the identification and analysis of clay minerals. Oxford University Press, New York.

Muckenhirn, R.J., Whiteside, E.P., Templin, E.H. (1949). Soil classification and the genetic factors of soil formation. *Soil Sci.* **(67)**:93-105.

Naidu, R., Bolan, N.S., Kookana, R.S., Tiller, K.G. (1994). Ionic strength and pH effects on the sorption of cadmium and the surface charge of soils. *Euro. J. Soil. Sc.* **(45)**: 419-429.

NASA. (2000). National Aeronautics and Space Administration. Jet Propulsion Laboratory. Shuttle Radar Topography Mission North America Images. http://www2.jpl.nasa.gov/srtm/northAmerica.html/(accessed March 2008).

NASS. (2010). National Agricultural Statistics Service. Fargo, North Dakota.

NCDC. (2010). National Climatic Data Center. Ashville, North Carolina. http://www.ndsu.edu/ndsco/climatography/lang.pdf./(accessed August 2010).

NDAWN. (2010). North Dakota Agricultural Weather Network. Fargo, North Dakota. http://ndawn.ndsu.nodak.edu/index.html(accessed August 2010).

Nijenhuis, I.A., Bosch, H.J., Sinninghe Damste´, J.S., Brumsack,H.-J., de Lange, G.J. (1999). Organic matter and trace element rich sapropels and black shales: a geochemical comparison. *Earth Planet. Sci. Lett.* **(169):** 277– 290.

Norvell, W.A., Wu, J., Hopkins, D.G. and Welch, R.M. (2000). Association of cadmium in durum wheat grain with soil chloride and chelate-extractable soil cadmium. *Soil Sci Soc Am J.* **(64):**2162-2168.

Nowak, B. (1998). Contents and relationship of elements in human hair for a non-industrialized population in Poland. *Sci. Total Environ.* **(209)**:59Y68

Oertel, A.C. (1961). Relation between trace element concentrations in soil and parent material. *Journal of Soil Science.* **(12):**119-128.

Onyedika, G.O., Nwosu, G.U. (2008). Lead, Zinc and Cadmium in Root Crops from Mineralized Galena-Sphalerite Mining Areas and Environment. *Pakistan Journal of Nutrition.* 7 **(3)**:418-420.

Page, A.L., Bingham, F.T. (1973). Cadmium residues in the environment. *Residue Rev.*

(48):1-44.

Perilli, P., Mitchell, L.G., Grant, C.A., Pisante, M. (2010). Cadmium concentration in durum wheat grain (*Triticum turgidum*) as influenced by nitrogen rate, seeding date and soil type. *J Sci Food Agric.* **(90):**813-822.

Pickering, W. (1980). Cadmium in the environment. In: Nriagu, J.O. (Ed). Ecological Cycling Part 1. John Wiley and Sons, New York.

Pulls, R.W., Bohn, H.L. (1988). Sorption of cadmium, nickel and zinc by kaolinite and montmorillonite suspensions. *Soil Soc.Am. J.* **(52)**:1289-1292.

Raiswell, R., Plant, J. (1980). The incorporation of trace elements into pyrite during diagenesis of black shales, Yorkshire, England. *Economic Geology.* **(75)**:684-699.

Schaetzl, R.J., Anderson, S. (2005). Soils: Genesis and Geomorphology. Cambridge University Press. Cambridge, UK.

Schoeneberger, P.J., Wysocki, D.A. (1998). Field book for describing and sampling soils. Version 1.1. Natural Resources Conservation Service, USDA, National Soil Survey Center, Lincoln, Nebraska.

Schultz, L.G., Tourtelot, H.A., Gill, J.R., Boerngen, J.G. (1980). Composition and properties of the Pierre Shale and equivalent rocks, Northern Great Plains Region. U.S. Geological Survey Prof. Pap.# A1064. United States Government Printing Office, Washington D.C

Schultz, L.G., Tourtelot, H.A., Gill, J.R., Boerngen, J.G. (1980). Composition and properties of the Pierre Shale and equivalent rocks, Northern Great Plains Region. U.S. Geological Survey Prof. Pap.# B1064. United States Government Printing Office, Washington D.C.

Shute, T., Macfie, S. M. (2006). Cadmium and zinc accumulation in soybean: A threat to food safety? *Science of the Total Environment.* **(37):** 63–73.

Shacklette, H.T., Boerngen, J.G. (1984). Element concentrations in soils and other surficial materials of the conterminous United States. U.S.Geological Survey Professional Paper # 1270:105.

Siemiatycki, J., Dewar, R., Nadon, L., Gerin, M. (1994). Occupational risk factors for bladder cancer, Results from a case control study in Montreal, Quebec, *Canada. Am J Epidemiol.* **(140):** 1061-1080.

Simmons, M., Moos, D.K. (1990). Soil Survey of Cavalier County, North Dakota. United States Government Printing Office, Washington D.C.

Singh, A.K., Clarke, J.M., DePauw, R.M., Knox, R.E., Clarke, F.R., Fernandez, M.R., McCaig, T.N. (2010). Enterprise durum wheat. *Can. J. Plant Sci.* **(90)**:353-357.

Smith, R.E., Michalyna, G., Wilson, G. (1973). Soils of the Morden-Winkler area. Soils Report #18. Manitoba Dept. of Agric. Winnipeg.

Smith D.B., Cannon, W.F., Woodruff, L.G., Garrett, R.G., Klassen, R., Kilburn, J.E., Horton, J.D., King, H.D., Goldhaber, M.B., Morrison, J.M. (2005). Major- and trace element concentrations in soils from two continental-scale transects of the United States and Canada. US Geol. Surv. Open-File Rep. #1253. <http://pubs.usgs.gov/of/2005/1253/>.

Smith, D.B., Woodruff, L.G., O'Leary, R.M., Cannon, W. F., Garrett, R. G., Kilburn, J. E. and Goldhaber, M. B.(2009). Pilot studies for the North American Soil Geochemical Landscapes Project – Site selection, sampling protocols, analytical methods, and quality control protocols. *Applied Geochemistry*. 24**(8)**: 1357-1368.

Sposito, G. (1983). The chemical forms of trace metals in soils.In: Thornton, I. (Ed.) Applied Environmental Geochemistry. Academic Press, New York.

Sposito, G. (1989). The chemistry of soils. Oxford University Press, Oxford, U.K.

Sterckeman, T., Douay, F., Baize, D., Fourrier, H., Proix, N., Schwartz, C., Carignan, J. (2006). Trace element distribution in soils developed in loess deposits from northern France. *European Journal of Soil Science*. **(57)**:392-410.

Storer, D. A. (1984). A simple high sample volume ashing procedure for determination of soil organic matter. *Soil Sci. Plant Anal.* 15 **(7)**: 759-772.

Tills, A.R., Alloway, B.J. (1983). The use of liquid chromatography in the study of cadmium speciation in soil solution from polluted soils. *Journal of Soil Science*. **(34)**: 769-781.

Tourtelot, H.A., Huffman, C. Jr., Rader, L.F. (1964). Cadmium in samples of the Pierre Shale and equivalent units, Great Plains Region. U.S. Geol. Surv. Prof. Paper # 475-D:73-78.

Tucker, P.G. (2008). Case Studies in Environmental Medicine (CSEM): Cadmium Toxicity. Agency for Toxic Substances and Disease Registry. 63 pp. http://www.atsdr.cdc.gov/csem/cadmium/index. html/(accessed May 2010).

Tuttle, L.W.M, Breit, G.N., Goldhaber, M.B. (2003). Geochemical Data from New Albany Shale, Kentucky: A Study in Metal Mobility During Weathering of Black Shales. U.S.G.S. Open File Report 03-207.

Tuttle, L.W.M., Fahy, J., Grauch, R.I., Ball, B.A., Chong, G.W., Elliott, J.G., Kosovich, J.J., Livo, K.E., Stillings, L.L. (2007). Results of Chemical Analyses of Soil, Shale, and Soil/Shale Extract from the Mancos Shale Formation in the Gunnison Gorge National Conservation Area, Southwestern Colorado, and at Hanksville, Utah. U.S.G.S. Mineral Resources Program. Open-File Report 2007-1002D.

Upham,Warren. (1895). The glacial Lake Agassiz. USGS Monograph **(25)**: 658.

Vine, J.D., Tourtelot, E.B. (1970). Geochemistry of black shale deposits - a summary report. Econ. Geol. **(65)**: 253–272.

Waalkes, M.P. (2000). Cadmium carcinogenesis in review. *J Inorg Biochem.* **(79)**: 241-244.

Warning, B and Brumsback, H.J. (2000). Trace metal signatures of Mediterranean sapropels. *Palaeogeogr.Palaeoclimatol. Palaeoecol.***(158)**:293-309.

Wichard, T., Mishra, B., Myneni, S.C.B., Bellenger, J.-P., Kraepiel, A.M.L. (2009). Storage and bioavailability of molybdenum in soils increased by organic matter complexation. *Nature Geoscience.* **(2)**:625-629.

Wignall, P.B. (1994). Black Shales. Oxford Monographs on Geology and Geophysics. Clarendon Press.Oxford.

White, J.G.,Welch, R.M., Norvell, W.A. (1997). Soil zinc map using geostatistics and geographic information systems. *Soil Sci Soc Am J.* **(61)**:185-194.

White, R.E., (1994). Principles and Practice of Soil Science-The Soil as a Natural Resource. 3rd ed. Blackwell Science, United Kingdom.

Woodruff, L.G., Cannon, W.F., Eberl, D.D., Smith, D.B., Kilburn, J. E., Horton, J.D., Garrett, R.G. and Klassen, R. (2009). Continental-scale patterns in soil geochemistry and mineralogy: results from two transects across the United States and Canada. *Applied Geochemistry.* 24 **(8)**: 1369–1381.

Yaalon, D.H. (1971). Soil-forming intervals in time and space. In, Yaalon, D.H. (Ed.). Paleopedology . (p. 29-39). Israel University Press. Jerusalem.

APPENDIX A. SOIL CORE DESCRIPTIONS

Core 1 F3, 1500N, 0W

A 0-24 cm; black (10YR 2/1) moist and very dark grayish brown (10YR 3/2) dry; fine- medium granular; many, very fine roots in the matrix.

B_t1 24-69 cm; olive brown (2.5Y 4/3) moist and light yellowish brown (2.5Y 6/3) dry; moderate, medium prismatic; common, prominent, black (7.5YR 2/1) charcoal/black lenses (0.5-2) mm; few, medium, prominent, masses yellowish brown (10YR 5/8) dry, redox accumulations at 41 cm; common, very fine roots between the ped faces. Stratifications in the horizon were found.

B_{t2} 69- 105 cm; light brownish gray (2.5Y 6/2) dry; moderate- strong, medium prismatic; few, fine, prominent, dry, irregular, dark yellowish brown (10YR 4/6) redox accumulations; 1cm shale fragments; common, very fine-coarse roots in matrix; colluvial/alluvial nature of material in the horizon.

B_{t3} 105-120 cm; light yellowish brown (2.5Y 6/3) dry; moderate to strong, fine, prismatic; few, coarse, distinct, dry, irregular, yellowish brown (10YR 5/6), redox concretions; few, fine-medium roots in the matrix.

BC 120-168 cm; light yellowish brown(2.5Y 6/3) dry; moderate to strong, fine, prismatic; few, fine, sharp, irregular, distinct, dry, dark yellowish brown (10YR 4/6) redox concretions between (145-168) cm.

C 168-235 cm; olive gray (5Y 4/2) and dark olive gray (5Y 3/2) dry, imbricated sedimentary structure; few, very fine roots between the ped faces.

Remarks

No effervescence was found throughout the core (Fig. A.1.). Very well organized

deep soil found in all the horizons for this core. Grayish white color throughout the profile. Charcoal lenses found all over the profile having size range between (2-3mm to 0.5 cm). Charcoal lenses when crushed have brownish black color. Very porous soil. Pedogenic structure at 105 cm where clay films cover shale fragments. Soil texture determination was not done for this core. The location of the core at the downslope position could be responsible for the fine textured and organized material in the core. The grayish white material could be silans over the soil horizons.

Core 2 F3, 1900N, 1250W

A 0-7 cm; black (10YR 2/1) and very dark grayish brown (10YR 3/2) dry;fine-medium granular; many, very fine-fine roots in the matrix.

E1and E2 7-30 cm; dark gray- very dark grayish brown(2.5Y 4/1-2.5Y 3/2) crushed and rubbed and (2.5Y 4/2) dry; organic matter staining with thick organic matter; no platy structure or sand grains; many, very fine roots between ped faces. Silt coating on the ped faces.

B_t 31-67 cm; very dark gray- dark grayish brown (2.5Y 3/1-2.5Y 4/2) crushed and rubbed and (2.5Y 4/1) dry; moderate prismatic structure; at 48 cm, few, fine, distinct, dry, irregular, brownish yellow (10YR 6/8) redox accumulations; many, fine roots, in the matrix.

BC 67-78 cm; dark grayish brown (2.5Y 3/1) dry; common, very fine roots in the matrix on the top of the horizon.

BC_1 79-86 cm; first brownish yellow (10YR 6/8) ash layer at 82cm; fine, angular (2-3) mm grains.

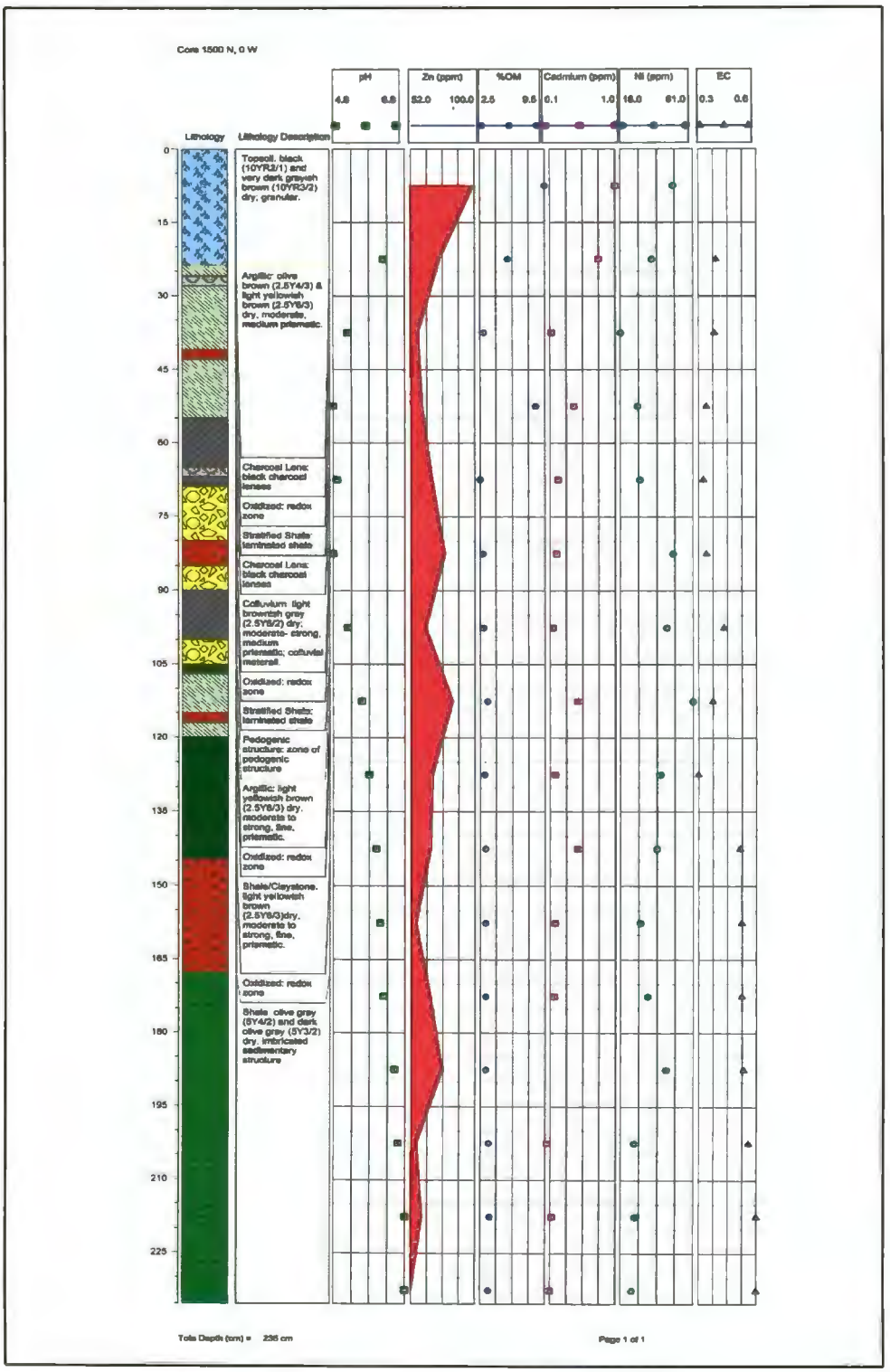

Fig.A.1. Graphical representation of core 1 showing lithology and chemical properties.

C 86-240 cm; grayish black shale with acute angled orientations; common, very fine roots between the ped faces; 2nd prominent ash layer with yellow (2.5Y 8/8) munsell color at 123 cm. Third ash layer at 227 cm.

Remarks

No effervescence seen in the upper horizons (Fig. A.2.). Roots found throughout the profile. Gypsum grains in masses with size (2-7)mm at 120 cm. Shale laminations near 129 cm. Jarosite mineral with yellow 5Y 8/6 munsell color found near profile at 98 cm and more dominant in the lower profile from 130-240 cm.

Core 3 F3, 1900N, 1500W

A 0-16 cm; very dark brown (10YR 2/2) and very dark grayish brown (10YR 3/2) dry; fine granular parting to (fine –medium) sub-angular blocky; many fine roots in the matrix on the top of the horizon.

B_{t1} 16-53 cm; dark grayish brown (10YR 4/2) and brown (10YR 5/3) dry; weak, medium prismatic parting to blocky; common, fine, coarse sand sized pebbles of different lithology like charcoal; common, fine, prominent, dry irregular, sharp, dark yellowish brown (10YR 4/6) dry redox accumulations; more heterogeneous, more porous; common, fine roots between the ped faces.

B_{t2} 53-62 cm; olive brown (2.5Y 4/4) and dark grayish brown (2.5Y 4/2) dry; moderate, medium prismatic; common, very fine roots between ped faces.

B_{t3} 62-85 cm; olive brown (2.5Y 4/4) and light olive brown (2.5Y 5/6) dry; shiny surface that may be clay skin, mini slicken slides or pressure face; common, fine, prominent, sharp, irregular, dark yellowish brown (10YR 4/6) dry redox concretions; few,

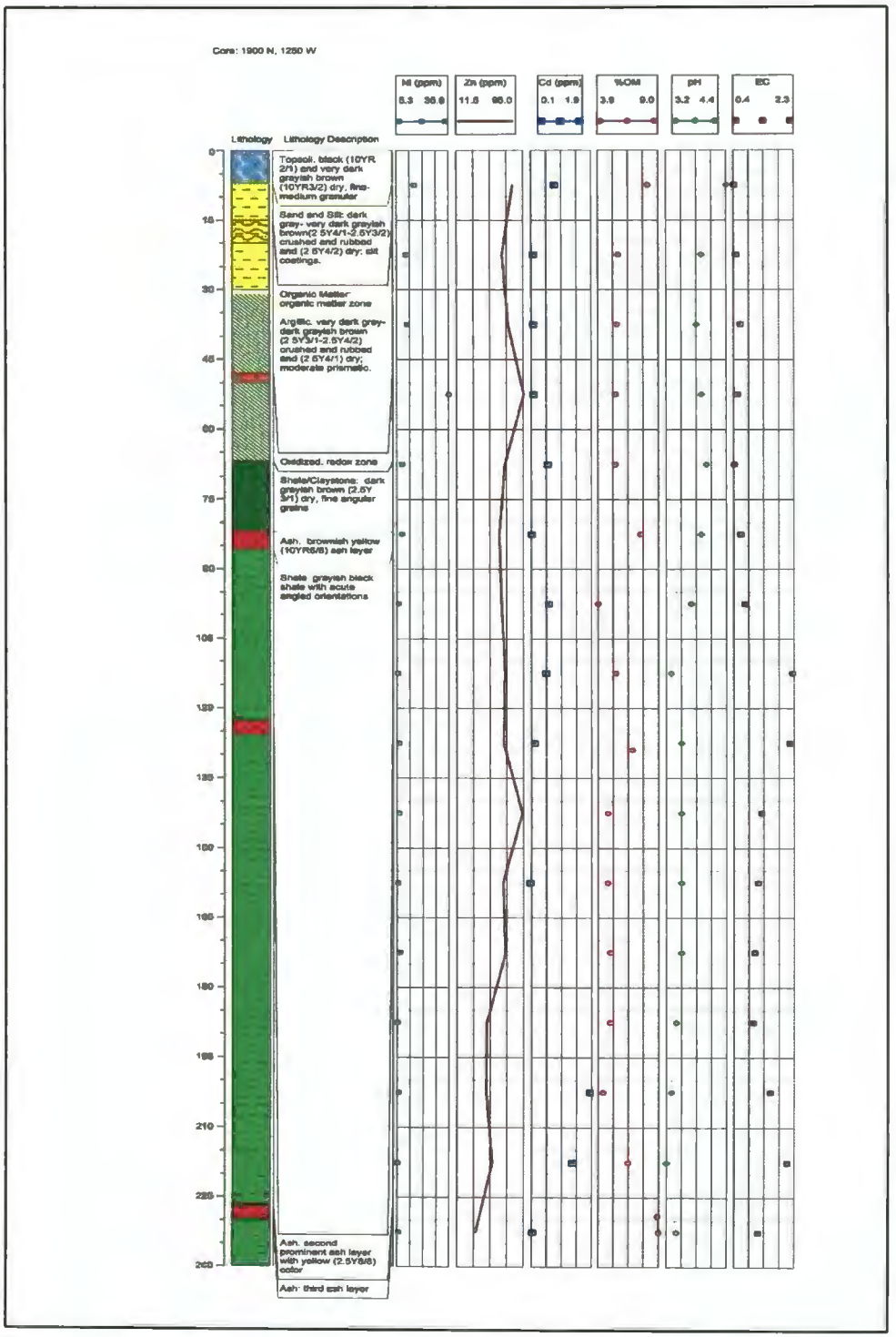

Fig.A.2. Graphical representation of core 2 showing lithology and chemical properties.

fine, prominent, yellow (5Y 7/6) jarosite mass; common, very fine roots, between ped faces.

C_r 85- 111 cm; dark olive gray (5Y 3/2) dry; weak prismatic; many, very fine roots between ped faces.

R 111-220 cm; dark olive gray (5Y 3/2) dry; angular laminated shale; few, very fine roots between the ped faces.

Remarks

Very shallow soil found for this horizon (Fig. A.3.). At 45 cm very small coherent ped faces without clay skin but are organized materials. At 52 cm root channels that are reorganized over the course of time . Entire profile was leached therefore no effervescence with HCl. Different jarosite lenses throughout the profile. First Fe Oxide presence at about 40 cm, then at 85 cm, 110 cm , 139 cm upto the bottom. Many, fine roots surrounded by few, very coarse roots at 90 cm. At 140 cm, yellowish brown (2.5Y 5/6) dry jarosite, ash layer at 145 cm (10YR 6/8). Yellow (5Y 7/8) dry jarosite stains near the bottom of the core. High amount of roots found throughout the core indicate the presence of pre existing forests in this area. Location of this core was also near the now existing forested area at upslope position in field three.

Core 4 F3 1500N 250W

A 0-11cm; very dark brown or very dark grayish brown (10 YR 2/2) and (10 YR 3/2) dry; medium to coarse granular; silty clay loam, firmly consistent when moist, many (fine- medium) roots in the matrix.

E 11-24 cm; light gray or pale yellow (2.5Y 7/2) and (2.5Y 7/3) dry for whitish

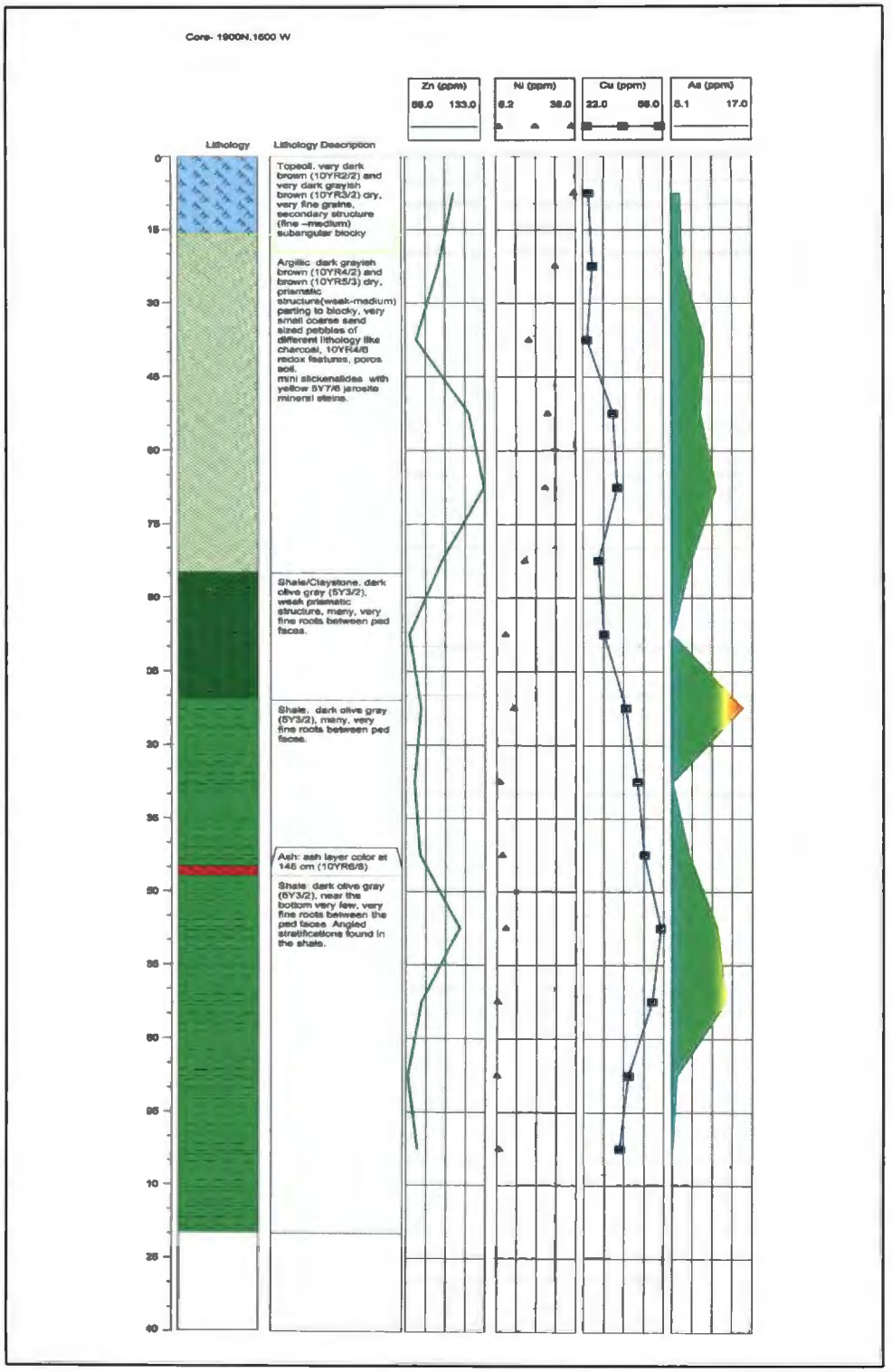

Fig.A.3. Graphical representation of core 3 showing lithology and chemical properties.

gray coating in the horizon with dark grayish brown or very dark grayish brown (2.5Y 4/2) and (2.5Y 3/2) color for the matrix; silty clay loam+ silty clay-; no platy structure but medium prismatic structure parting to medium sub-angular blocky; few, medium roots in the matrix on top of the horizon; few, fine moist, irregular, hard, diffuse, brown (10YR 4/3) Iron- Manganese concretions near 17 cm; small quartz single grain 1 (mm) in size near 20 cm.

B_t1 24-50 cm; very dark grayish brown (2.5Y 4/3) and light yellowish brown (2.5Y 6/3) dry; clay (50-55%); (5-10%) sand; moderate to strong, fine prismatic parting to secondary structure; common, faint, pale yellow (2.5Y 7/3) dry, discontinuous, illuvial clayfilms on the vertical faces of peds; common, very fine roots in the matrix; silt coatings are soft when tried to scratch and expand with clay matrix.

Bt2 50-112 cm; light brownish gray (2.5Y 6/2) for white coating and dark grayish brown (2.5/Y 4/2) moist and light gray 2.5Y 7/2 dry, for the matrix; silty clay; moderate to strong, fine to medium, prismatic; few, very fine roots in the matrix, (0.5-2) cm, many, fine, prominent, very dark gray (7.5 YR 3/1) dry, irregular, clear black concretions in the matrix present all over the Bt horizon, these black concretions are arranged differently in the soil ; in some cases appear as embedded between clay while sometimes they are present continuously between the fissures; these concretions when pressed get flattened. It might be organic matter or some secondary iron mineral; (1-2) cm long friable shale fragments.

BC 112-147 cm; light olive brown (2.5Y 5/3) dry, laminar/layered structure; common, fine roots in the matrix, no shale fragments present but whitish gray material (2.5Y6/2) dry; (2-4) mm gypsum grain near 122 cm; stratifications in the last 20 cm.

C 147-233 cm; olive gray (2.5Y 4/2) dry; weak prismatic, no roots; intense whitish

material; pale yellow (2.5Y 7/3) moist jarosite with friable shale; common, fine, moist, irregular, hard, diffused strong brown (7.5Y 4/6) Iron- Manganese concretions.

Remarks

Upper soil is more homogenous. Very thin (thinner than a human hair) fungal hyphae found near 85 cm (Fig. A.4.). Very porous soil with water movement. Material is very intensely reorganized. Whole soil profile is bleached with intense redox features, whitish gray material and thick clay waxy coatings.

Well developed ped faces longer than wide with black stains found in the upper profile. There might be a presence of Glossic horizon where E goes down in argillic horizon and thus ped faces in Bt horizon have whitish coatings. Shale fragments found high up in the profile.

Core 5 F3, 1500N, 500W

A 0-20 cm; black (10YR 2/1) and very dark grayish brown (10YR 3/2) dry; silt loam; fine- medium granular, medium sub-angular blocky parting to granular; many fine-medium roots on the matrix in the horizon.

E 20-28 cm; light gray (2.5Y 7/2) coatings to very dark grayish brown color for the matrix (2.5Y 3/2), (2.5Y 7/1) light gray to (2.5Y 5/2) grayish brown (dry) color for the matrix; silty clay loam; (fine – medium) moderate prismatic with continuous coating of silt particles on the ped faces in the horizon; common, very fine-fine roots in the matrix; common, fine, faint, redox accumulations; common, distinct, continuous, shiny silans (silt coatings) on the ped faces.

B_t 28-57 cm; very dark grayish brown (2.5Y 4/3) and (2.5Y 6/3) light yellowish

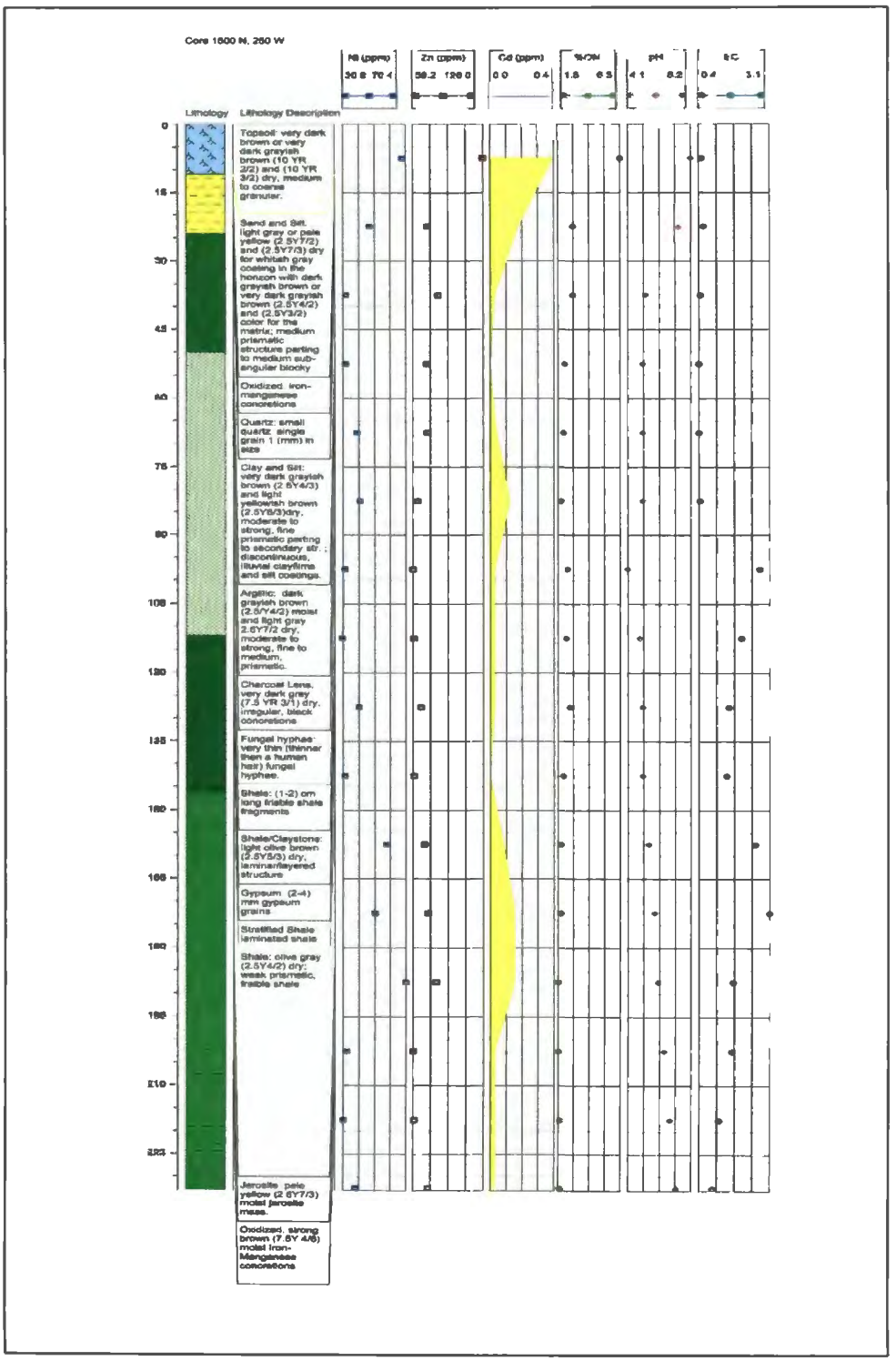

Fig.A.4. Graphical representation of core 4 showing lithology and chemical properties.

brown dry; silty clay, moderate-strong, very fine, prismatic; many, fine to medium roots in the matrix, many, faint, continuous clay films on all the ped faces; clay films in the horizon are very shiny; common, fine, prominent, irregular, redox concentrations on the horizontal ped faces.

B_{t2} 57-80 cm; grayish brown (2.5Y 5/2) white coating with dark grayish brown (2.5Y 4/2) matrix and light yellowish brown (2.5Y 6/3) dry; many very fine to fine roots on the ped faces; moderate to strong, medium prismatic structure; distinct, common, fine, irregular-threadlike, olive yellow (2.5Y 6/6)dry and black (2.5Y 2.5/1) dry redox accumulations; (0.5-2) cm, dark grayish black, shale fragments when crushed gave brown color; black redox accumulations were spherical in shape with a size < 1mm; These black bodies could be either organic matter or secondary precipitation.

C_1 80-111 cm; light yellowish brown (2.5Y 6/3) and light brownish gray (2.5Y 6/2) dry, with matrix as grayish brown (2.5Y 5/1); fine to medium, sub-angular blocky structure; few, very fine, roots on the peds; common, fine, irregular, distinct, yellowish brown (10YR 5/8)dry and black (2.5Y 2.5/1)dry redox features; (0-2) cm shale fragments; sub-angular, blocky, coarse, black(2.5Y 2.5/1) fragments found near 98 cm.

C_2 111-144 cm; very dark grayish brown (2.5Y 3/2) and grayish brown (2.5Y 5/1) dry; moderate, fine-medium, prismatic; common, very fine roots on the ped faces; laminations in shale fragments can be seen, shale fragments have a size within a range of (1-2) cm; common, fine, distinct, yellowish brown (10YR 5/6) dry and black (2.5Y 2.5/1)dry redox accumulations; very distinct ped faces.

C_3 144- 192 cm; light brownish gray (2.5Y 6/2) alternating color with grayish brown (2.5Y 5/1) matrix; few, very fine, roots on the ped faces; fine-coarse, sub- angular

shale aggregates; common, fine, prominent, dark brown (7.5YR 3/4) dry, strong brown (7.5YR 4/6) dry and yellow (10YR 7/6) dry redox accumulations; shale aggregates were very friable; slight – moderately hard when dry.

C_4 192-215 cm; light olive brown (2.5Y 5/3) moist matrix color and grayish brown (2.5Y 5/1) dry; weak- moderate, fine to medium prismatic; roots were absent, distinct, prominent, fine, irregular, yellowish brown (10YR 5/8) dry, very dark brown (10YR 2/2) dry ash layers/ redox accumulations; alternating light (2.5Y 7/3) dry pale yellow and dark (7.5YR 4/4) dry brown dry colors on the ped faces; massive ash layer (4-5) cm without shale aggregates having alternating light and dark bands; the ped faces were very hard when dry.

C_5 215-239 cm; very dark grayish brown (2.5Y 3/2) moist matrix and light yellowish brown (2.5Y 6/3) dry whitish material in the shale; roots were absent; very friable shale aggregates (can be broken with hands) without laminations; common, distinct, fine, irregular to threadlike yellowish red (5YR 5/8) dry redox accumulations in the horizon..

Remarks

No effervescence was seen all over the profile. Distinct clay films and silans were found in horizons (Fig. A.5.). Two distinct ash layers/redox features found at (193-197) cm and (209-212) cm. Intensive white coating can be found in many lower horizons. It might be a weathering product. Reoccurrence of moderate prismatic structure in C horizon with ash layers having different colors. Very small Quartz/Gypsum grains were seen near 228 cm. Roots were found to be abundant before 85 cm and then afterwards, they tend to thin out in the lower profile.

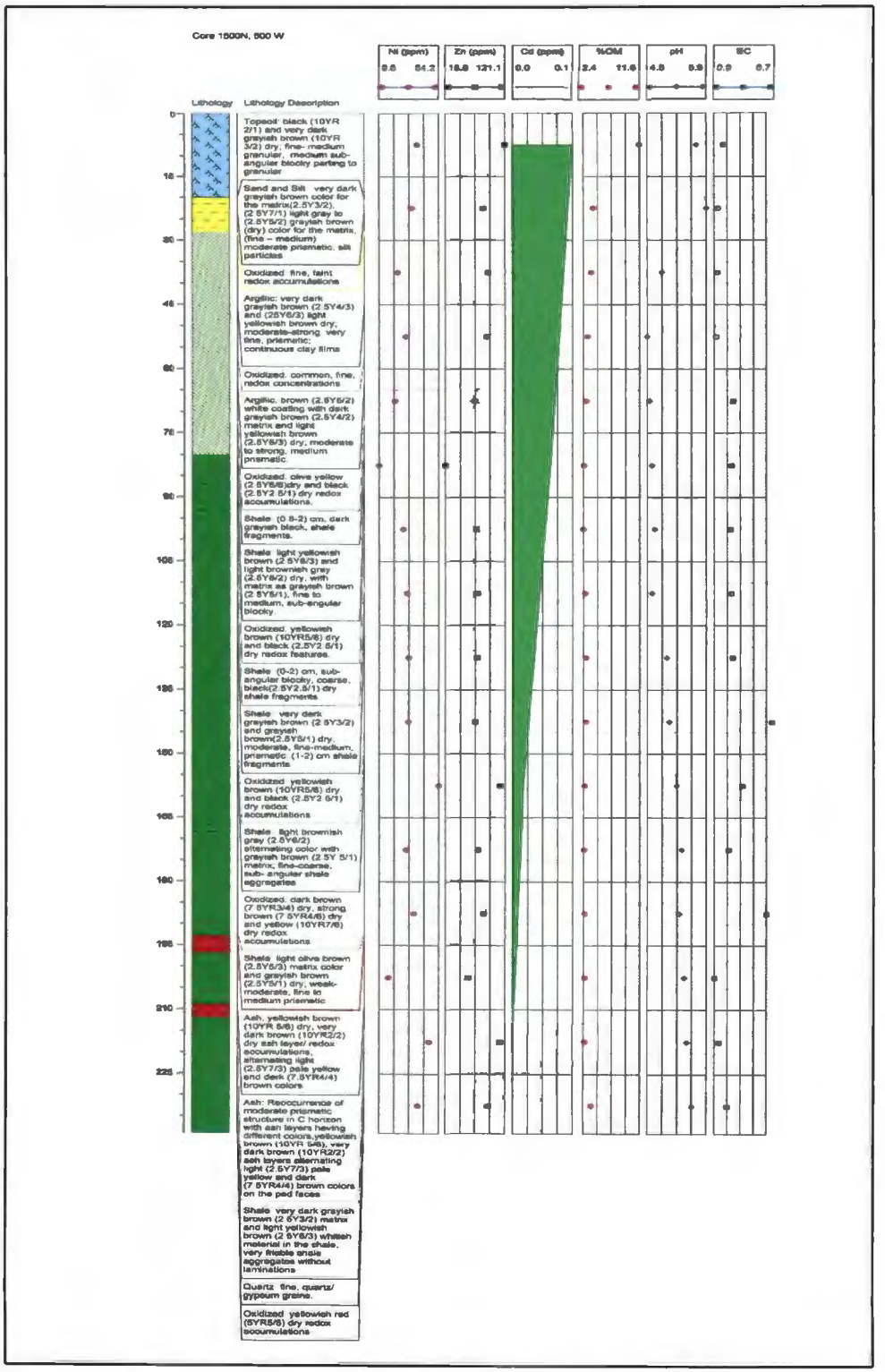

Fig.A.5. Graphical representation of core 5 showing lithology and chemical properties.

Core 6 F3, 1500N, 750W

A 0-19 cm; black (10YR 2/1) and very dark gray (10YR 3/1) dry; silt loam; (fine-medium) granular, medium sub-angular blocky parting to granular; fine-medium roots in the matrix.

E 19-26 cm; grayish brown (10YR 5/2) and light brownish gray (10YR 7/1) dry; silty clay loam; moderate, (fine- medium), prismatic structure; common, (very-fine-fine), roots on the ped faces; many, faint, continuous, silans on ped faces; abrupt boundary.

B_{t1} 26-40 cm; dark grayish brown (10YR 4/2) and grayish brown (10YR 5/2) dry; silty clay; moderate, fine, prismatic structure; many, faint, continuous clay films on ped faces; many, very fine- fine, roots on ped faces; many, faint, continuous silans; few faint, redox accumulations.

B_{t2} 40- 58 cm; olive brown (10YR 4/3) and light yellowish brown (10YR 6/3) dry; silty clay; strong, fine-medium, prismatic structure; slightly hard when dry; many, faint, continuous clay films on ped faces; common, faint, silans; few, faint, yellowish brown (10YR 5/6), redox accumulations; common, very-fine, roots, on the ped faces.

B_{t3} 58- 83 cm; dark grayish brown (2.5Y 4/2) and light yellowish brown (2.5Y 6/3) dry; moderate- strong, fine- medium, prismatic structure; slightly hard when dry; small black spherical bodies (organic/redox accumulations) on the ped faces; faint, continuous clay films; few, very-fine roots, (< 5 mm) shale fragments embedded between the ped faces and clay films; few, fine, distinct, brownish yellow (10YR 6/6) and black (10YR 2/1) redox accumulations.

BC 83- 120 cm; light olive brown (2.5Y 5/3) and light brownish gray (2.5Y 6/2) dry; weak, prismatic structure; discontinuous, faint clay films; (5mm- 1cm), angular, shale

fragments; common, medium, prominent, yellowish brown (10YR 5/8) redox accumulations; few, very-fine roots; clear boundary.

C_1 120-151 cm; very dark grayish brown (2.5Y 3/2) and light brownish gray (2.5Y 6/2) dry; moderate, fine-medium, prismatic structure; very soft when dry; many, (1 cm) wide angular shale fragments; few, shale fragments (3 cm long) very- fine granular material; many, fine, prominent, distinct brownish yellow (10YR 6/6) and very dark brown (10YR2/2) redox accumulations; few, very-fine roots.

C_2 151- 174 cm, very dark grayish brown (2.5Y 3/2) and light brownish gray (2.5Y6/2) dry; strong,fine-medium, prismatic structure; hard when dry; anomalous sedimentary zone with very fine grained material and less shale fragments between (151-160 cm); no roots; fine, prominent, distinct, strong brown (7.5YR 5/6) and brownish yellow (10YR 6/8) and very dark brown (10YR 2/2) redox accumulations; shale fragments start increasing near 160 cm and are soft when dry.

$C_3$174- 203 cm; very dark grayish brown (2.5Y 3/2) and light yellowish brown (2.5Y 6/3) dry; very fine granular material; fine, prominent, distinct, strong brown (7.5YR 5/6) and brownish yellow (10YR 6/8) and very dark brown (10YR 2/2) and very pale brown (10YR7/4) redox accumulations; no roots; angular very soft (1-2) cm shale fragments.

C_4 203- 357 cm; olive brown (2.5Y 4/3) and light gray (2.5Y 7/2) dry; moderate, fine-medium, prismatic structure; many, irregular-threadlike, prominent, distinct, 1 cm thick organic matter/redox accumulations with black (10YR 2/1), brownish yellow (10YR 6/6) and strong brown (7.5YR 5/6) color; anomalous sedimentary zone again from (204-227) cm, with less shale but fragments tend to increase after 232 cm; no roots; very fine

granular material abundant between (271-311) cm; many (1-1.5) cm soft shale fragments in this zone; few shale fragments slightly hard when dry between (311-350) cm; shale fragments increase near the bottom (350) cm onwards and are soft when dry.

Remarks

No effervescence over the profile. Distinct, continuous clay films and silans upto 90 cm. Two anomalous sedimentary zones between (151-160) cm and (204-227) cm. Very fine grained material in the lower profile. Black spherical bodies when crushed gave blackish brown color. Shale fragments high up in the profile (Fig. A.6.). Soil might be colluvial/alluvial deposits. Angled shale fragments embedded in clay films. Fine granular material indicates slopewash over the shale regolith. Lots of redox accumulations all over the profile. Very thick root near 300 cm.

Core 7 F3, 1500N, 1000W

A 0-15 cm; very dark brown (10YR 2/2) and very dark grayish brown (10YR 3/2) dry; silty clay loam; (fine-medium) granular, medium sub-angular blocky parting to granular; many, very-fine to fine roots in the matrix and in the cracks; slightly hard in consistence; abrupt, smooth boundary.

B_{t1} 17-43 cm; olive brown (2.5Y 4/3) and grayish brown (2.5Y 5/2) dry; strong, (fine-medium) prismatic structure; silty clay; moderately hard when dry; many, very-fine to fine, roots on the ped faces; many, faint, continuous clay films on ped faces; common, faint, discontinuous skeletans on the ped faces; abrupt smooth boundary.

B_{t2} 43-65cm; grayish brown (2.5Y 5/2) and light brownish gray (2.5Y 6/2) dry; moderate, (fine-medium) prismatic structure; silty clay; moderately hard in consistence;

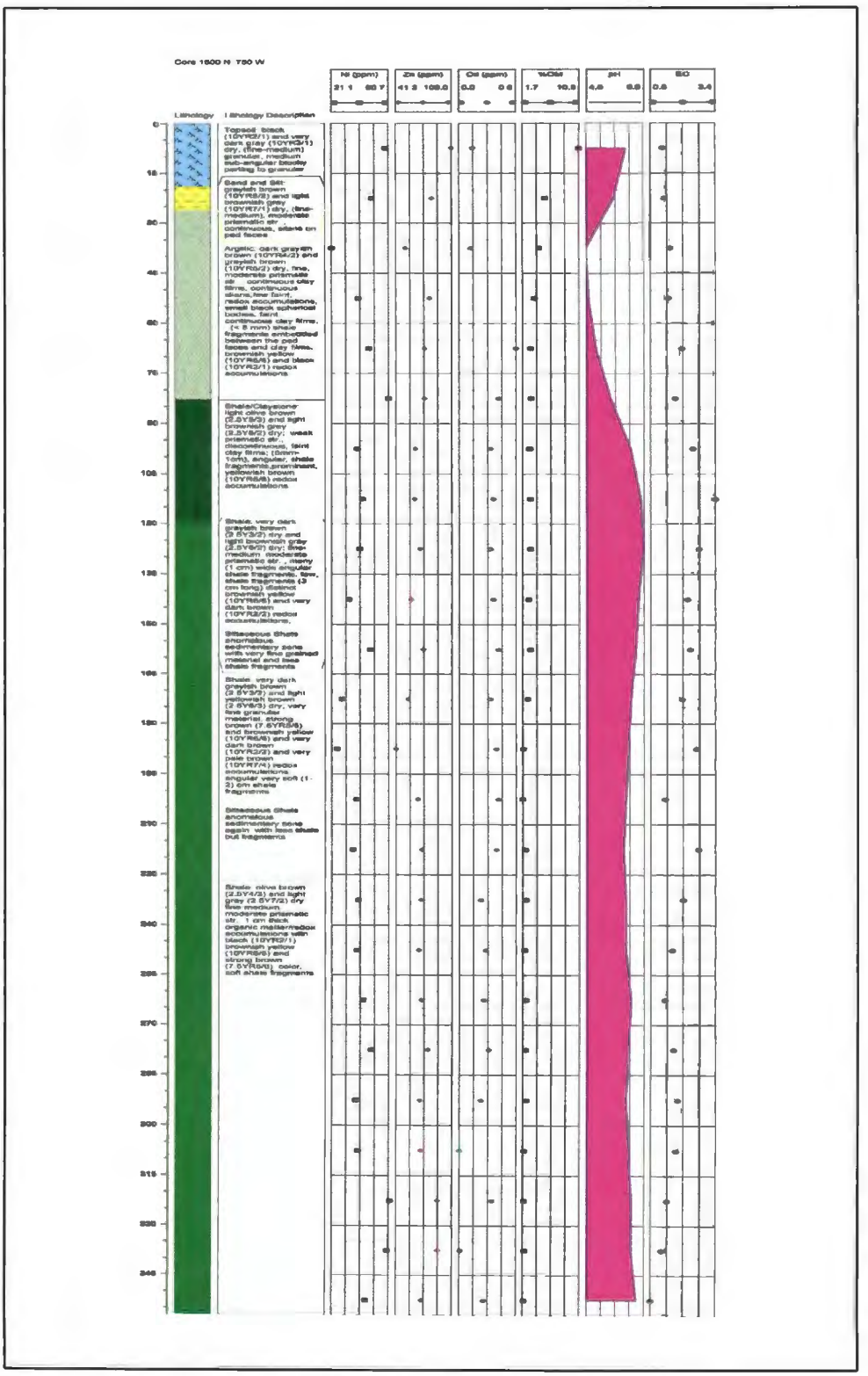

Fig.A.6. Graphical representation of core 6 showing lithology and chemical properties.

many, very-fine to fine, roots on the ped faces; common, faint discontinuous clay films; common, faint, discontinuous skeletans; common,(fine-medium), irregular, clear, black (2.5Y 2.5/1), organic matter accumulations; abrupt and wavy boundary.

B_{k1} 65-118 cm; light brownish gray (2.5Y 6/2) and light gray (2.5Y 7/2) dry; moderate, (fine-medium), prismatic structure; silty clay loam; very hard in consistence; common, faint, discontinuous clay films; many, prominent, threadlike root channels; common, (fine-medium), prominent, olive yellow (2.5Y 6/8), spherical-irregular, redox concretions; many, (fine-medium), prominent, white (2.5Y 8/1), irregular, carbonate nodules in the matrix; common, very-fine roots matted on ped faces; abrupt and smooth boundary.

B_{k2} 118-144 cm; dark grayish brown (2.5Y 4/2) and light yellowish brown (2.5Y 6/3) dry; moderate, medium, prismatic structure; sily clay loam; moderately hard in consistence; few, very-fine roots; common, faint, discontinuous clay films; few,(fine-medium), prominent, spherical-irregular, olive yellow (2.5Y 6/8) and dark yellowish brown (10YR 3/6) redox concretions; very-fine granular material; abrupt and smooth boundary.

C_1 144-181 cm; grayish brown (2.5Y 5/2) and light brownish gray (2.5Y 6/2)dry; weak, (fine-medium), prismatic structure; silt loam; moderately hard; few, root channels; few, very-fine roots; very-fine granular material; common, (fine-medium), prominent, soft, sharp, very dark brown (10YR 2/2) Fe nodules; organic matter/redox accumulation between (148-151) cm; common, fine, spherical charcoal bodies;1 mm shale fragments; non-effervescent; abrupt and smooth boundary.

C_2 181-211 cm; light brownish gray (2.5Y 6/2) and light gray (2.5Y 7/2) dry; abrupt and smooth boundary; weak ,(fine-medium), prismatic structure; very hard in

consistence; few, very-fine roots; few, fine, prominent, threadlike, very dark gray (10YR 3/1) and very dark brown (7.5YR 2.5/2),many, thin, discontinuous Fe coatings mixed with clay; few, faint shiny grains on the ped faces; fine shale fragments embedded between the ped faces; Organic matter zone (181-186) cm.

C_3 211-238 cm; light gray (2.5Y 7/2) and light gray (5Y 7/1) dry; massive structure; very soft in consistence; no roots; very friable shale aggregates; (2-3) cm long shale fragments; many, prominent, irregular, brown (7.5YR 4/4) and strong brown (7.5YR 5/8) Fe oxide stains; abrupt and smooth boundary.

Remarks

Carbonate/ lime concretions starting near 69 cm. Matrix (73-144) cm fizzed with HCl. Common, root channels in the horizons. First core to show effervescence with HCl. Fine, black spherical charcoal bodies found in the upper horizon of the core. Very thin E horizon (15-17) cm (Fig. A.7.) with light brownish gray (10YR 6/2) moist and light gray (10YR 7/1) dry; (fine-medium) moderate prismatic structure; few, very-fine roots in the matrix; common, faint, silt grains; abrupt and smooth boundary for the horizon. Thin illuvial horizon found for this core indicates extreme erosional processes operating in the escarpment soils. Location of this core at the upslope position could be responsible for aggravating erosional processes.

Core 8 F 3, 1500N, 1250W

A 0-14 cm; very dark brown (10YR 2/2) and very dark grayish brown (10YR 3/2) dry; silt loam; (fine-medium) granular, moderate, medium sub-angular blocky parting to granular; slightly hard when dry; many, very-fine to fine roots in the matrix; abrupt, wavy boundary.

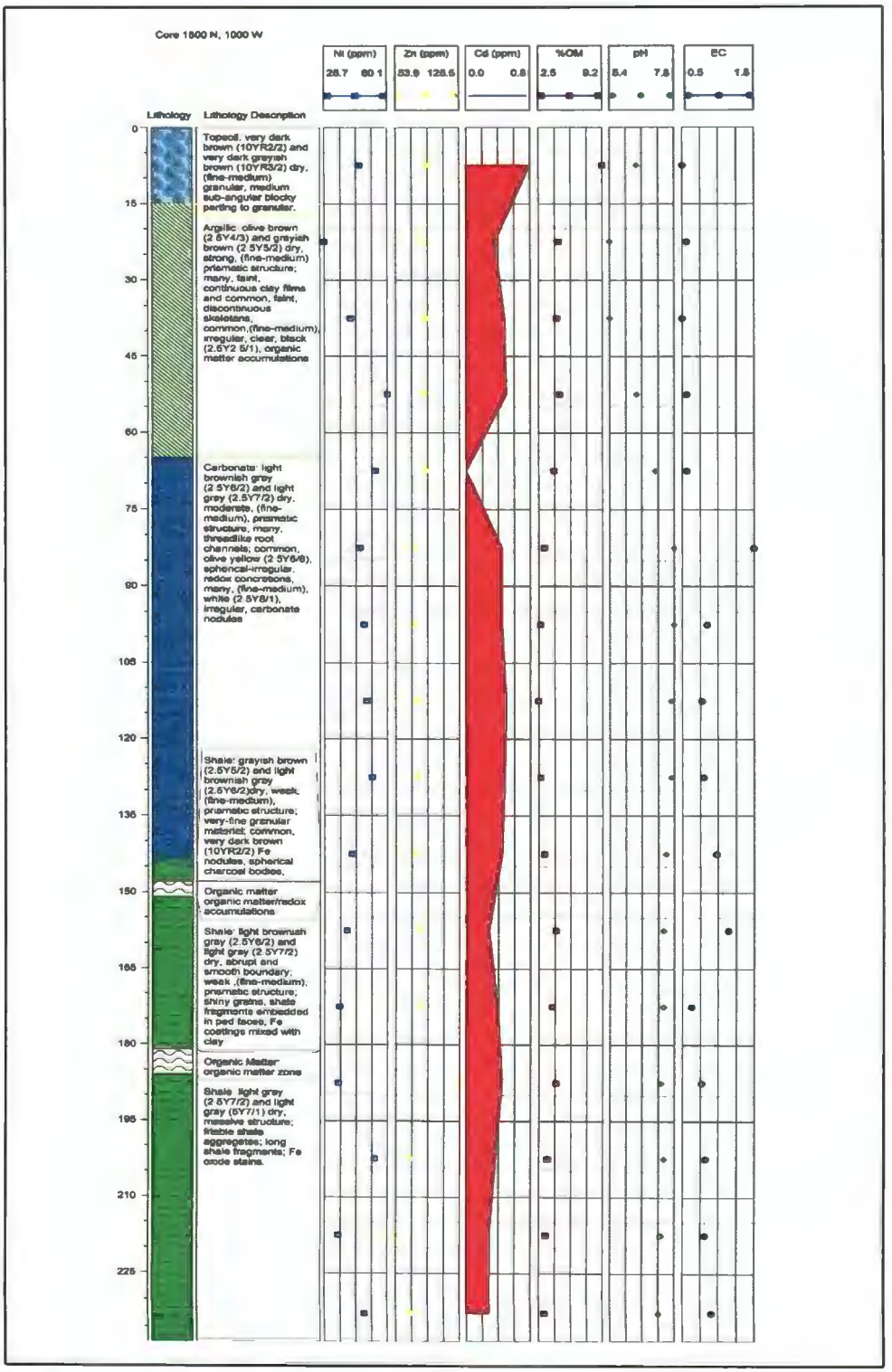

Fig.A.7. Graphical representation of core 7 showing lithology and chemical properties.

B_{t1} 14-32 cm; very dark grayish brown (10YR 3/2) and dark grayish brown (10YR 4/2) dry; silty clay loam; moderate ,medium prismatic structure; moderately hard when dry; many, very-fine to fine, roots on the ped faces; many, faint, continuous clay films on ped faces; common, faint, discontinuous skeletans on the ped faces; abrupt smooth boundary.

Bt2 32-45 cm; dark grayish brown (2.5Y 4/2) and grayish brown (2.5Y 5/2) dry; silty clay; strong, medium, prismatic structure; moderately hard when dry; many, fine to medium, roots on the ped faces; many, faint, continuous clay films on ped faces; common, faint, discontinuous skeletans on the ped faces; organic matter at 38 cm; abrupt wavy boundary.

B_{t3} 45-88 cm; very dark gray (2.5Y 3/1) and grayish brown (2.5Y 5/2) dry; silty clay; strong, medium prismatic structure; soft in consistence when dry; common, fine roots on ped faces, thick medium root matted on the matrix on the ped face; very few, fine, prominent yellow (2.5Y 8/6) jarosite masses; light colored (10YR 7/2) material between (75-80) cm; abrupt smooth boundary.

Cr-(88-238) cm, black (5Y 2.5/1) and grayish brown (2.5Y 5/2) dry; angular laminated shale; hard when dry; very fine granular material over the shale aggregates between (77-79) cm; shale aggregates are soft when dry near the bottom of the horizon; many, fine grained gypsum lenses from 135-138 cm, again between (154-156) cm and (175-176) cm; (3-4) mm gypsum grains from (228-238) cm; pale yellow(2.5Y8/2) and yellow (2.5Y8/6) volcanic ash layer from 216-222 cm ; yellowish brown (10YR 5/4) organic debris laterally matted on the matrix from 232-238 cm; many, prominent, fine-medium, light olive brown (25Y 5/4) and yellowish brown (10YR 5/6) redox accumulations on the shale aggregates; common, fine, prominent yellow(2.5Y8/6) jarosite

masses.

Remarks

Entire profile was leached, thus no effervescence found in the core. Gypsum lenses first appear between (135-138) cm (Fig. A.8.). Ash like fine grained light colored material from (75-80) cm. Jarosite mineral grains in the lower profile. Shale aggregates are highly oxidized. Very shallow soil, C- horizon starts near 88cm (). Organic matter/roots found at depth (232-238) cm in the profile.

Core 9 F 3, 1500N, 1500W

A 0-9 cm; very dark brown (10YR 2/2) and very dark grayish brown (10YR 3/2) dry; silty clay; (fine-medium) granular parting to moderate, medium, sub angular blocky; friable when moist and soft when dry; many, very fine- fine roots on the ped faces; very fine material near the abrupt wavy boundary.

B_{t1} 9-37 cm; brown (10YR 4/3) and brown (10YR 5/3) dry; silty clay; weak, medium prismatic parting to (fine-medium) sub angular blocky; firm when moist and slightly hard when dry; few, faint spherical black charcoal lens in the matrix; many, faint continuous clay films on ped faces; common, fine roots on ped faces; abrupt smooth boundary.

B_{t2} 37-67 cm; very dark gray (2.5Y 3/2) and dark grayish brown (2.5Y 4/2) dry; silty clay; weak, medium prismatic parting to (fine-medium) sub angular blocky; firm when moist and slightly hard when dry; many, faint continuous clay films on ped faces; few, fine, pale yellow (5Y 7/4) jarosite masses, organic matter/root zone between (52-57) cm and (65-69) cm; few, finely disseminated, faint, very fine grains on the matrix from

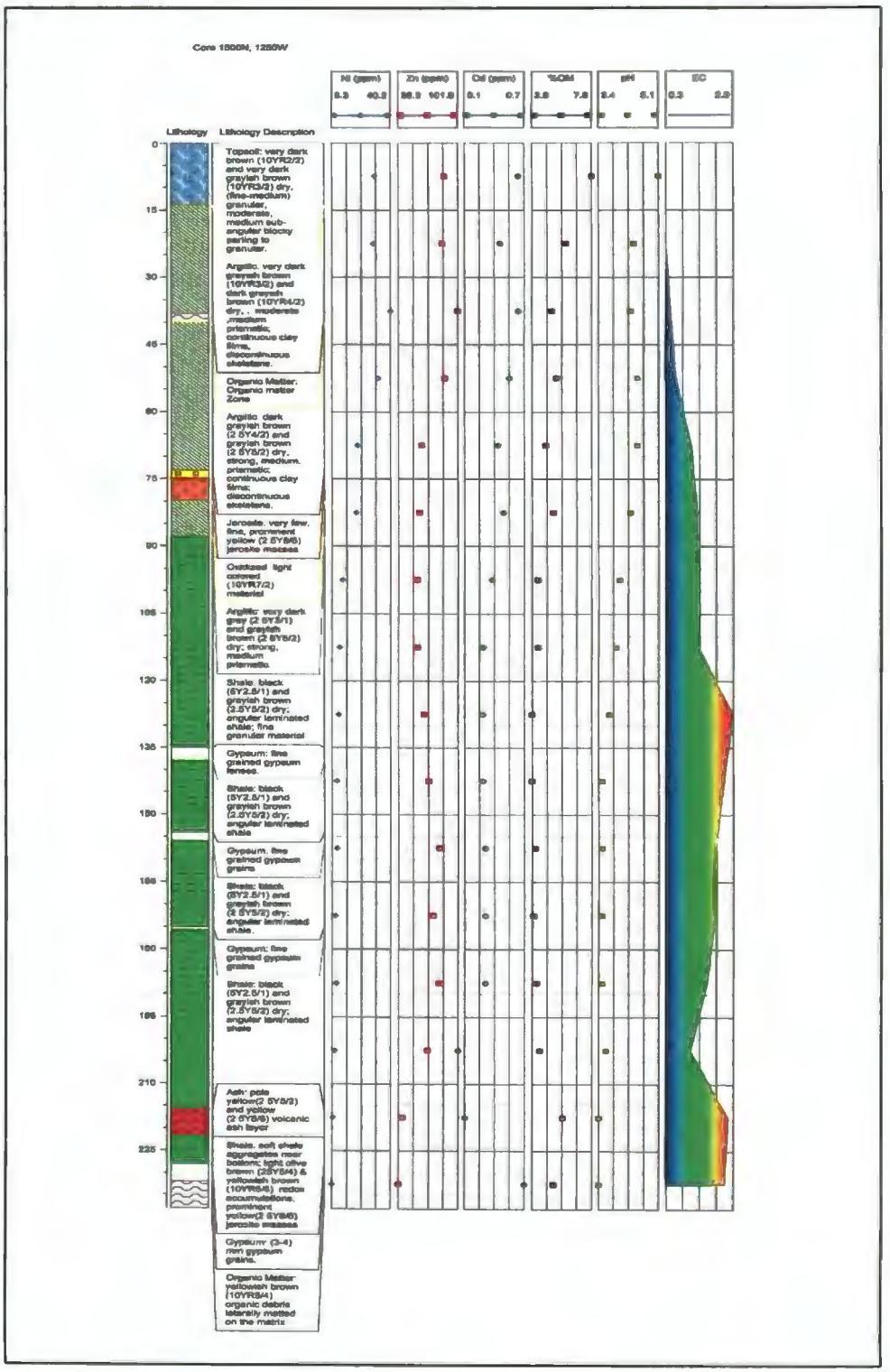

Fig.A.8. Graphical representation of core 8 showing lithology and chemical properties.

(60-64) cm; common, very fine-fine roots on ped faces; abrupt smooth boundary.

C_r 67-239 cm; very dark gray (2.5Y 3/1),gray (2.5Y 5/1) and dark gray (2.5Y 4/1), gray (2.5Y 6/1) dry; silty clay; angular laminated shale; gray (5Y 6/1) and gray 5Y 5/1) dry organic shale zone between (120-124) cm; very firm when moist and slightly hard when dry; pale yellow (2.5Y 7/4) and yellowish brown (10YR 5/8) ash layer between (104-110) cm; common,(fine-medium), irregular, prominent pale yellow (2.5Y 7/4) and light olive brown (2.5Y 5/4) redox accumulations; medium, prominent, irregular, yellow (10YR 7/8) moist redox accumulations at 225 cm; few, fine, prominent, pale yellow(5Y 7/4) jarosite masses at 132 cm; few, fine roots between (148-163) cm and (189-215) cm.

Remarks

Entire profile was leached. Moderately deep soil. Ash layer from (104-110) cm (Fig. A.9.). Thick redox zones before and after ash layer. First redox accumulation near 72 cm. Highly oxidized shale. Many, fine roots upto 67 cm; few very fine roots in Cr. Cr very up in the profile; starts at 67 cm.

Core 10 F 3, 1500N, 1750W

A 0-14 cm; very dark brown (10YR 2/2) and light brownish gray (10YR 5.5/1) dry; silty clay; (fine-medium) granular parting to moderate, medium sub-angular blocky; very friable when moist and moderately hard when dry; many, fine-medium roots on ped faces.

B_{t1} 14-37 cm; very dark gray (10YR 3/1) and light brownish gray(10YR 5/2)dry; silty clay; moderate, medium prismatic; friable when moist and slightly hard when dry; many, faint, continuous, clay films on ped faces; common, distinct, spherical, black charcoal lenses; common, fine, spherical grains embedded in the matrix; common,

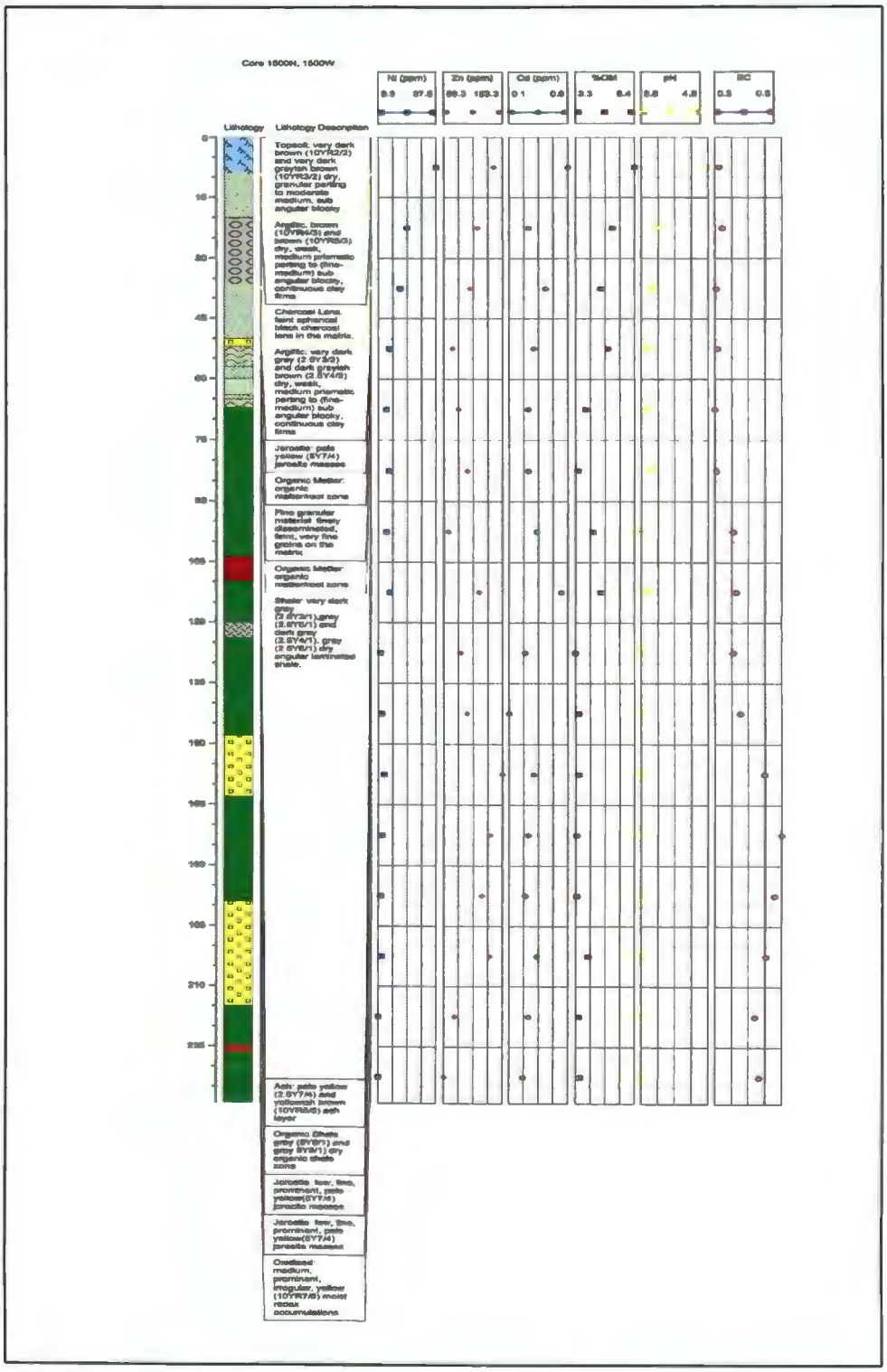

Fig.A.9. Graphical representation of core 9 showing lithology and chemical properties.

medium, prominent, dark yellowish brown (10YR 4/4)and yellowish brown (10YR 5/4) dry, sharp, redox accumulations or weathered zone from (14-22) cm; many, fine-medium roots in the matrix.

B_{t2} 37-75 cm; very dark gray (2.5Y 3/2) and dark gray (2.5Y 4/2) dry; silty clay; strong, medium prismatic; friable when moist and hard when dry; common, faint, continuous, clay films; common, fine, spherical grains; many, medium, prominent, brownish yellow (10YR 6/6) and yellow (2.5Y 7/6) and pale yellow (2.5Y 7/3) and pale yellow (2.5Y 8/3) dry, redox accumulations/ spherical grains (46-57) cm; many, medium, prominent, irregular, light yellowish brown (2.5Y 6/3) dry, redox depletions (58-73); common, fine, sub-angular, shale fragments; many, very fine-fine roots on the ped faces.

BC 75-90 cm; very dark gray (2.5Y 3/1) and dark gray (2.5Y 4/1) dry; silty clay; weak, medium prismatic; friable when moist and hard when dry; few, medium, prominent, irregular, light yellowish brown (2.5Y 6/3) dry, redox depletions; common, fine, (1-2) cm sub-angular, shale fragments; few, very fine roots on ped faces.

C_r 90-236 cm; black (2.5Y 2.5/1) and black (5Y 2.5/1) moist and gray (2.5Y 5/1) and dark gray (2.5Y 4/1) dry; silt clay; angular, laminated shale; firm when moist and hard when dry; few, medium, prominent, irregular, brownish yellow (10YR 6/6) and yellow (2.5Y7/6) dry, redox accumulations; many, fine-medium, pale yellow (5Y 7/4) jarosite masses from (71-93) cm; few, very fine roots.

Remarks

Entire profile leached. Very dark colored shale near 120 cm (Fig. A.10.). Very shallow soil. Shale fragments found high up in the profile. First redox accumulations near 46 cm. Many, fine spherical grains in the argillic horizon. Jarosite masses in lower profile.

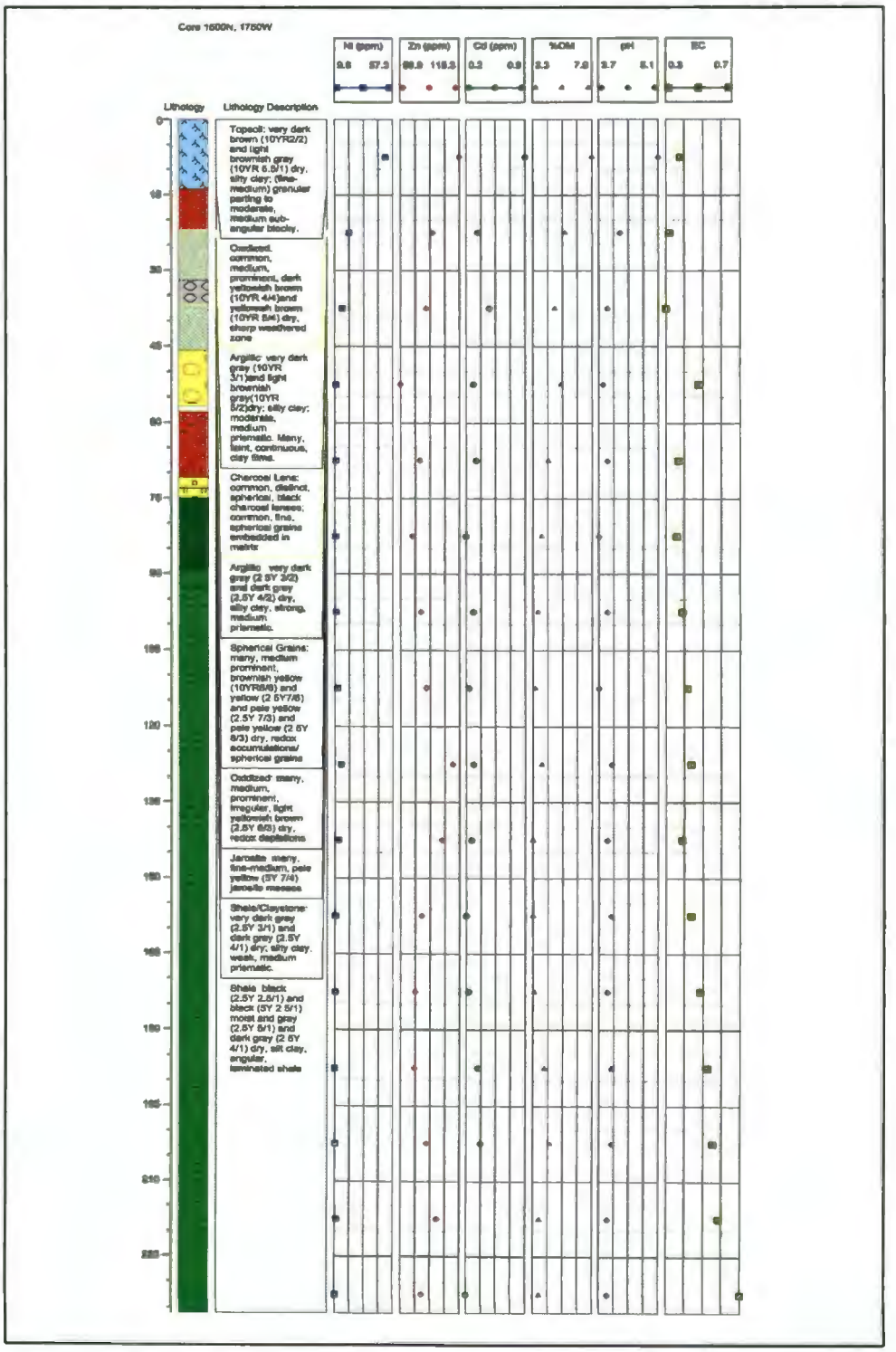

Fig.A.10. Graphical representation of core 10 showing lithology and chemical properties.

Core 11 F3, 1700N, 1250W

A (0-11) cm; very dark brown (10YR 2/2) and light brownish gray (10YR 6/2) dry; silty clay; fine-medium granular parting to moderate, medium sub-angular blocky; very friable when moist and slightly hard when dry; many, fine-medium roots on ped faces.

E (11-18) cm; dark grayish brown (10YR 4/2) and light brownish gray (10YR 6.5/2) dry; silty clay; moderate, fine prismatic parting to fine sub-angular blocky; very friable when moist and moderately hard when dry; many, faint, very fine sand grains; few, fine, prominent, black (10YR 2/1) dry, sub-angular charcoal/organic matter mass in the matrix, black when crushed, many, fine-medium roots on ped faces.

B_{t1} (18-38) cm; olive brown (2.5Y 4/4) and grayish brown (10YR 5.5/2) dry; silty clay; moderate, medium prismatic; very friable when moist and hard when dry; many, faint, continuous clay films; common, fine, prominent, sharp, light yellowish brown (2.5Y 6/3) dry, redox depletion masses between (30-33) cm; few, fine, prominent, sub-angular, black (10YR 2/1) dry, charcoal/organic matter in the matrix; few, fine-medium, faint, sub-angular-spherical, grains/shale fragments; many, fine roots on ped faces.

B_{t2} (38-71) cm; very dark gray (2.5Y 3/1) and grayish brown (2.5Y 5/2) dry; silty clay; strong, medium prismatic; friable when moist and slightly hard when dry; common, faint, continuous clay films; common, fine-medium, faint, sub-angular to spherical grains; few, fine, prominent, pale yellow (2.5Y 7/4) dry, jarosite mass/redox accumulations at 48 cm; very friable, granular, anomalous sedimentary zone from (60-65) cm; common, fine, prominent, pale yellow (2.5Y 7/4) dry irregular and threadlike jarosite at 67 cm and in the sedimentary zone; (0.5-1) cm, fine, shale fragments from (59-65) cm; common, fine-medium roots on ped faces.

BC (71-106) cm; dark gray (2.5Y 4/1) and gray (2.5Y 5/1) dry; silty clay; weak, medium prismatic; friable when moist and slightly hard when dry; common, discontinuous clay films; common, fine, shale fragments embedded in the matrix; few, fine, prominent, black (10YR 2/1) dry, charcoal/organic matter concentrations; few, fine, threadlike, pale yellow (2.5Y 7/4) dry jarosite between (75-78) cm; common, (1 cm) shale fragments in the lower part near 94 cm; few, very fine-fine roots in the matrix; root/organic matter zone at 110 cm.

Cr (106-236) cm; black (5Y 2.5Y/1) moist and gray (2.5Y 5/1) dry; silty clay; angular laminated shale; friable when moist and slightly-moderately hard when dry; few, fine, prominent, yellowish brown (10YR 5/6) dry redox accumulations at 117 cm; few, fine, prominent, pale yellow (2.5Y 7/4) dry jarosite mass; few, medium, prominent, irregular, brownish yellow (10YR 6/6) dry redox accumulations between (160-163) cm; few, medium, prominent, irregular, very pale brown (10YR 8/2) dry ash layer from (163-168) cm; few, medium, threadlike pale yellow (2.5Y 7/4) dry jarosite mass in the ash layer; organic matter zone from (165-177) cm, and (188-197) cm and (228-234) cm.

Remarks

Entire profile leached for this core, thus no effervescence seen. First redox depletions seen at 30 cm (Fig. A.11.). Sub-angular to spherical charcoal/organic matter in the argillic horizon. Irregular, thread like jarosite mineral found in the whole soil profile. Shale is highly oxidized. Redox accumulations followed by ash layer from (163-168) cm. Several organic matter zones in the lower soil profile. Anomalous fine grained sedimentary zone from (60-65) cm. Fine shale fragments in the argillic horizon up in the profile. These shale fragments found up in the profile suggest shallow shale horizons for upslope location.

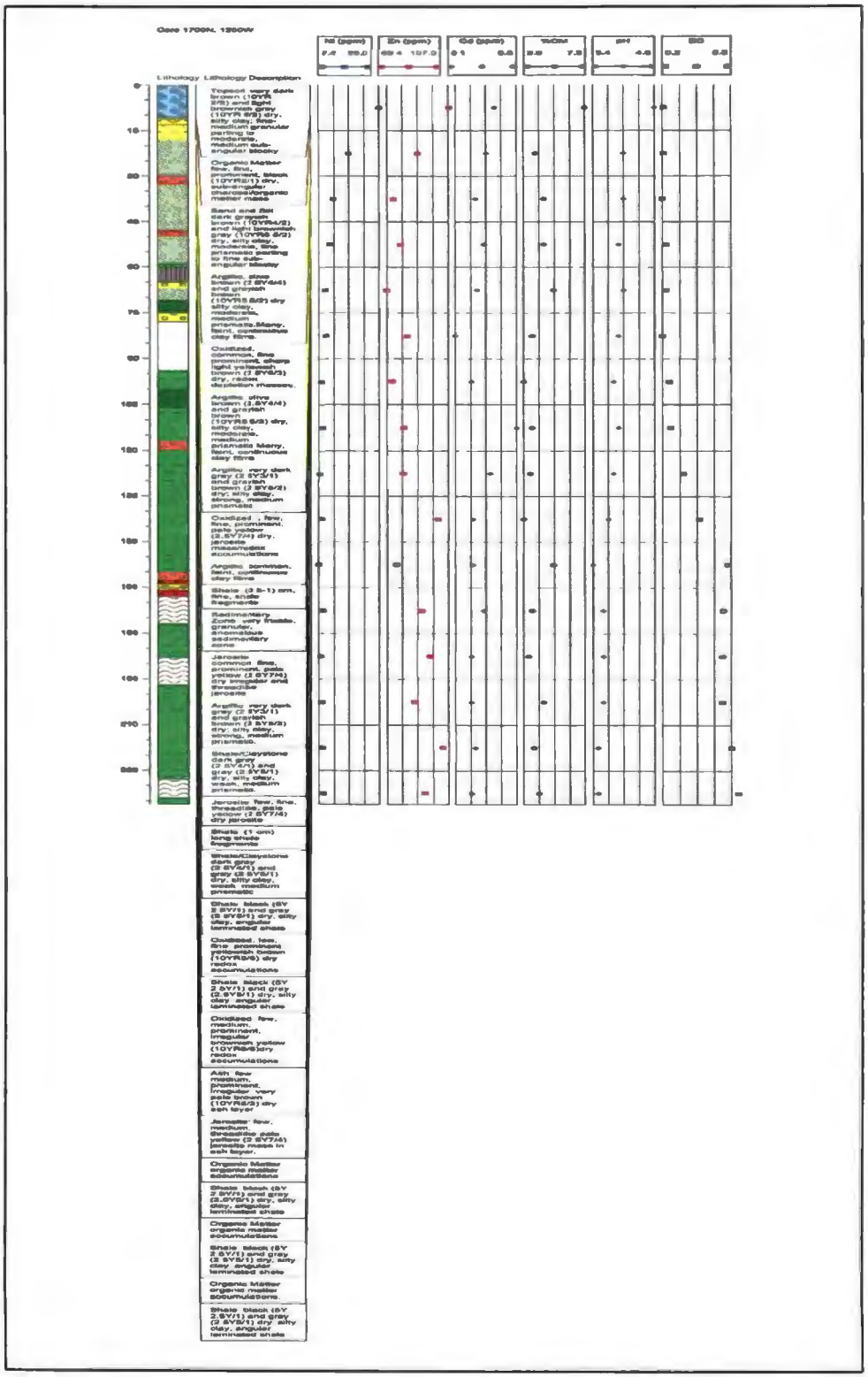

Fig.A.11. Graphical representation of core 11 showing lithology and chemical properties.

Core 12 F3, 1700N, 1500W

A (0-16) cm; very dark brown (10YR 2/2) and very dark grayish brown (10YR 4/1) dry; silty clay loam; fine-medium granular parting to moderate, medium sub-angular blocky; very friable when moist and slightly hard when dry; many, fine-medium roots in the matrix.

E (16-26) cm; dark grayish brown and pale brown (10YR 6/3) dry; silty clay; moderate, medium prismatic; very friable when moist and slightly hard when dry; many, very fine sand grains; common, very-fine roots on ped faces.

B_{t1} (26-52) cm; very dark grayish brown (2.5Y 3/2) and light olive brown (2.5Y 5/3) dry; silty clay loam; strong, medium prismatic; friable when moist and moderately hard when dry; common, discontinuous clay films; common, fine, prominent, pale yellow (5Y 7/4) dry jarosite mass; common, medium, prominent, light olive brown (2.5Y 5/4) dry redox accumulations; many, fine roots on ped faces.

B_{t2} (52-66) cm; very dark grayish brown (2.5Y 3/2) and grayish brown (2.5Y 5/2) dry; silty clay loam; weak, medium prismatic parting to moderate, fine sub-angular blocky; friable when moist and slightly hard when dry; anomalous zone between (53-57) cm with fine, shale fragments; organic matter zone from (57-60) cm; few, fine, prominent, irregular dark yellowish brown (10YR 4/6) dry redox accumulations; common, fine, prominent, pale yellow (5Y 7/4) dry jarosite mass; common, continuous clay films; fine, granular material over the matrix; many, medium roots on ped faces.

B_{t3} (66-84) cm; dark olive gray (5Y 3/2) and grayish brown (2.5Y 5/2) dry; silty clay; strong, medium prismatic; friable when moist and moderately hard when dry; common, fine, sub-angular shale fragments embedded between the ped faces; few,

discontinuous clay films; anomalous oxidized/leached zone from (80-101) cm; common, medium, prominent, pale yellow (5Y 7/4) dry jarosite mass; many, medium prominent, irregular, dark yellowish brown (10YR 4/6) dry and white (2.5Y 8/1) dry and light gray (2.5Y 7/1) dry redox accumulations; organic debris at 100cm; common, very fine roots on ped faces.

$\mathbf{C_r}$ (84-236) cm; black (5Y 2.5/1) and gray (2.5 Y5/1) dry; silty clay; angular laminated shale; firm when moist and hard when dry; common, prominent, irregular light gray (2.5Y 7/2) dry ash layer from (124-127) cm; many, medium, prominent, pale yellow (5Y 7/4) dry jarosite mass; many, fine-medium, prominent, irregular dark yellowish brown (10YR 4/6) dry redox accumulations; many, medium, prominent, pale yellow (5Y 7/4) dry jarosite mass zone from (160-165) cm; many, medium, prominent, irregular, light gray (2.5Y 7/2) dry and very pale brown (10YR 8/2) dry and brownish yellow (10YR 6/6) dry ash layer from (165-169) cm; few, very fine roots in the matrix.

Remarks

Entire profile was leached. Anomalous zone with fine shale fragments from (53-57) cm (Fig. A.12.). Ash layers from (124-127) cm and (165-169) cm. Jarosite zone from (165-169) cm. Highly oxidized/leached zone from (80-101) cm. Jarosite and redox accumulations upto the bottom of the profile.

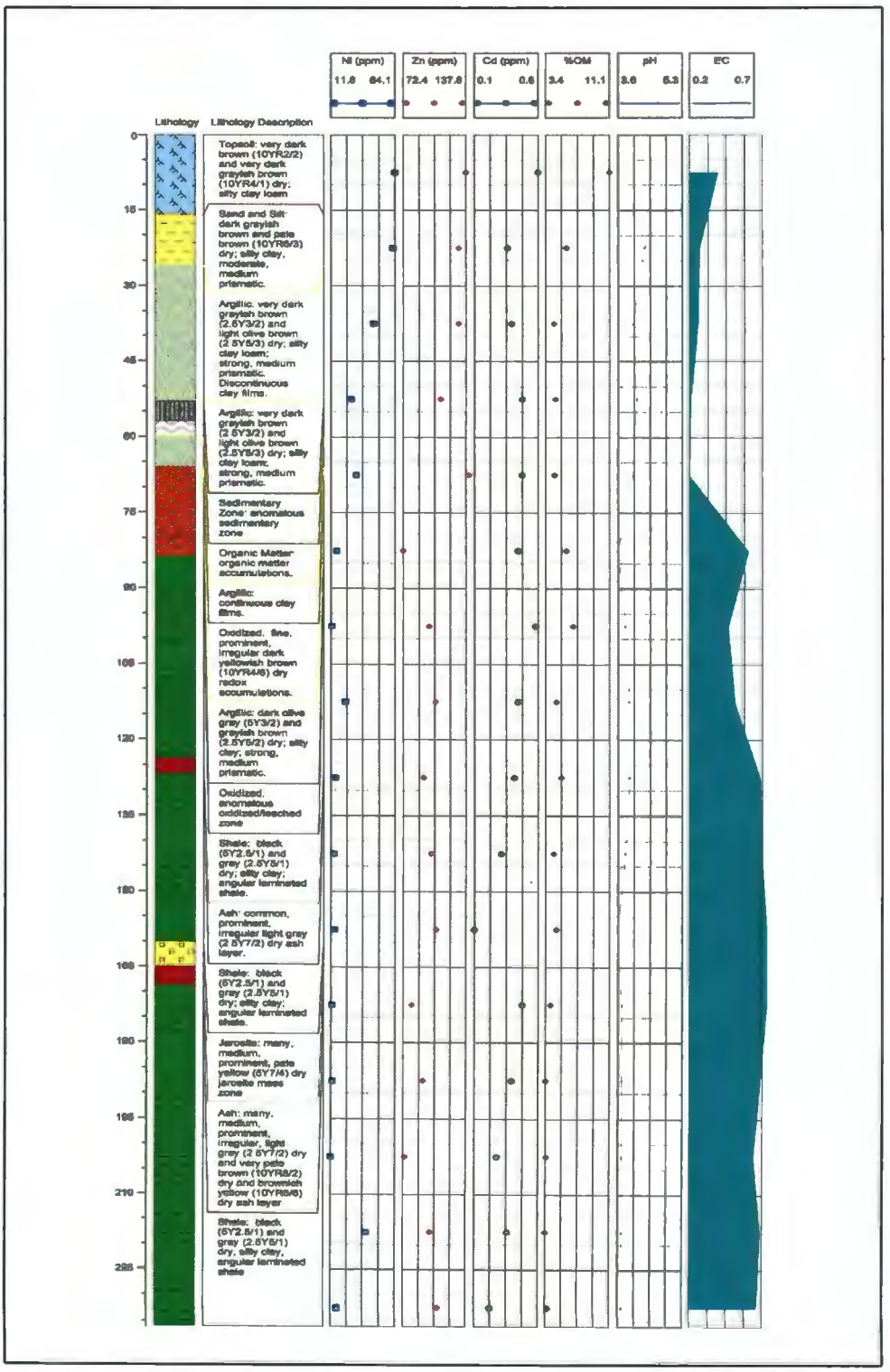

Fig.A.12. Graphical representation of core 12 showing lithology and chemical properties.

APPENDIX B. PARTICLE SIZE ANALYSIS

Table B.1. Particle size analysis for surface and core samples.

	Texture		
Sample No.	**% Sand**	**%Silt**	**%Clay**
1	18.28	33.48	48.25
2	3.30	32.66	64.04
3	17.03	36.54	46.44
4	2.45	42.35	55.20
5	15.48	36.12	48.40
6	16.28	34.27	49.45
7	6.45	37.52	56.03
8	15.63	33.02	51.35
9	16.98	31.17	51.85
10	7.55	36.92	55.53
11	17.10	35.72	47.18
12	28.68	33.59	37.74
13	17.08	36.75	46.17
14	16.18	33.54	50.28
15	16.20	34.32	49.48
16	13.28	38.01	48.72
17	6.20	37.85	55.95
18	12.73	35.22	52.06
19	17.70	34.33	47.97
20	3.35	32.55	64.10
21	0.73	28.62	70.66
22	7.85	34.94	57.21
23	15.05	36.41	48.54
24	7.20	26.31	66.49
25	7.32	40.40	52.27
26	8.20	47.98	43.82
27	9.75	48.86	41.39
28	11.75	52.62	35.63
29	9.00	50.90	40.10
30	2.90	51.88	45.22
31	3.53	48.69	47.78
32	7.43	55.82	36.76
33	1.83	54.29	43.89
34	5.58	44.95	49.48
35	1.68	50.73	47.59
36	15.35	46.79	37.86
37	9.70	54.69	35.61
38	6.98	55.42	37.61
39	1.63	30.27	68.10

Table B.1. (continued)

40	3.85	38.96	57.19
41	7.83	48.98	43.20
42	5.95	48.38	45.67
43	3.98	51.27	44.75
44	8.35	53.45	38.20
45	16.30	54.01	29.69
46	2.80	45.69	51.51
47	1.35	32.03	66.62
48	6.05	29.29	64.66
49	8.55	39.94	51.51
50	1.30	30.59	68.11
51	9.43	37.47	53.10
52	6.88	48.11	45.02
53	4.78	35.23	60.00
54	4.05	33.09	61.96
55	4.08	39.56	56.36
56	2.83	39.72	57.45
57	7.20	37.19	55.61
58	0.85	43.54	55.61
59	2.30	39.45	58.25

Table B.2. Summary of sample identification for particle size analysis.

Sample Name	Sample ID
PE (0-15)	1
PS (30-50)	2
PN (0- 15)	3
PE (30-50)	4
PS (0-15)	5
PN (30-50)	6
PW (30-50)	7
PC (0-15)	8
PC (15-30)	9
PC (30-50)	10
PD1(0-15)	11
PD3 (0-15)	12
CRP1 (0-15)	13
CRP1 (30-50)	14
PW (0-15)	15
PD2 (0-15)	16
CRP1 (114-130)	17
CRP2 (0-15)	18
CRP2 (30-50)	19

Table B.2. (continued)

CRP2 (10" to auger handle)	20
CRP2 (Brown oxides)	21
CRP2 (7cm to handle)	22
CRP3 (0-15)	23
CRP3 (30-50)	24
CRP3 (5'Lime layer)	25
1500N, 0W (0-24)	26
1500N, 0W(24-69)	27
1500N, 0W (69-105)	28
1500N, 0W (105-120)	29
1500N, 0W (120-168)	30
1500N, 0W (168-225)	31
1500N, 250W (0-11)	32
1500N, 250W (11-24)	33
1500N, 250W (24-50)	34
1500N,250W(50-112)	35
1500N, 250W (112-147)	36
1500N, 250W (147-233)	37
1500N, 1000W (0-15)	38
1500N, 1000W (17-43)	39
1500N, 1000W (43-65)	40
1500N,1000W(65-118)	41
1500N, 1000W (118-144)	42
1500N, 1000W (144-181)	43
1500N, 1000W (186-211)	44
1500N, 1000W (211-238)	45
1500N, 1500W (0-9)	46
1500N, 1500W (9-37)	47
1500N, 1500W (37-67)	48
1500N, 1500W (67-104)	49
1500N, 1500W (111-161)	50
1500N, 1500W(161-209)	51
1500N, 1500W (209-239)	52
1500N, 1750W (0-14)	53
1500N, 1750W (14-37)	54
1500N, 1750W (37-75)	55
1500N, 1750W (75-90)	56
1500N, 1750W (90-147)	57
1500N, 1750W (147-204)	58
1500N, 1750W (204-236)	59

APPENDIX C. CLAY MINERAL ANALYSIS

Table C.1. Summary of sample identification for X-Ray diffraction.

Sample Name	Sample ID
PE (0-15)	1
PS (30-50)	2
PN (0- 15)	3
PE (30-50)	4
PS (0-15)	5
PN (30-50)	6
PW (30-50)	7
PC (0-15)	8
PC (15-30)	9
PC (30-50)	10
PD1(0-15)	11
PD3 (0-15)	12
CRP1 (0-15)	13
CRP1 (30-50)	14
PW (0-15)	15
PD2 (0-15)	16
CRP1 (114-130)	17
CRP2 (0-15)	18
CRP2 (30-50)	19
CRP2 (10" to auger handle)	20
CRP2 (Brown oxides)	21
CRP2 (7cm to handle)	22
CRP3 (0-15)	23
CRP3 (30-50)	24
CRP3 (5'Lime layer)	25

X-Ray diffraction conditions including peak lists, position (°2Th.), height (cts), d-spacing (Å), relative intensity (Rel. Int) (%) and patterns after air dried and glycolated exposures have been recorded for samples 1 through 25 with diffraction diagrams from Fig.C.1.-Fig. C.25 with red line indicating air dried pattern and black line indicating glycolated pattern. The X-axis marks the position (°2Th.) and Y-axis marks height in counts.

Sample 1

Table C.2. Peak list for air dried sample 1.

Pos. [°2Th.]	Height [cts]	d-spacing [Å]	Rel. Int. [%]
12.2238	120.17	7.23483	55.06
17.6383	23.84	5.02426	10.92
24.7958	218.25	3.58781	100.00
26.6306	178.13	3.34462	81.62
37.6133	27.47	2.38944	12.58

Table C.3. Peak list for glycolated sample 1.

Pos. [°2Th.]	Height [cts]	d-spacing [Å]	Rel. Int. [%]
5.3296	279.13	16.56811	62.78
8.7178	48.27	10.13499	10.86
12.3155	129.01	7.18120	29.01
15.6860	2.85	5.64490	0.64
17.7216	35.77	5.00081	8.05
20.7189	7.71	4.28366	1.73
24.8525	216.74	3.57974	48.75
26.6894	444.63	3.33739	100.00
29.3511	58.34	3.04051	13.12
37.6906	30.48	2.38473	6.86

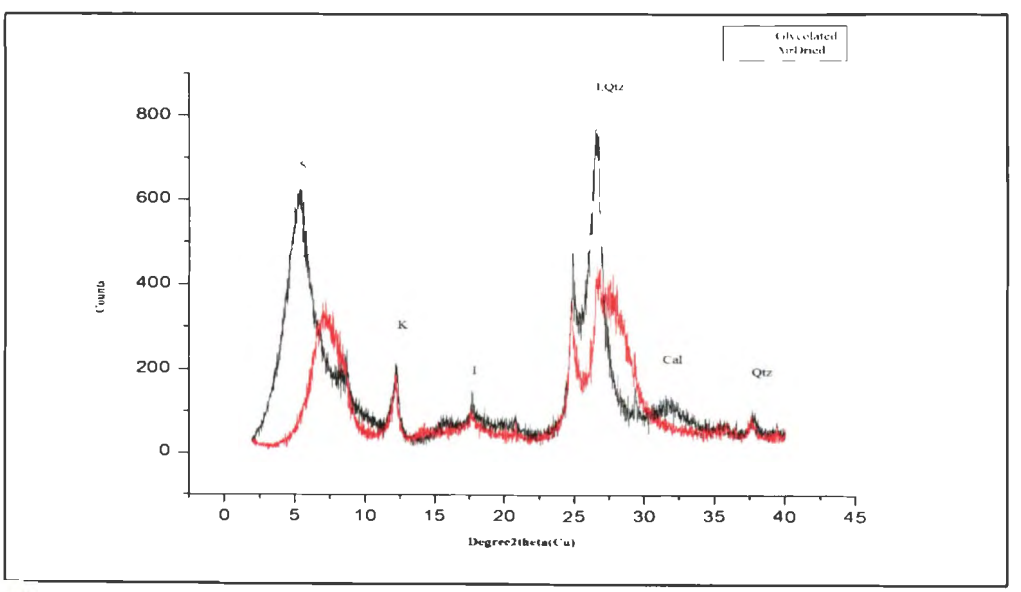

Fig.C.1. X-Ray diffraction patterns for major clay and other minerals for air dried and glycolated sample 1. S: Smectite, K: Kaolinite, I: Illite, Qtz: Quartz, Cal: Calcite.

Sample 2

Table C.4. Peak list for air dried sample 2.

Pos. [°2Th.]	Height [cts]	d-spacing [Å]	Rel. Int. [%]
5.8247	598.26	15.16094	100.00
12.3065	69.60	7.18643	11.63
17.6174	30.63	5.03015	5.12
24.9025	73.50	3.57268	12.29
29.4104	311.73	3.03452	52.11

Table C.5. Peak list for glycolated sample 2.

Pos. [°2Th.]	Height [cts]	d-spacing [Å]	Rel. Int. [%]
5.1384	578.13	17.18433	100.00
10.3562	16.30	8.53501	2.82
12.2251	58.03	7.23407	10.04
15.6908	29.61	5.64319	5.12
24.8567	47.70	3.57914	8.25
26.6331	145.16	3.34431	25.11
29.3810	222.09	3.03748	38.42
31.6120	14.54	2.82802	2.51

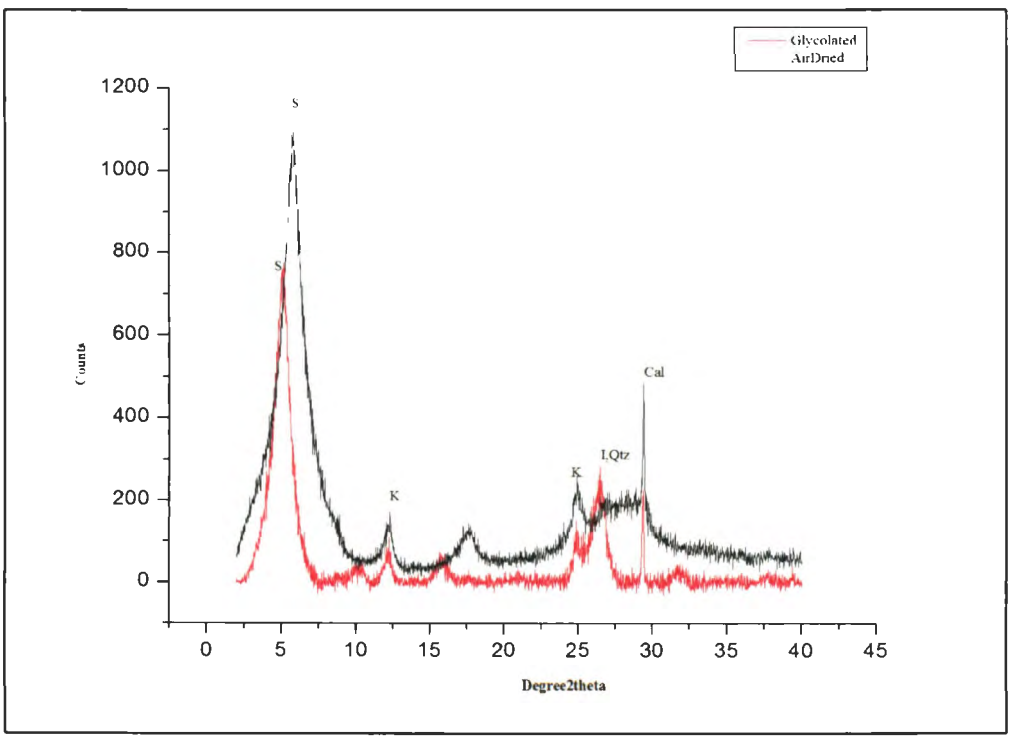

Fig.C.2. X-Ray diffraction patterns for major clay and other minerals for air dried and glycolated sample 2. S: Smectite, K: Kaolinite, I:I llite, Qtz: Quartz, Cal: Calcite.

Sample 3

Table C.6. Peak list for air dried sample 3.

Pos. [°2Th.]	Height [cts]	d-spacing [Å]	Rel. Int. [%]
8.6736	95.16	10.18650	32.88
12.2633	120.06	7.21164	41.49
17.6335	24.42	5.02562	8.44
20.7393	40.85	4.27949	14.12
24.7681	165.36	3.59175	57.14
26.5444	289.40	3.35529	100.00
29.2925	228.63	3.04647	79.00
37.5995	28.25	2.39029	9.76
39.3351	34.25	2.28873	11.84

Table C.7. Peak list for glycolated sample 3.

Pos. [°2Th.]	Height [cts]	d-spacing [Å]	Rel. Int. [%]
8.6087	23.99	10.26321	5.29
12.1703	97.59	7.26651	21.53
17.6205	29.53	5.02928	6.51
20.6779	43.86	4.29205	9.68
24.7501	180.12	3.59432	39.73
26.4533	453.37	3.36664	100.00
29.2556	254.44	3.05022	56.12
37.5379	30.90	2.39407	6.82

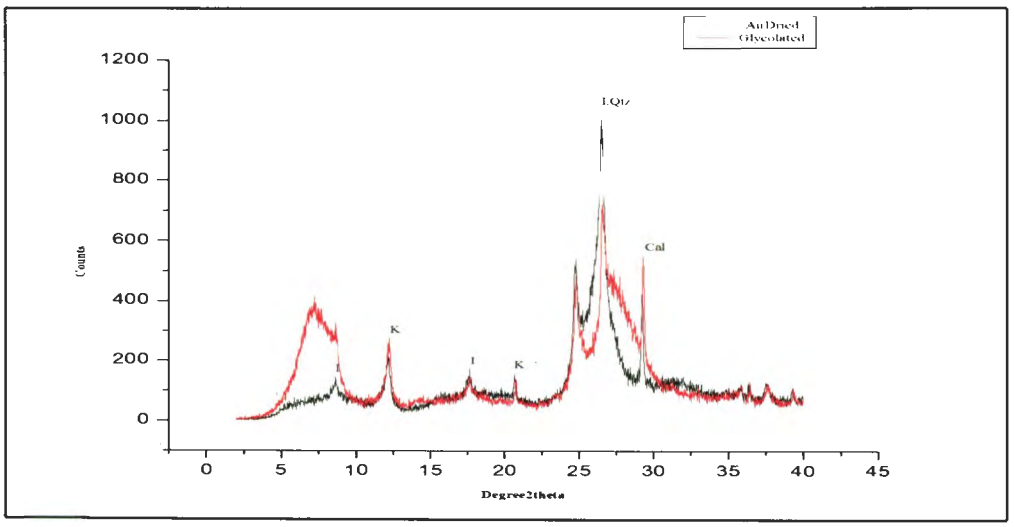

Fig.C.3. X-Ray diffraction patterns for major clay and other minerals for air dried and glycolated sample 3.S: Smectite, K: Kaolinite,I:Illite,Qtz:Quartz, Cal:Calcite.

Sample 4

Table C.8. Peak list for air dried sample 4.

Pos. [°2Th.]	Height [cts]	d-spacing [Å]	Rel. Int. [%]
7.2087	221.00	12.25297	8.97
12.3417	107.23	7.16600	4.35
17.7469	13.93	4.99376	0.57
24.9035	168.47	3.57252	6.84
26.7729	66.11	3.32717	2.68
28.1870	56.46	3.16338	2.29
29.4071	2463.71	3.03485	100.00
35.9698	121.18	2.49477	4.92
37.7055	26.59	2.38381	1.08
39.4131	194.63	2.28438	7.90

Table C.9. Peak list for glycolated sample 4.

Pos. [°2Th.]	Height [cts]	d-spacing [Å]	Rel. Int. [%]
5.1458	139.96	17.15946	5.79
12.2993	88.10	7.19061	3.65
24.8766	128.92	3.57633	5.34
26.6157	188.11	3.34646	7.79
29.3792	2415.11	3.03767	100.00
35.9572	109.13	2.49561	4.52
37.7256	22.16	2.38259	0.92
39.3753	207.44	2.28649	8.59

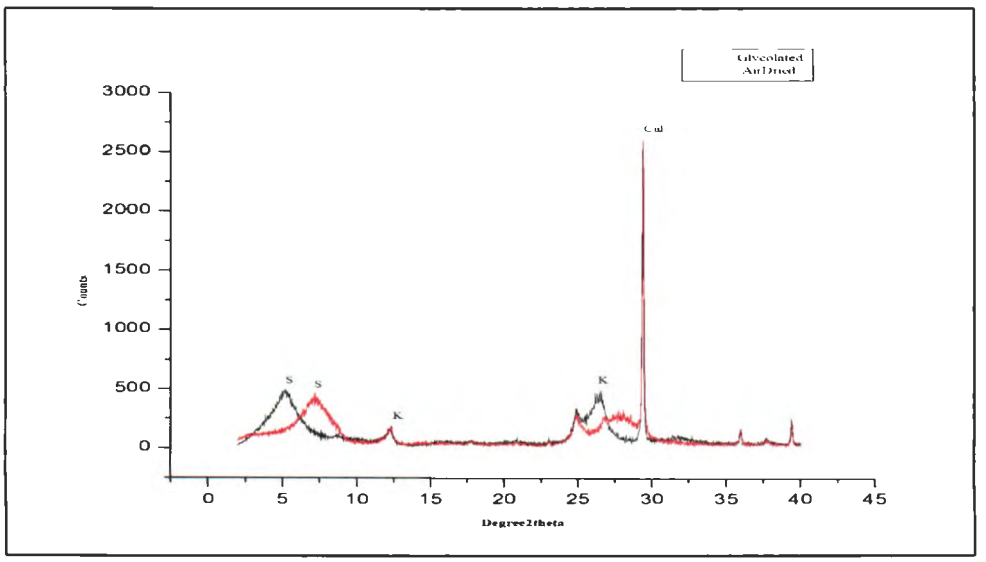

Fig.C.4. X-Ray diffraction patterns for major clay and other minerals for air dried and glycolated sample 4. S: Smectite,K: Kaolinite, Cal: Calcite.

Sample 5

Table C.10. Peak list for air dried sample 5.

Pos. [°2Th.]	Height [cts]	d-spacing [Å]	Rel. Int. [%]
7.0529	371.27	12.52322	59.06
8.8298	138.98	10.00674	22.11
12.3863	159.66	7.14031	25.40
17.7535	42.04	4.99191	6.69
24.9167	253.67	3.57067	40.36
26.6353	319.04	3.34404	50.75
29.4157	628.60	3.03398	100.00
35.9531	40.69	2.49588	6.47
37.6965	28.92	2.38436	4.60

Table C.11. Peak list for glycolated sample 5.

Pos. [°2Th.]	Height [cts]	d-spacing [Å]	Rel. Int. [%]
5.5227	327.45	15.98937	55.98
8.8286	47.58	10.00810	8.13
12.3997	130.42	7.13263	22.29
17.7779	33.73	4.98511	5.77
24.8985	274.60	3.57323	46.94
26.6705	584.09	3.33971	99.85
29.4324	584.99	3.03230	100.00
35.9898	42.76	2.49343	7.31
37.6988	28.25	2.38422	4.83

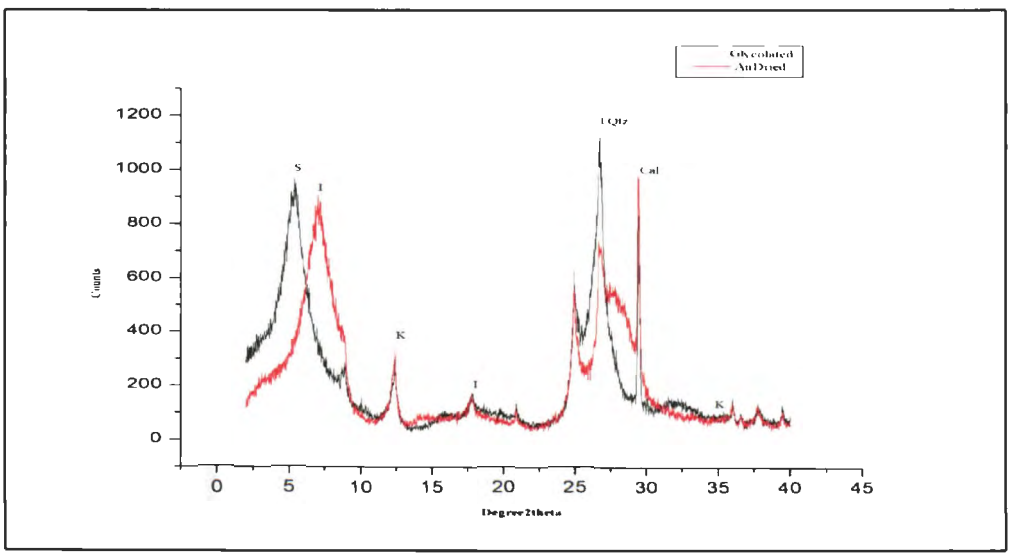

Fig.C.5. X-Ray diffraction patterns for major clay and other minerals for air dried and glycolated sample 5. S: Smectite, K: Kaolinite, I: Illite, Qtz: Quartz, Cal: Calcite.

Sample 6

Table C.12. Peak list for air dried sample 6.

Pos. [°2Th.]	Height [cts]	d-spacing [Å]	Rel. Int. [%]
7.0614	250.20	12.50830	21.77
8.6520	112.72	10.21190	9.81
12.3123	151.72	7.18305	13.20
17.7219	27.06	5.00073	2.35
24.8622	232.14	3.57837	20.20
26.6569	183.17	3.34138	15.93
29.3771	1149.50	3.03788	100.00
35.9449	80.24	2.49643	6.98
37.6700	25.56	2.38598	2.22
39.3744	95.04	2.28653	8.27

Table C.13. Peak list for glycolated sample 6.

Pos. [°2Th.]	Height [cts]	d-spacing [Å]	Rel. Int. [%]
5.0873	330.33	17.35687	27.08
8.7803	43.42	10.06299	3.56
12.3139	140.43	7.18212	11.51
15.7400	13.48	5.62565	1.11
17.7036	24.26	5.00586	1.99
24.8585	245.55	3.57889	20.13
26.6463	432.08	3.34269	35.43
29.3835	1219.66	3.03723	100.00
35.9469	85.69	2.49630	7.03
37.6850	32.77	2.38506	2.69
39.3768	108.66	2.28640	8.91

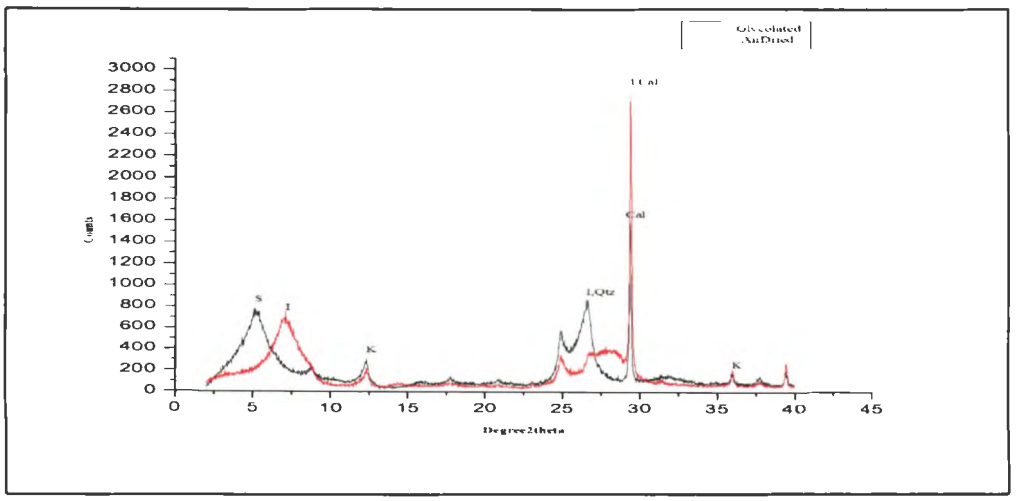

Fig.C.6. X-Ray diffraction patterns for major clay and other minerals for air dried and glycolated sample 6. S: Smectite, K: Kaolinite, I: Illite, Qtz: Quartz, Cal: Calcite.

Sample 7

Table C.14. Peak list for air dried sample 7.

Pos. [°2Th.]	Height [cts]	d-spacing [Å]	Rel. Int. [%]
6.9514	237.04	12.70598	10.99
12.3185	85.06	7.17943	3.94
17.7740	6.54	4.98619	0.30
24.8940	124.55	3.57387	5.78
26.7545	67.60	3.32942	3.13
29.4066	2156.66	3.03490	100.00
35.9731	125.42	2.49454	5.82
39.4093	164.41	2.28459	7.62

Table C.15. Peak list for glycolated sample 7.

Pos. [°2Th.]	Height [cts]	d-spacing [Å]	Rel. Int. [%]
5.2145	342.27	16.93347	15.49
12.3092	85.11	7.18485	3.85
15.7037	14.58	5.63857	0.66
20.8861	19.01	4.24974	0.86
24.8577	129.64	3.57901	5.87
26.6504	292.54	3.34219	13.24
29.3913	2209.72	3.03644	100.00
35.9570	116.33	2.49562	5.26
37.7025	17.86	2.38400	0.81
39.3863	189.56	2.28587	8.58

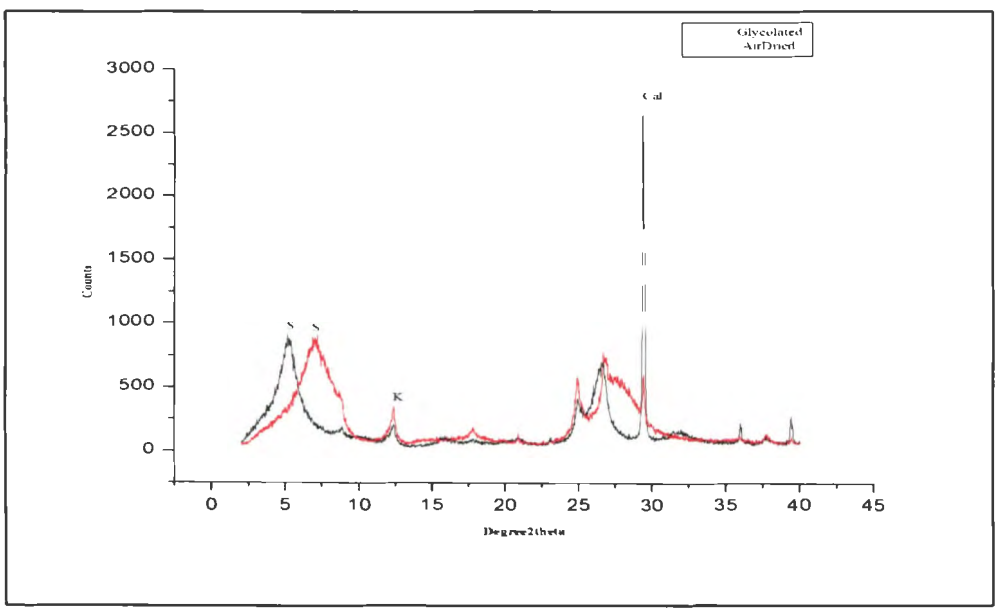

Fig.C.7. X-Ray diffraction patterns for major clay and other minerals for air dried and glycolated sample 7. S: Smectite, K: Kaolinite, Cal: Calcite.

Sample 8

Table C.16. Peak list for air dried sample 8.

Pos. [°2Th.]	Height [cts]	d-spacing [Å]	Rel. Int. [%]
8.7481	140.23	10.10000	41.83
12.3223	181.14	7.17725	54.03
17.7202	38.22	5.00122	11.40
24.8684	267.79	3.57749	79.87
26.6100	335.27	3.34717	100.00
29.3881	303.92	3.03676	90.65
37.7447	30.67	2.38143	9.15
8.7481	140.23	10.10000	41.83

Table C.17. Peak list for glycolated sample 8.

Pos. [°2Th.]	Height [cts]	d-spacing [Å]	Rel. Int. [%]
5.2061	365.50	16.96082	62.65
8.8097	70.43	10.02951	12.07
12.3198	150.84	7.17869	25.86
15.6953	5.55	5.64160	0.95
17.7199	44.92	5.00130	7.70
20.7127	11.25	4.28492	1.93
24.8786	264.15	3.57605	45.28
26.5968	583.37	3.34880	100.00
29.3764	249.18	3.03795	42.71
37.7173	27.38	2.38309	4.69

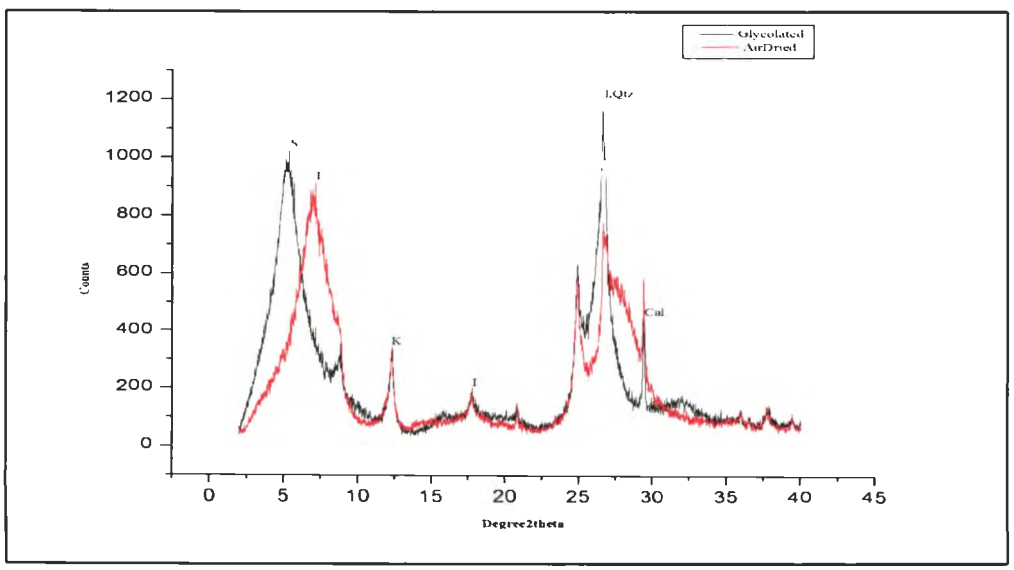

Fig.C.8. X-Ray diffraction patterns for major clay and other minerals for air dried and glycolated sample 8. S: Smectite, K: Kaolinite, I: Illite, Qtz: Quartz, Cal: Calcite.

Sample 9

Table C.18. Peak list for air dried sample 9.

Pos. [°2Th.]	Height [cts]	d-spacing [Å]	Rel. Int. [%]
3.1054	6.12	28.42819	1.53
7.2543	399.17	12.17610	100.00
8.7913	161.60	10.05039	40.48
12.3368	238.45	7.16886	59.74
17.7170	44.96	5.00212	11.26
24.8164	322.28	3.58487	80.74
26.6019	301.01	3.34816	75.41
29.3872	318.22	3.03686	79.72
35.8462	20.65	2.50308	5.17
37.6499	52.48	2.38721	13.15

Table C.19. Peak list for glycolated sample 9.

Pos. [°2Th.]	Height [cts]	d-spacing [Å]	Rel. Int. [%]
5.2428	464.40	16.84236	61.92
8.8068	89.29	10.03277	11.91
12.3548	206.57	7.15845	27.54
15.7400	13.70	5.62568	1.83
17.7251	59.09	4.99984	7.88
20.8627	22.36	4.25446	2.98
24.8713	398.97	3.57707	53.19
26.6034	750.03	3.34798	100.00
29.3752	273.45	3.03807	36.46
31.9275	24.70	2.80079	3.29
37.7348	49.38	2.38203	6.58

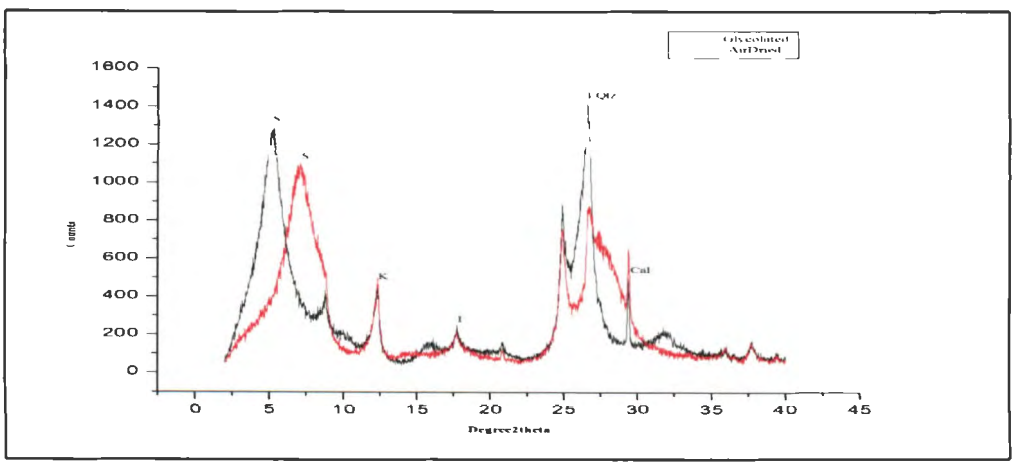

Fig.C.9. X-Ray diffraction patterns for major clay and other minerals for air dried and glycolated sample 9. S: Smectite,, K: Kaolinite, I: Illite, Qtz: Quartz, Cal: Calcite.

Sample 10

Table C.20. Peak list for air dried sample 10.

Pos. [°2Th.]	Height [cts]	d-spacing [Å]	Rel. Int. [%]
7.0527	456.31	12.52359	81.04
12.3221	141.63	7.17737	25.15
17.7935	14.38	4.98078	2.55
24.9161	189.02	3.57075	33.57
26.8776	112.94	3.31445	20.06
29.4165	563.09	3.03390	100.00
35.9313	23.45	2.49735	4.16
37.7130	19.81	2.38336	3.52

Table C.21. Peak list for glycolated sample 10.

Pos. [°2Th.]	Height [cts]	d-spacing [Å]	Rel. Int. [%]
5.2681	609.85	16.76137	100.00
12.3599	107.47	7.15548	17.62
15.6856	32.80	5.64507	5.38
20.8182	11.71	4.26343	1.92
24.8938	182.99	3.57390	30.01
26.6405	432.36	3.34340	70.90
29.3838	527.16	3.03721	86.44
31.8181	24.01	2.81017	3.94
37.6895	21.14	2.38479	3.47
39.3996	50.67	2.28513	8.31

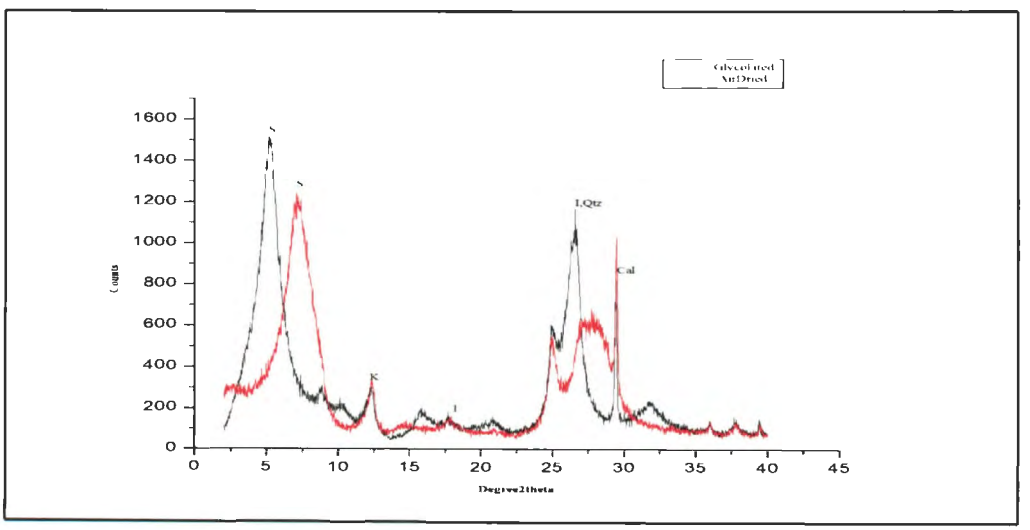

Fig.C.10. X-Ray diffraction patterns for major clay and other minerals for air dried and glycolated sample 10. S: Smectite, K: Kaolinite, I: Illite, Qtz: Quartz, Cal: Calcite.

Sample 11

Table C.22. Peak list for air dried sample 11.

Pos. [°2Th.]	Height [cts]	d-spacing [Å]	Rel. Int. [%]
12.2112	42.51	7.24227	8.94
17.6281	10.06	5.02712	2.12
20.7177	31.74	4.28390	6.68
24.7384	110.02	3.59600	23.14
26.5186	200.62	3.35849	42.20
29.2742	475.39	3.04832	100.00
35.8430	34.13	2.50330	7.18
39.3090	49.39	2.29019	10.39

Table C.23. Peak list for glycolated sample 11.

Pos. [°2Th.]	Height [cts]	d-spacing [Å]	Rel. Int. [%]
8.5944	8.38	10.28028	1.41
12.2499	44.33	7.21948	7.44
17.8594	7.50	4.96254	1.26
20.7354	27.18	4.28028	4.56
24.7916	106.25	3.58840	17.82
26.5059	292.61	3.36007	49.09
29.3100	596.10	3.04469	100.00
35.8664	48.34	2.50172	8.11
37.6606	17.38	2.38656	2.92
39.3203	76.76	2.28956	12.88

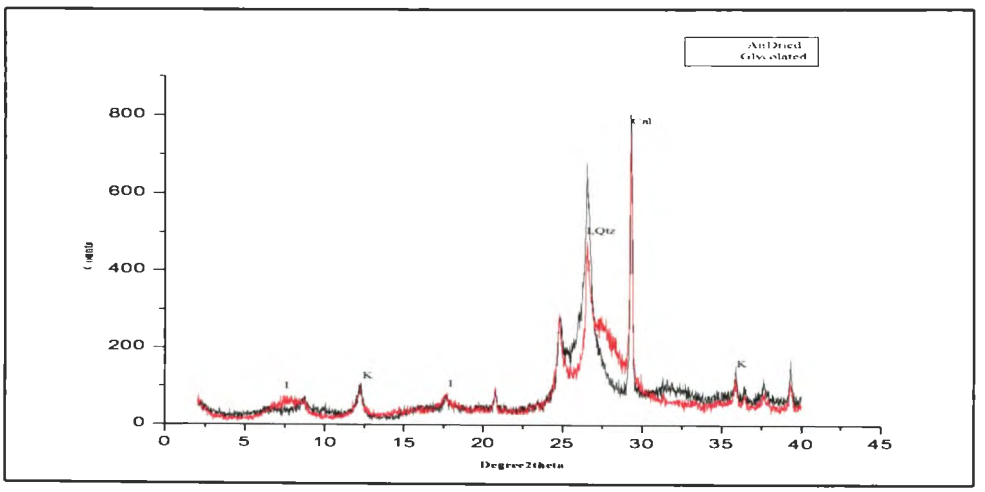

Fig.C.11. X-Ray diffraction patterns for major clay and other minerals for air dried and glycolated sample 11. S: Smectite, K: Kaolinite, I: Illite, Qtz: Quartz, Cal: Calcite.

Sample 12

Table C.24. Peak list for air dried sample 12.

Pos. [°2Th.]	Height [cts]	d-spacing [Å]	Rel. Int. [%]
8.8048	122.64	10.03504	27.95
12.3612	99.95	7.15476	22.78
17.7101	33.13	5.00404	7.55
20.8701	77.72	4.25295	17.72
24.8816	160.04	3.57562	36.48
26.6518	438.72	3.34201	100.00

Table C.25. Peak list for glycolated sample 12.

Pos. [°2Th.]	Height [cts]	d-spacing [Å]	Rel. Int. [%]
8.7445	44.07	10.10416	13.78
12.3030	66.81	7.18844	20.89
17.7179	15.41	5.00185	4.82
20.7925	40.36	4.26864	12.62
24.8271	70.91	3.58334	22.18
26.5883	319.76	3.34985	100.00

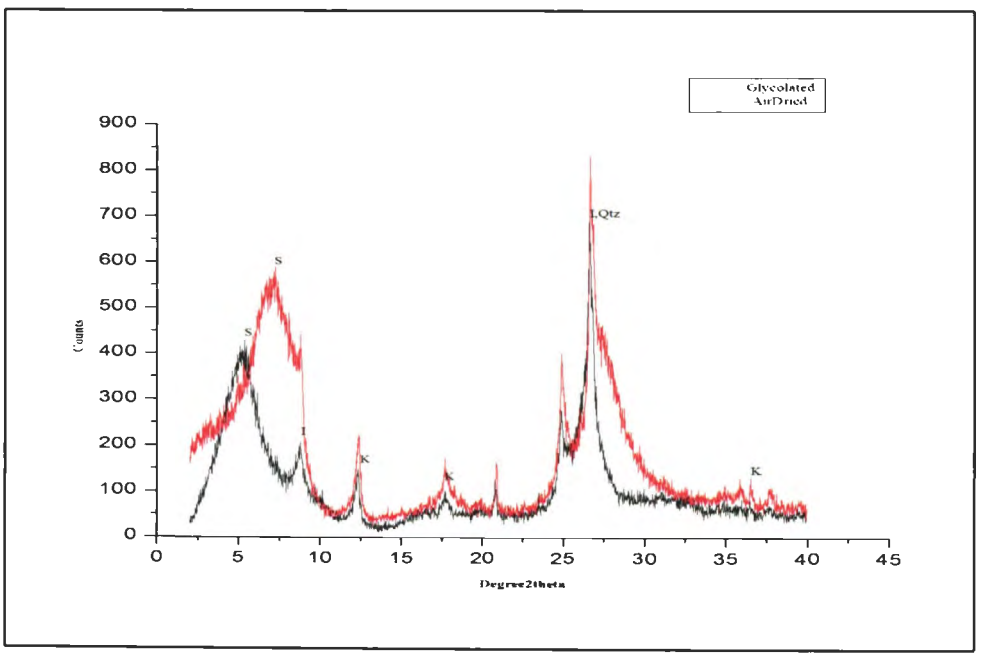

Fig.C.12. X-Ray diffraction patterns for major clay and other minerals for air dried and glycolated sample 12. S: Smectite, K: Kaolinite, I: Illite, Qtz: Quartz, Cal: Calcite.

Sample 13

Table C.26. Peak list for air dried sample 13.

Pos. [°2Th.]	Height [cts]	d-spacing [Å]	Rel. Int. [%]
8.6130	57.84	10.25804	14.57
12.2901	106.72	7.19596	26.89
17.6089	23.53	5.03256	5.93
20.7655	37.60	4.27414	9.47
24.7833	177.57	3.58958	44.74
26.5837	396.93	3.35041	100.00
29.3307	299.29	3.04258	75.40
37.5929	25.05	2.39069	6.31

Table C.27. Peak list for glycolated sample 13.

Pos. [°2Th.]	Height [cts]	d-spacing [Å]	Rel. Int. [%]
12.1034	42.10	7.30656	10.02
15.6244	5.20	5.66703	1.24
17.5223	8.46	5.05724	2.01
20.5476	25.20	4.31897	5.99
24.6379	128.76	3.61043	30.63
26.4022	420.33	3.37304	100.00
29.1384	170.18	3.06222	40.49
37.4225	19.65	2.40119	4.68

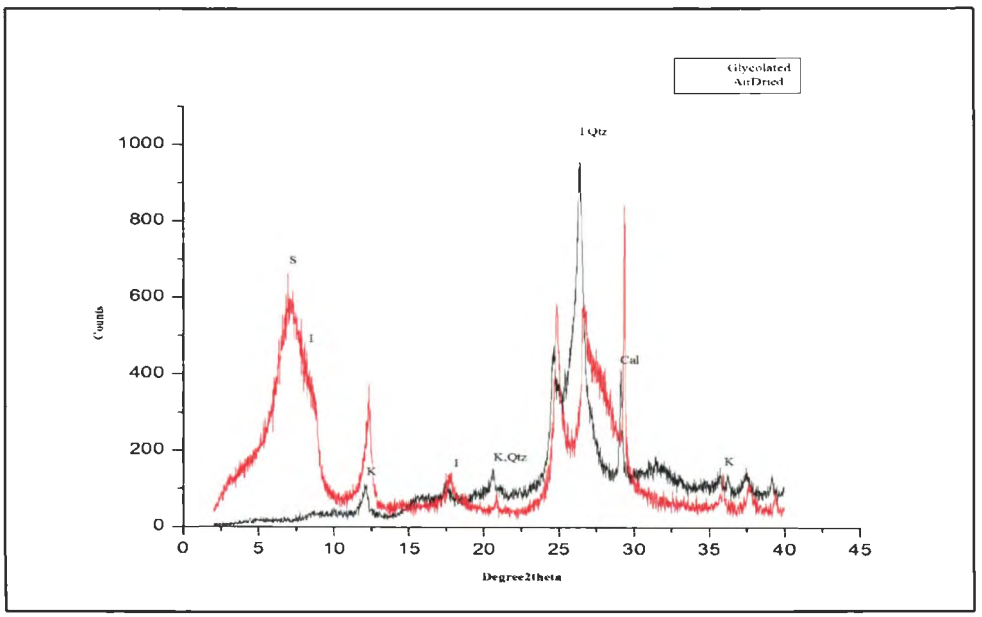

Fig.C.13. X-Ray diffraction patterns for major clay and other minerals for air dried and glycolated sample 13. S: Smectite, K: Kaolinite, I: Illite, Qtz: Quartz, Cal: Calcite.

Sample 14

Table C.28. Peak list for air dried sample 14.

Pos. [°2Th.]	Height [cts]	d-spacing [Å]	Rel. Int. [%]
3.0601	1.94	28.84842	0.29
7.0811	260.41	12.47347	39.24
8.7831	135.17	10.05982	20.37
12.3490	259.82	7.16176	39.15
17.7224	51.49	5.00060	7.76
24.8936	399.09	3.57392	60.14
26.6212	310.68	3.34579	46.82
29.3907	663.58	3.03651	100.00
35.9436	74.12	2.49652	11.17
37.6897	45.61	2.38478	6.87

Table C.29. Peak list for glycolated sample 14.

Pos. [°2Th.]	Height [cts]	d-spacing [Å]	Rel. Int. [%]
5.1645	384.23	17.09753	54.18
8.8119	86.45	10.02694	12.19
12.3064	265.61	7.18650	37.46
15.7690	15.48	5.61538	2.18
17.7436	53.29	4.99468	7.51
20.7730	21.83	4.27262	3.08
24.8686	458.72	3.57746	64.69
26.7107	654.77	3.33478	92.34
29.3683	709.13	3.03878	100.00
35.9104	59.37	2.49875	8.37
37.7194	63.17	2.38297	8.91
39.3826	70.90	2.28608	10.00

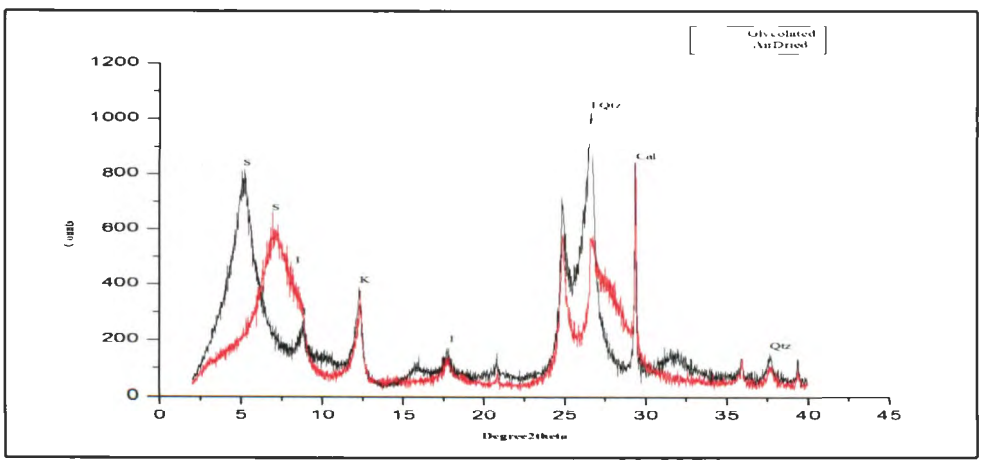

Fig.C.14. X-Ray diffraction patterns for major clay and other minerals for air dried and glycolated sample 14. S: Smectite, K: Kaolinite, .I: Illite, Qtz: Quartz, Cal: Calcite.

Sample 15

Table C.30. Peak list for air dried sample 15.

Pos. [°2Th.]	Height [cts]	d-spacing [Å]	Rel. Int. [%]
7.0244	173.25	12.57400	43.78
8.7901	104.85	10.05185	26.50
12.3781	133.54	7.14503	33.74
17.7318	29.49	4.99798	7.45
20.8733	71.18	4.25230	17.99
24.8804	195.23	3.57579	49.33
26.6443	395.73	3.34293	100.00
29.4104	210.46	3.03451	53.18
37.7742	21.65	2.37964	5.47

Table C.31. Peak list for glycolated sample 15.

Pos. [°2Th.]	Height [cts]	d-spacing [Å]	Rel. Int. [%]
5.2244	200.13	16.90157	33.40
8.7749	72.01	10.06922	12.02
12.3048	126.17	7.18740	21.06
15.8234	6.08	5.59618	1.02
17.7323	39.25	4.99782	6.55
20.8175	51.08	4.26359	8.52
24.8454	179.78	3.58074	30.00
26.6007	599.21	3.34832	100.00
29.3658	172.94	3.03903	28.86

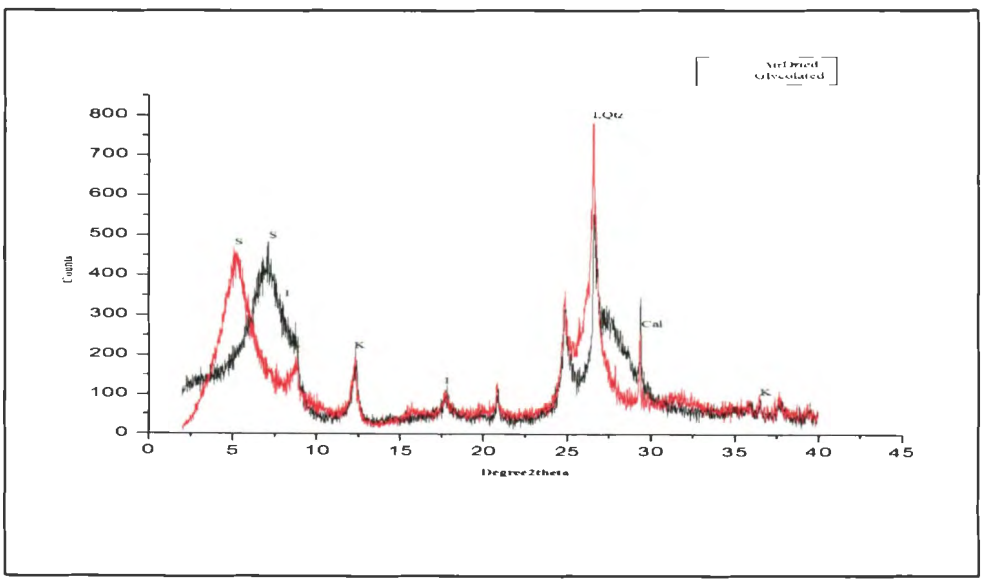

Fig.C.15. X-Ray diffraction patterns for major clay and other minerals for air dried and glycolated sample 15. S: Smectite, K: Kaolinite, I: Illite, Qtz: Quartz, Cal: Calcite.

Sample 16

Table C.32. Peak list for air dried sample 16.

Pos. [°2Th.]	Height [cts]	d-spacing [Å]	Rel. Int. [%]
2.1200	137.76	41.63956	57.30
2.3637	139.92	37.34618	58.20
8.8205	105.49	10.01724	43.88
12.4087	89.50	7.12747	37.23
17.7274	24.62	4.99921	10.24
20.8650	37.31	4.25398	15.52
24.8893	129.15	3.57454	53.72
26.6656	240.42	3.34031	100.00
29.4482	170.11	3.03071	70.76

Table C.33. Peak list for glycolated sample 16.

Pos. [°2Th.]	Height [cts]	d-spacing [Å]	Rel. Int. [%]
5.2093	192.56	16.95057	43.46
8.7692	54.02	10.07569	12.19
12.2967	86.12	7.19214	19.44
15.8358	3.57	5.59184	0.81
17.6928	20.81	5.00889	4.70
20.7699	36.33	4.27324	8.20
24.8319	146.97	3.58267	33.17
26.5596	443.10	3.35341	100.00
29.3439	219.34	3.04124	49.50

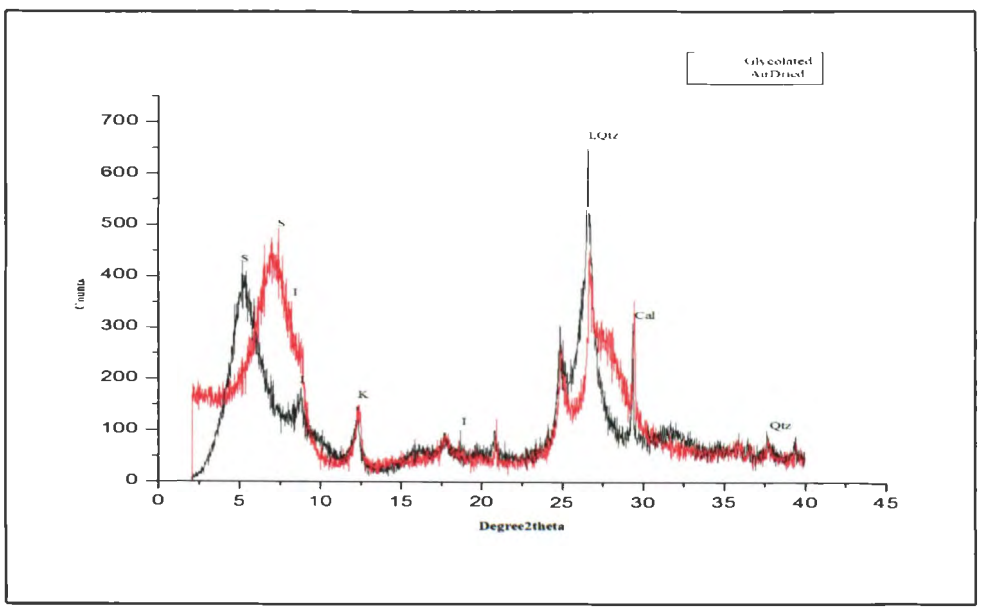

Fig.C.16. X-Ray diffraction patterns for major clay and other minerals for air dried and glycolated sample 16. S: Smectite, K: Kaolinite, I: Illite, Qtz: Quartz, Cal: Calcite.

Sample 17

Table C.34. Peak list for air dried sample 17.

Pos. [°2Th.]	Height [cts]	d-spacing [Å]	Rel. Int. [%]
7.1101	1258.56	12.42276	100.00
12.2717	32.27	7.20671	2.56
14.2651	67.97	6.20382	5.40
21.2398	19.13	4.17975	1.52
24.9983	53.11	3.55919	4.22
28.6975	302.36	3.10826	24.02
29.4138	483.51	3.03418	38.42

Table C.35. Peak list for glycolated sample 17.

Pos. [°2Th.]	Height [cts]	d-spacing [Å]	Rel. Int. [%]
5.2307	1951.26	16.88129	100.00
10.4556	54.73	8.45410	2.81
12.2878	28.83	7.19731	1.48
15.7792	119.68	5.61179	6.13
21.0317	41.05	4.22065	2.10
24.9526	23.96	3.56560	1.23
26.4310	416.24	3.36943	21.33
29.4098	411.08	3.03458	21.07
31.7831	72.79	2.81318	3.73

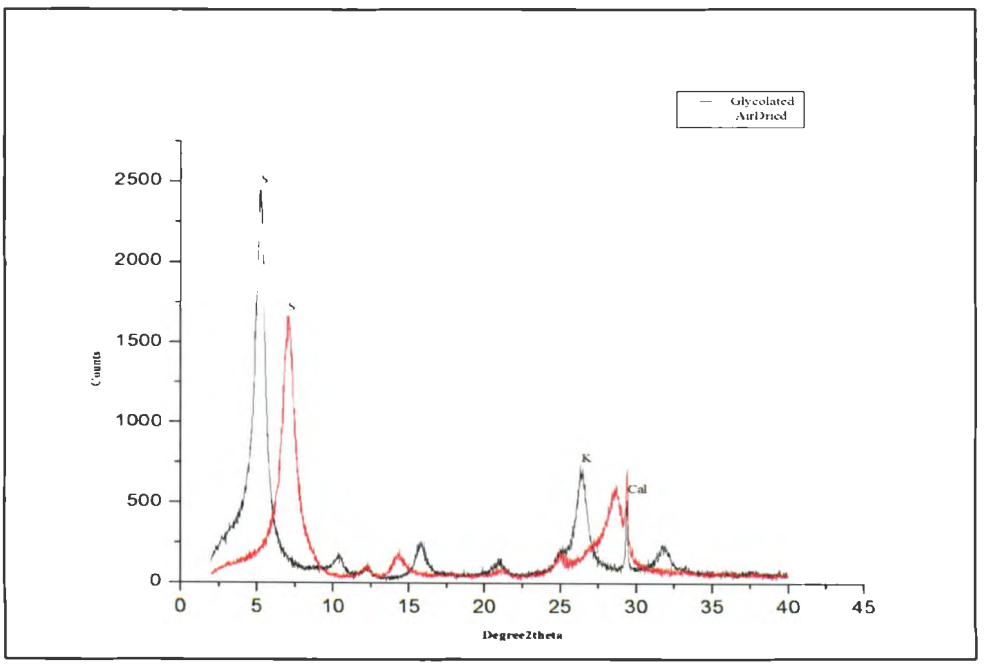

Fig.C.17. X-Ray diffraction patterns for major clay and other minerals for air dried and glycolated sample 17. S: Smectite, K: Kaolinite, Cal: Calcite.

Sample 18

Table C.36. Peak list for air dried sample 18.

Pos. [°2Th.]	Height [cts]	d-spacing [Å]	Rel. Int. [%]
8.8453	104.54	9.98924	16.49
12.3725	138.82	7.14824	21.90
17.7674	29.70	4.98804	4.69
20.8924	36.40	4.24846	5.74
24.9072	200.71	3.57200	31.67
26.6776	320.56	3.33884	50.57
29.4334	633.84	3.03220	100.00
36.0118	44.03	2.49195	6.95
37.7287	38.30	2.38240	6.04

Table C.37. Peak list for glycolated sample 18.

Pos. [°2Th.]	Height [cts]	d-spacing [Å]	Rel. Int. [%]
5.2498	216.19	16.81976	30.81
8.8721	77.39	9.95908	11.03
12.3797	143.02	7.14410	20.38
15.9363	3.40	5.55680	0.48
17.7624	44.35	4.98943	6.32
20.8878	48.84	4.24940	6.96
24.9305	214.99	3.56872	30.64
26.6776	462.48	3.33884	65.90
29.4359	701.76	3.03195	100.00
35.9876	52.21	2.49357	7.44
37.7025	22.33	2.38400	3.18
39.4363	64.82	2.28309	9.24

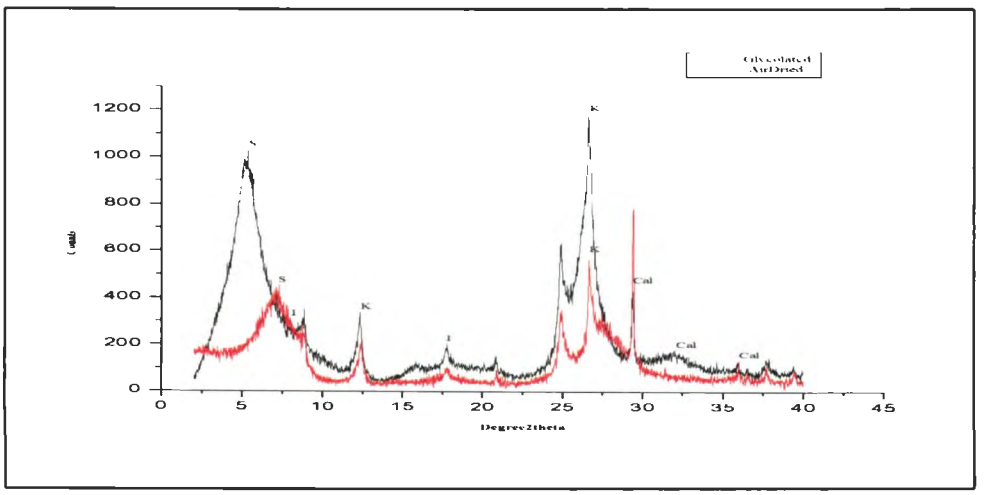

Fig.C.18. X-Ray diffraction patterns for major clay and other minerals for air dried and glycolated sample 18. S: Smectite, K: Kaolinite, I: Illite, Cal: Calcite.

Sample 19

Table C.38. Peak list for air dried sample 19.

Pos. [°2Th.]	Height [cts]	d-spacing [Å]	Rel. Int. [%]
12.3305	119.73	7.17251	55.76
14.4819	3.66	6.11141	1.71
17.6125	12.23	5.03155	5.70
24.8388	166.80	3.58169	77.67
26.7825	109.84	3.32600	51.15
29.3767	214.74	3.03792	100.00
35.9117	27.22	2.49867	12.67
37.6649	20.64	2.38629	9.61

Table C.39. Peak list for glycolated sample 19.

Pos. [°2Th.]	Height [cts]	d-spacing [Å]	Rel. Int. [%]
5.1371	740.25	17.18850	100.00
10.2654	31.26	8.61031	4.22
12.3096	103.19	7.18461	13.94
15.6289	28.94	5.66542	3.91
17.7328	22.63	4.99769	3.06
20.6140	6.56	4.30522	0.89
24.8387	177.66	3.58170	24.00
26.6341	496.45	3.34420	67.07
29.3594	206.62	3.03967	27.91
35.8483	14.48	2.50294	1.96
37.6068	14.64	2.38984	1.98

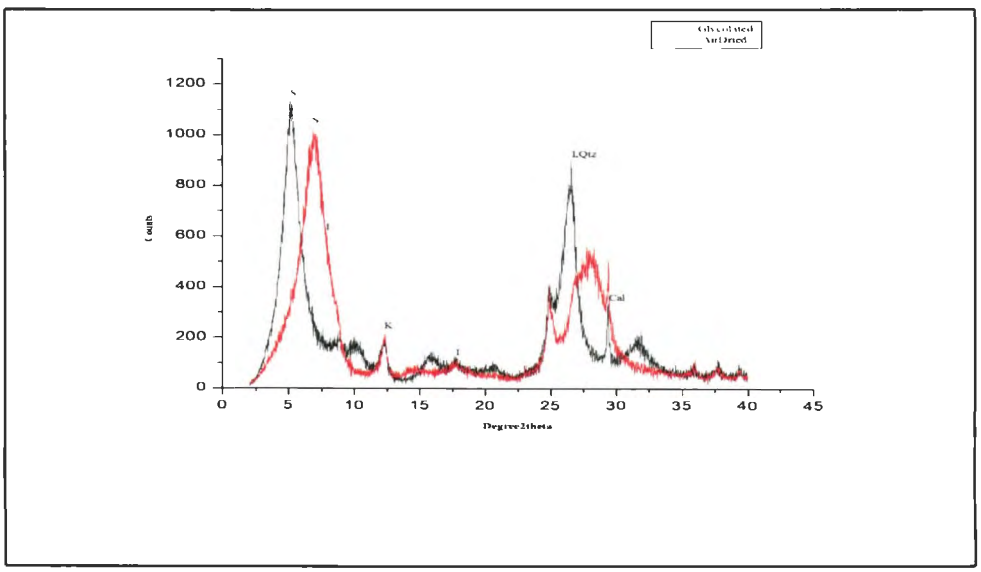

Fig.C.19. X-Ray diffraction patterns for major clay and other minerals for air dried and glycolated sample 19. S: Smectite, K: Kaolinite, I: Illite, Qtz: Quartz, Cal: Calcite.

Sample 20

Table C.40. Peak list for air dried sample 20.

Pos. [°2Th.]	Height [cts]	d-spacing [Å]	Rel. Int. [%]
6.1775	280.47	14.29583	100.00
7.0871	276.95	12.46289	98.74
12.2930	20.33	7.19427	7.25
14.2763	9.13	6.19897	3.25
17.5334	71.63	5.05406	25.54
21.2034	17.97	4.18686	6.41
25.0115	29.63	3.55735	10.57
28.6541	219.04	3.11286	78.10

Table C.41. Peak list for glycolated sample 20.

Pos. [°2Th.]	Height [cts]	d-spacing [Å]	Rel. Int. [%]
5.1832	513.23	17.03593	100.00
10.3848	26.55	8.51154	5.17
12.2055	18.78	7.24565	3.66
15.7775	81.90	5.61236	15.96
17.4560	67.64	5.07631	13.18
21.0747	25.71	4.21214	5.01
26.5770	199.78	3.35125	38.93
28.5884	120.21	3.11987	23.42
29.0595	123.81	3.07035	24.12
29.3637	124.43	3.03923	24.24
31.8780	56.68	2.80503	11.04

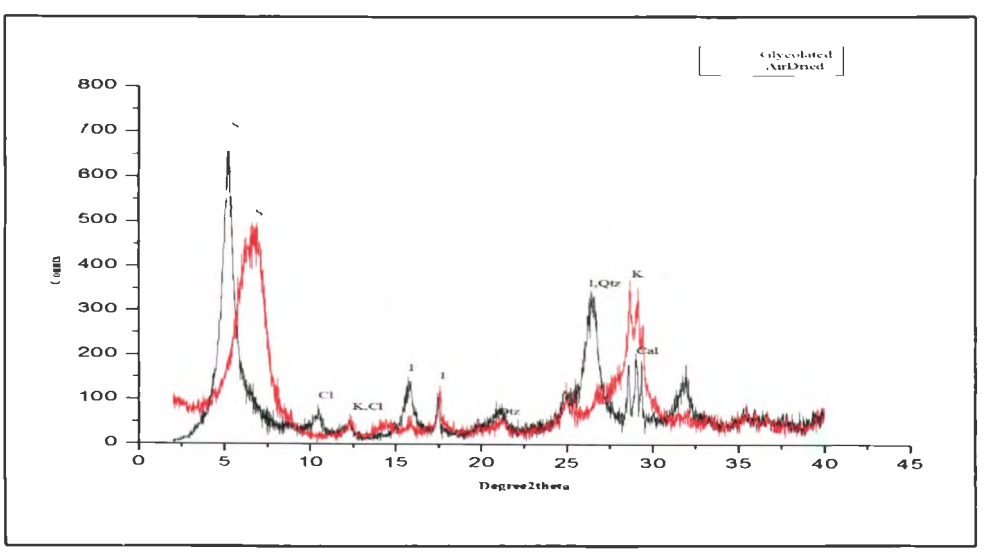

Fig.C.20. X-Ray diffraction patterns for major clay and other minerals for air dried and glycolated sample 20. S: Smectite, K: Kaolinite, I: Illite, Qtz: Quartz, Cal: Calcite, Cl: Chlorite.

Sample 21

Table C.42. Peak list for air dried sample 21.

Pos. [°2Th.]	Height [cts]	d-spacing [Å]	Rel. Int. [%]
12.3394	132.75	7.16736	53.51
17.7367	19.99	4.99661	8.06
21.1226	18.27	4.20268	7.36
24.9296	196.87	3.56884	79.36
26.8727	141.71	3.31504	57.13
28.4351	122.17	3.13634	49.25
29.4159	248.07	3.03396	100.00
37.7588	24.57	2.38057	9.91

Table C.43. Peak list for glycolated sample 21.

Pos. [°2Th.]	Height [cts]	d-spacing [Å]	Rel. Int. [%]
5.1746	450.29	17.06398	100.00
12.2918	119.14	7.19500	26.46
20.9877	11.86	4.22939	2.63
24.9171	209.91	3.57061	46.62
26.5786	439.35	3.35106	97.57
29.3683	219.75	3.03877	48.80
37.7204	22.60	2.38291	5.02

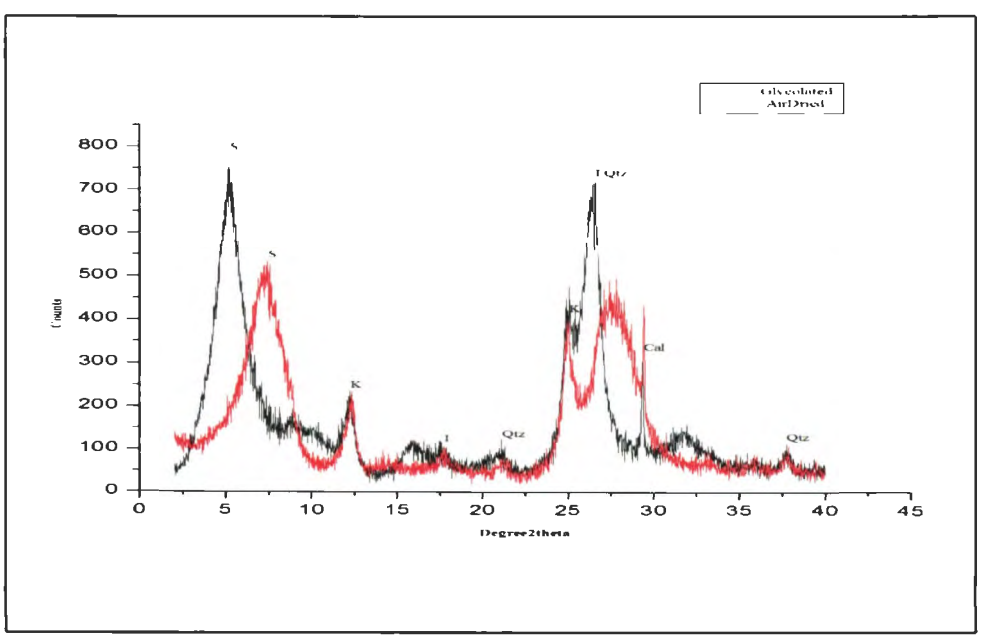

Fig.C.21. X-Ray diffraction patterns for major clay and other minerals for air dried and glycolated sample 21. S: Smectite, K: Kaolinite, I: Illite, Qtz: Quartz.

Sample 22

Table C.44. Peak list for air dried sample 22.

Pos. [°2Th.]	Height [cts]	d-spacing [Å]	Rel. Int. [%]
3.0265	8.46	29.16903	1.66
7.0631	292.94	12.50514	57.52
12.3242	81.75	7.17614	16.05
17.7901	11.63	4.98172	2.28
21.2452	9.83	4.17871	1.93
24.9172	113.45	3.57060	22.28
26.8931	108.51	3.31257	21.31
29.4109	509.32	3.03447	100.00

Table C.45. Peak list for glycolated sample 22.

Pos. [°2Th.]	Height [cts]	d-spacing [Å]	Rel. Int. [%]
12.2536	70.77	7.21733	16.21
15.8586	14.95	5.58384	3.42
21.1269	24.39	4.20183	5.59
24.9037	124.36	3.57250	28.49
26.6289	324.47	3.34484	74.33
29.4098	436.56	3.03458	100.00

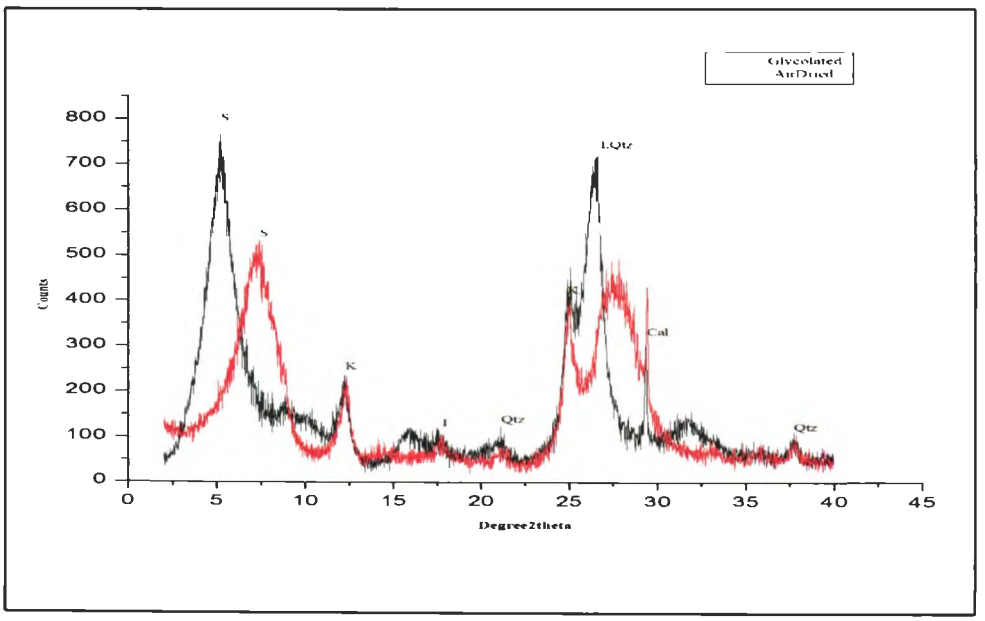

Fig.C.22. X-Ray diffraction patterns for major clay and other minerals for air dried and glycolated sample 22. S: Smectite, K: Kaolinite, I: Illite, Qtz: Quartz, Cal: Calcite.

Sample 23

Table C.46. Peak list for air dried sample 23.

Pos. [°2Th.]	Height [cts]	d-spacing [Å]	Rel. Int. [%]
8.7027	121.49	10.15259	21.33
12.2585	181.83	7.21443	31.92
17.6388	54.87	5.02412	9.63
20.7959	77.91	4.26796	13.68
24.7897	265.40	3.58867	46.60
26.5433	569.57	3.35543	100.00
35.8941	7.67	2.49985	1.35
36.4393	32.62	2.46369	5.73
37.6365	22.88	2.38803	4.02

Table C.47. Peak list for glycolated sample 23.

Pos. [°2Th.]	Height [cts]	d-spacing [Å]	Rel. Int. [%]
5.1170	119.79	17.25592	16.94
8.7671	102.98	10.07811	14.56
12.3096	180.35	7.18464	25.51
17.6944	73.75	5.00846	10.43
20.7859	81.27	4.26999	11.49
24.8495	235.98	3.58017	33.37
26.5627	707.12	3.35302	100.00
35.9201	3.01	2.49810	0.43
36.4700	29.16	2.46169	4.12
37.6199	42.33	2.38904	5.99

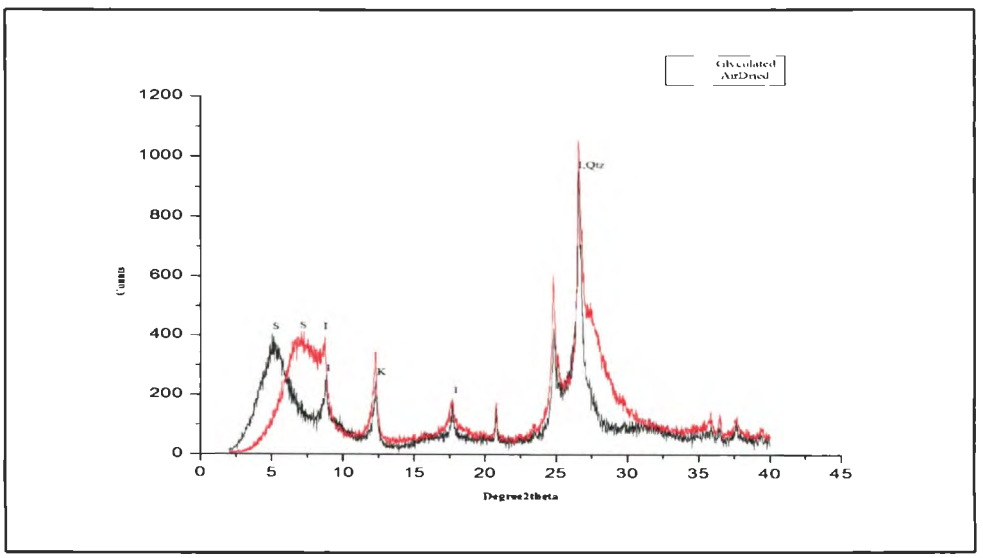

Fig.C.23. X-Ray diffraction patterns for major clay and other minerals for air dried and glycolated sample 23. S: Smectite, K: Kaolinite, I:I llite, Qtz: Quartz.

Sample 24

Table C.48. Peak list for air dried sample 24.

Pos. [°2Th.]	Height [cts]	d-spacing [Å]	Rel. Int. [%]
7.0682	340.58	12.49629	90.39
8.7854	129.78	10.05712	34.44
12.3276	207.03	7.17418	54.95
17.7057	51.93	5.00528	13.78
20.8179	76.68	4.26350	20.35
24.8587	302.91	3.57886	80.39
26.6028	376.79	3.34805	100.00
36.5000	36.09	2.45973	9.58
37.6758	38.05	2.38562	10.10

Table C.49. Peak list for glycolated sample 24.

Pos. [°2Th.]	Height [cts]	d-spacing [Å]	Rel. Int. [%]
5.3422	451.90	16.52923	59.76
8.7996	89.14	10.04096	11.79
12.3438	182.43	7.16480	24.12
15.8443	15.25	5.58887	2.02
17.7038	55.57	5.00581	7.35
20.7895	68.47	4.26926	9.05
24.8605	270.20	3.57861	35.73
26.6026	756.23	3.34808	100.00
31.8897	11.33	2.80403	1.50
37.6588	40.51	2.38666	5.36

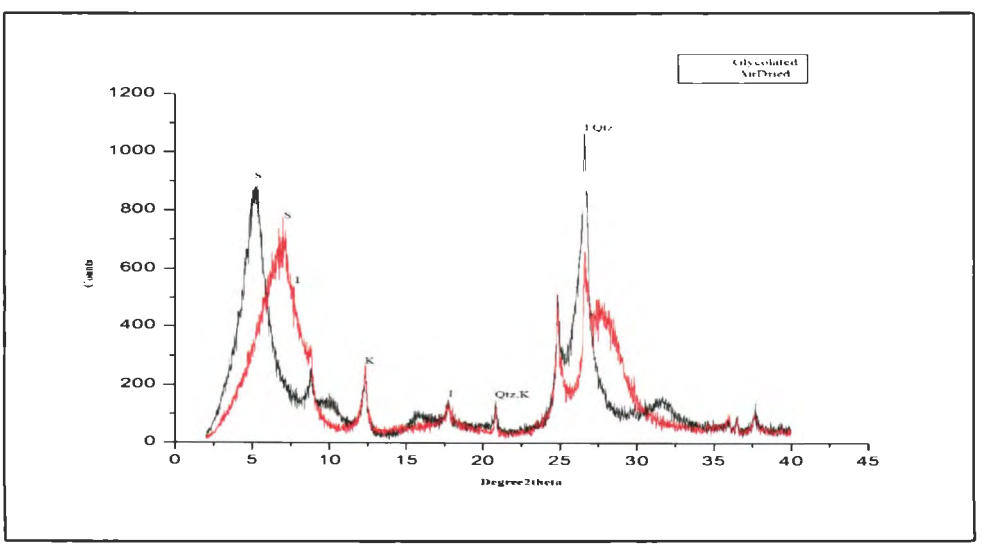

Fig.C.24. X-Ray diffraction patterns for major clay and other minerals for air dried and glycolated sample 24. S: Smectite, K: Kaolinite, I: Illite, Qtz: Quartz.

Sample 25

Table C.50. Peak list for air dried sample 25.

Pos. [°2Th.]	Height [cts]	d-spacing [Å]	Rel. Int. [%]
12.3090	16.92	7.18496	0.57
14.6320	16.17	6.04907	0.54
22.9940	128.45	3.86470	4.33
26.5558	103.70	3.35388	3.49
29.3430	2968.46	3.04133	100.00
31.3615	41.90	2.85003	1.41
35.9060	327.88	2.49905	11.05
39.3477	552.01	2.28802	18.60

Table C.51. Peak list for glycolated sample 25.

Pos. [°2Th.]	Height [cts]	d-spacing [Å]	Rel. Int. [%]
12.1652	12.98	7.26959	0.47
14.5529	6.83	6.08177	0.25
22.9690	95.59	3.86885	3.44
24.8005	21.97	3.58713	0.79
26.5117	117.64	3.35935	4.23
29.2916	2780.09	3.04656	100.00
31.3206	52.68	2.85366	1.89
35.8612	337.89	2.50207	12.15
39.2951	531.70	2.29096	19.13

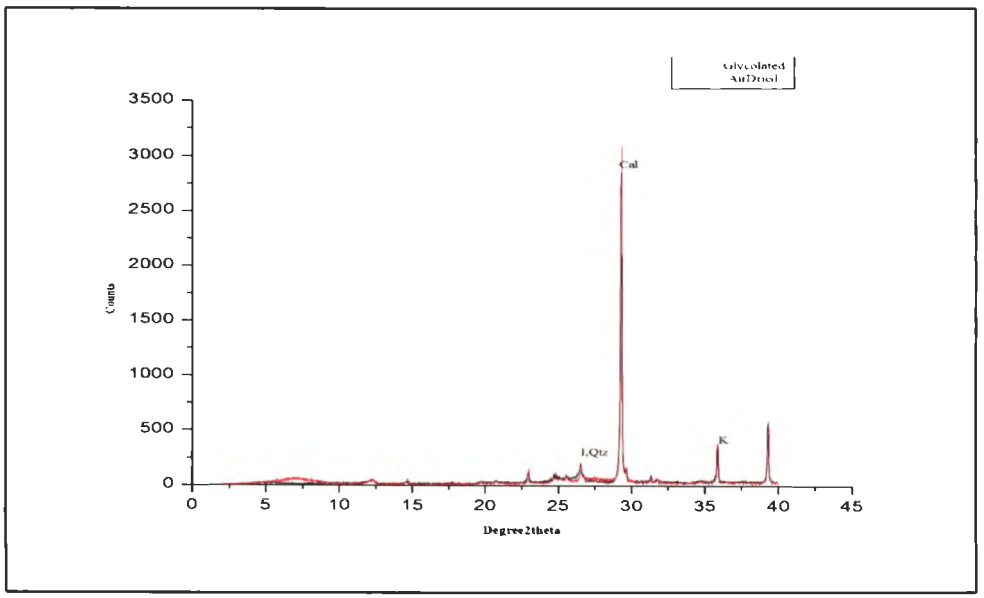

Fig.C.25. X-Ray diffraction patterns for major clay and other minerals for air dried and glycolated sample 25. K: Kaolinite, I: Illite, Qtz: Quartz, Cal: Calcite.

APPENDIX D. SOIL CHARACTERIZATION

Table D.1. Soil characteristics for surface samples.

Sample ID	%OM	pH	EC (microS/cm)
2A-15	9.37	6.40	0.20
2A-30	5.90	6.50	0.49
2B-15	9.79	6.50	0.48
2B-30	5.29	6.30	0.45
2C-15	8.99	6.10	0.51
2C-30	5.21	5.50	0.50
2D-15	10.22	6.20	0.48
2D-30	3.83	5.60	0.42
2-E-15	12.04	6.50	0.51
2-E-30	4.63	5.90	0.51
2F-15	6.35	5.60	0.48
2F-30	4.37	4.90	0.46
2G-15	11.83	6.00	0.56
2G-30	5.00	4.90	0.53
2H-15	6.61	5.00	0.37
2H-30	5.38	4.40	0.31
2I-15	9.29	5.10	0.33
2I-30	5.93	4.90	0.38
2J-15	9.53	6.30	0.46
2J-30	7.50	6.40	0.38
6K-15	9.92	6.30	0.45
6K-30	8.77	6.20	0.44
6L-15	8.14	6.20	0.45
6L-30	8.28	6.40	0.45
6M-15	13.30	6.40	0.39
6M-30	9.92	6.40	0.45
6N-15	5.55	6.30	0.45
6N-30	4.87	6.50	0.44
6O-15	8.16	6.20	0.43
6O-30	3.78	6.30	0.48
6P-15	9.29	5.80	0.47
6P-30	5.58	5.20	0.40
6Q-15	6.76	5.50	0.55
6Q-30	5.69	5.30	0.55
6R-15	5.25	4.60	0.41
6R-30	4.49	4.40	0.42

Table D.1. (continued)

6S-15	11.22	6.30	0.45
6S-30	7.38	6.30	0.45
11A-15	5.12	6.20	0.39
11A-30	3.04	6.30	0.35
11B-15	7.17	6.30	0.38
11B-30	3.05	6.10	0.52
11C-15	2.62	6.10	0.44
11C-30	4.85	6.20	0.41
11D-15	6.69	6.30	0.45
11D-30	3.59	6.30	0.44
11-E-15	7.07	6.10	0.44
11-E-30	2.81	5.60	0.45
11F-15	8.98	5.90	0.50
11F-30	4.11	5.30	0.54
Check	NA	7.80	0.33
11G-15	7.46	5.10	0.33
11G-30	4.03	4.30	0.32
11H-15	5.78	6.00	0.60
11H-30	5.19	6.70	0.66
11-I-15	5.41	6.90	1.20
11-I-30	5.72	7.00	2.90
15A-15	8.96	6.30	0.52
15A-30	3.22	6.20	0.45
15B-15	5.53	6.20	0.45
15B-30	2.92	6.20	0.40
15C-15	5.18	6.40	0.52
15C-30	3.84	6.40	0.46
15D-15	5.33	6.30	0.40
15D-30	4.80	6.40	0.37
15-E-15	6.95	6.30	0.44
15-E-30	2.61	6.50	0.43
15F-15	9.57	6.40	0.52
15-F-30	5.07	6.60	0.44
15G-15	8.57	6.10	0.46
15G-30	4.67	5.80	0.42
15H-15	9.28	5.90	0.46
15H-30	4.19	5.20	0.46
15-I-15	8.77	5.30	0.37
15-I-30	4.48	4.40	0.40
15J-15	9.41	5.10	0.36
15J-30	5.54	4.30	0.30

Table D.1. (continued)

15K-15	8.44	5.00	0.33
15K-30	5.21	4.50	0.27
15L-15	5.81	5.80	0.66
15L-30	4.37	6.10	1.30
15M-15	4.52	5.70	0.51
15M-30	3.32	5.60	0.52
15N-15	3.59	6.00	0.44
15-N-30	1.77	4.90	0.51
16A-15	7.52	6.20	0.42
16A-30	4.76	6.10	0.36
16B-15	8.35	6.20	0.48
16B-30	6.76	6.20	0.41
16C-15	7.89	6.10	0.46
16C-30	7.62	6.00	0.41
16D-15	9.05	6.10	0.46
16-E-15	6.04	6.30	0.40
16-E-30	8.30	6.00	0.47
16F-15	5.41	5.90	0.51
17A-15	8.42	6.20	0.48
17A-30	7.39	6.20	0.43
17B-15	9.07	6.00	0.44
17B-30	7.77	5.90	0.39
Check	NA	7.70	0.31
17C-15	6.70	5.70	0.52
17C-30	5.09	5.30	0.51
17D-15	10.07	5.90	0.55
17D-30	5.35	5.30	0.47
17-E-15	8.09	5.90	0.42
17-E-30	4.40	5.70	0.39
17F-15	9.02	5.20	0.38
17F-30	5.68	4.40	0.29
17G-15	8.21	4.90	0.33
17G-30	6.60	4.30	0.29
17H-15	8.31	4.50	0.30
17H-30	5.68	4.00	0.27
17-I-15	7.95	5.40	0.66
17-I-30	6.56	5.70	3.72
17J-15	7.06	6.30	0.39
17J-30	4.30	6.40	0.27
17K-15	4.91	6.20	0.43
17K-30	3.04	5.20	0.24

Table D.1. (continued)

17L-15	6.60	6.10	0.44
17L-30	5.56	6.20	0.35
19A-15	9.24	6.20	0.43
19A-30	4.37	6.10	0.31
19-B-15	8.30	6.20	0.42
19-B-15	6.09	6.20	0.35
19C-15	10.05	6.00	0.41
19C-30	6.00	6.40	0.48
19D-15	10.82	5.80	0.59
19D-30	8.69	5.90	0.52
19-E-15	8.30	7.00	0.72
19-E-30	6.82	6.30	0.44
19F-15	9.97	5.10	0.35
19F-30	5.53	4.30	0.24
19G-15	7.19	4.40	0.33
19G-30	5.73	4.00	0.32
19H-15	7.36	5.50	0.36
19H-30	4.24	4.80	0.34
19-I-15	6.98	5.50	0.53
19-I-30	6.12	5.20	0.98
19J-15	8.02	6.20	0.45
19J-30	5.77	6.30	0.41
19K-15	5.20	6.00	0.45
19K-30	3.50	5.80	0.47
19L-15	6.92	6.10	0.44
19L-30	5.22	6.10	0.40

NA-not analyzed

Table D.2. Soil characteristics for core samples.

Sample ID	**%OM**	**pH**	**EC (microS/cm)**
Core1			
15-C-0	9.52	NA	NA
15-C-15	5.52	6.20	0.39
Check	3.55	NA	NA
15-C-30	2.94	5.20	0.38
15-C-45	8.47	4.80	0.33
15-C-60	2.52	4.90	0.31
Check	3.60	7.60	0.33
15-C-75	2.84	4.80	0.33
15-C-90	2.88	5.20	0.44

Table D.2. (continued)

15-C-105	3.32	5.60	0.37
15-C-120	3.02	5.80	0.28
15-C-135	3.11	6.00	0.54
15-C-150	3.09	6.10	0.55
15-C-165	3.13	6.20	0.55
15-C-180	3.09	6.50	0.56
Check	3.82	NA	NA
15-C-195	3.39	6.60	0.59
15-C-210	3.47	6.80	0.64
15-C-225	3.42	6.80	0.64
Core2			
19-AC-0	8.07	4.40	0.43
19-AC-15	5.60	3.90	0.48
19-AC-30	5.54	3.80	0.62
19-AC-45	5.38	3.90	0.53
19-AC-60	5.37	4.00	0.43
Check	5.04	NA	NA
19-AC-75	7.48	3.90	0.63
19-AC-90	3.94	3.70	0.76
19-AC-105	5.37	3.30	2.26
19-AC-120	6.77	3.50	2.17
19-AC-135	4.74	3.50	1.28
Check	5.02	NA	NA
19-AC-150	4.68	3.50	1.18
19-AC-165	4.90	3.50	1.07
19-AC-180	4.94	3.40	1.02
19-AC-195	4.30	3.30	1.55
19-AC-210	6.37	3.20	2.08
19-AC-225	9.05	3.40	1.16
19-AC-226	8.90	NA	NA
Core3			
19BC-0	20.07	NA	NA
19-BC-15	6.15	4.40	0.30
19BC-30	5.49	NA	NA
19BC-45	4.61	NA	NA
19BC-60	4.04	NA	NA
19BC-75	5.33	NA	NA
19BC-90	3.68	NA	NA
Check	3.77	NA	NA
19BC-105	4.32	NA	NA
19BC-117	3.22	3.80	0.69

Table D.2. (continued)

19BC-135	4.69	3.40	1.81
19BC-150	3.26	NA	NA
19BC-165	3.18	NA	NA
19BC-180	2.99	3.70	0.86
19BC-195	3.14	NA	NA
19BC-210	2.96	3.80	0.66
Core4			
15-AC-0	6.33	6.20	0.50
15AC-15	2.89	5.80	0.57
15AC-30	2.89	4.70	0.46
Check	3.83	NA	NA
15AC-45	2.32	4.60	0.40
15AC-60	2.18	4.60	0.40
15AC-75	2.04	4.60	0.44
Check	NA	8.00	0.40
15AC-90	2.50	4.10	2.70
15AC-105	2.38	4.50	2.00
15AC-120	2.70	4.60	1.53
15AC-135	2.18	4.60	1.45
15AC-150	1.96	4.80	2.52
15AC-165	1.99	5.00	3.06
15AC-180	1.81	5.10	1.69
Check	3.87	NA	NA
Check	3.87	NA	NA
15AC-195	1.82	5.30	1.64
15AC-210	1.87	5.50	1.14
15AC-225	1.95	5.70	0.91
Core5			
15BC-0	11.63	6.50	1.91
15BC-15	4.01	6.90	1.33
15BC-30	3.75	5.10	1.25
15BC-45	3.05	4.50	1.10
15BC-60	2.86	4.60	2.98
15BC-75	2.55	4.70	2.84
15BC-90	2.39	4.80	2.69
Check	3.79	NA	NA
15BC-105	2.67	4.70	2.81
15BC-120	2.84	5.30	2.92
15BC-135	2.77	5.40	7.29
15BC-150	2.55	5.70	4.01
15BC-165	2.53	5.90	2.49

Table D.2. (continued)

15BC-180	2.58	5.80	6.67
15BC-195	2.61	6.00	0.90
15BC-210	2.57	6.10	1.41
15BC-225	3.68	6.30	2.30
Core6			
15CC-0	10.34	6.20	1.01
Check	4.16	NA	NA
15CC-15	5.12	5.70	1.10
15CC-30	4.22	4.60	1.36
15CC-45	3.55	4.70	1.27
15CC-60	2.95	5.00	1.88
15CC-75	3.01	5.60	1.58
15CC-90	2.81	6.40	2.39
15CC-105	2.94	6.80	3.41
15CC-120	2.86	6.90	2.66
15CC-135	2.57	6.70	2.15
15CC-150	2.93	6.60	2.27
15CC-165	2.52	6.40	1.89
Check	4.25	NA	NA
15CC-180	1.81	6.30	2.55
15CC-195	1.71	6.20	1.12
15CC-210	2.06	6.10	2.64
15CC-225	2.15	6.20	1.94
15CC-240	2.03	6.20	1.44
15CC-255	2.22	6.40	1.11
15CC-270	2.13	6.30	1.51
15CC-285	2.24	6.20	1.69
15CC-300	1.86	6.30	1.61
15CC-315	1.93	6.40	1.21
Check	3.49	NA	NA
15CC-330	2.00	6.40	0.96
Check		8.00	0.45
15CC-340	1.93	6.60	0.47
Core7			
15DC-0	9.24	6.40	0.47
15DC-15	4.60	5.40	0.54
15DC-30	4.41	5.40	0.46
15DC-45	4.69	6.40	0.54
15DC-60	4.11	7.10	0.54
15DC-75	3.07	7.80	1.82
15DC-90	2.71	7.80	0.93

Table D.2. (continued)

15DC-105	2.47	7.70	0.83
15DC-120	2.71	7.70	0.86
15DC-135	3.10	7.50	1.11
15DC-150	4.33	7.40	1.33
15DC-165	3.92	7.40	0.63
15DC-180	4.34	7.30	0.82
15DC-195	3.44	7.40	0.89
Check	4.51	NA	NA
15DC-210	3.16	7.30	0.88
15DC-225	3.08	7.20	1.01
Core8			
15EC-0	7.79	5.10	0.33
15EC-15	6.08	4.40	0.33
15EC-30	5.15	4.30	0.44
Check	4.39	NA	NA
15EC-45	5.54	4.50	0.58
15EC-60	4.84	4.50	0.97
15EC-75	5.33	4.30	1.12
15EC-90	4.32	4.00	1.18
15EC-105	4.30	3.90	1.15
Check	3.59	NA	NA
15EC-120	3.94	3.70	2.01
15EC-135	3.87	3.50	1.79
15EC-150	4.05	3.50	1.59
15EC-165	3.96	3.50	1.57
15EC-180	4.16	3.50	1.36
Check	4.89	NA	NA
15EC-195	4.36	3.60	0.94
15EC-210	5.91	3.40	1.89
15EC-225	5.30	3.40	1.80
Core9			
15FC-0	8.40	4.90	0.37
15FC-15	9.38	4.10	0.39
15FC-30	5.50	4.00	0.35
15FC-45	6.11	3.90	0.36
15FC-60	4.19	3.90	0.34
15FC-75	3.49	4.00	0.35
15FC-90	4.84	3.80	0.47
15FC-105	5.47	3.90	0.49
15FC-120	3.33	3.80	0.47
15FC-135	3.57	3.80	0.52

Table D.2. (continued)

15FC-150	3.64	3.80	0.69
15FC-165	3.42	3.80	0.81
15FC-180	3.43	3.80	0.76
15FC-195	4.35	3.80	0.70
15FC-210	3.60	3.80	0.62
15FC-225	3.71	3.80	0.65
Check	NA	8.00	0.34
Core10			
15GC-0	7.92	5.10	0.33
15GC-15	5.76	4.20	0.27
15GC-30	5.04	3.90	0.25
15GC-45	5.55	3.80	0.43
15GC-60	4.54	3.90	0.32
15GC-75	3.99	3.70	0.31
15GC-90	3.69	3.90	0.34
15GC-105	3.52	3.70	0.37
15GC-120	3.96	4.00	0.39
15GC-135	3.31	3.90	0.34
15GC-150	3.27	4.00	0.39
15GC-165	3.35	3.90	0.44
15GC-180	4.15	4.00	0.48
15GC-195	4.61	4.00	0.51
15GC-210	3.78	3.90	0.54
15GC-225	3.85	3.90	0.66
Core11			
17AC-0	7.31	4.60	0.25
17AC-15	4.25	4.00	0.25
17AC-30	4.81	4.00	0.24
17AC-45	4.76	3.90	0.27
17AC-60	5.40	4.00	0.27
17AC-75	4.13	3.90	0.24
17AC-90	3.63	3.80	0.30
17AC-105	4.06	3.90	0.31
17AC-120	4.03	3.80	0.42
17AC-135	3.56	3.70	0.56
17AC-150	5.35	3.40	0.81
17AC-165	4.13	3.60	0.77
17AC-180	3.94	3.60	0.76
17AC-195	4.76	3.60	0.76
17AC-210	4.24	3.50	0.84
17AC-225	4.47	3.50	0.90

Table D.2. (continued)

Core12			
17BC-0	11.09	5.30	0.41
17BC-15	5.94	4.30	0.30
17BC-30	4.38	4.00	0.29
17BC-45	4.64	4.10	0.25
17BC-60	4.51	4.00	0.24
17BC-75	5.85	3.60	0.59
17BC-90	6.73	3.80	0.47
17BC-105	4.66	3.90	0.51
17BC-120	5.28	3.90	0.66
17BC-135	4.42	3.80	0.67
17BC-150	4.73	3.60	0.70
17BC-165	3.97	3.70	0.70
17BC-180	3.42	3.70	0.66
17BC-195	3.48	3.70	0.62
17BC-210	3.43	3.70	0.66
17BC-225	3.68	3.70	0.64
Check	NA	8.00	0.36

*NA – Samples not analyzed

Table D.3. Summary of sample identification.

Sample Name	**Sample ID**
F1 200N,0W(0-15)	2A-15
F1 200N,0W(15-30)	2A-30
F1 200N,250W(0-15)	2B-15
F1 200N,250W(15-30)	2B-30
F1 200N,500W(0-15)	2C-15
F1 200N,500W(15-30)	2C-30
F1 200N,750W(0-15)	2D-15
F1 200N,750W(15-30)	2D-30
F1 200N,1000W(0-15)	2-E-15
F1 200N,1000W(15-30)	2-E-30
F1 200N,1250W(0-15)	2F-15
F1 200N,1250W(15-30)	2F-30
F1 200N,1500W(0-15)	2G-15
F1 200N,1500W(15-30)	2G-30
F1 200N,1750W(0-15)	2H-15
F1 200N,1750W(15-30)	2H-30

Table D.3. (continued)

F1 200N,2000W(0-15)	2I-15
F1 200N,2000W(15-30)	2I-30
F1 200N,-200W(0-15)	2J-15
F1 200N,-200W(15-30)	2J-30
F1 600N,0W(0-15)	6K-15
F1 600N,0W(15-30)	6K-30
F1 600N,250W(0-15)	6L-15
F1 600N,250W(15-30)	6L-30
F1 600N,500W(0-15)	6M-15
F1 600N,500W(15-30)	6M-30
F1 600N,750W(0-15)	6N-15
F1 600N,750W(15-30)	6N-30
F1 600N,1000W(0-15)	6O-15
F1 600N,1000W(15-30)	6O-30
F1 600N,1250W(0-15)	6P-15
F1 600N,1250W(15-30)	6P-30
F1 600N,1500W(0-15)	6Q-15
F1 600N,1500W(15-30)	6Q-30
F1 600N,1688W(0-15)	6R-15
F1 600N,1688W(15-30)	6R-30
F1 600N,-250W(0-15)	6S-15
F1 600N,-250W(15-30)	6S-30
F2 1100N, 0W(0-15)	11A-15
F2 1100N,0W(15-30)	11A-30
F2 1100N,250W(0-15)	11B-15
F2 1100N,250W(15-30)	11B-30
F2 1100N,500W(0-15)	11C-15
F2 1100N,500W(15-30)	11C-30
F2 1100N,750W(0-15)	11D-15
F2 1100N,750W(15-30)	11D-30
F2 1100N,1000W(0-15)	11-E-15
F2 1100N,1000W(15-30)	11-E-30
F2 1100N,1250W(0-15)	11F-15
F2 1100N,1250W(15-30)	11F-30
F2 1100N,1500W(0-15)	11G-15
F2 1100N,1500W(15-30)	11G-30
F2 1100N,1750W(0-15)	11H-15
F2 1100N,1750W(15-30)	11H-30
F2 1100N,2000W(0-15)	11-I-15

Table D.3. (continued)

F2 1100N, 2000W(15-30)	11-I-30
F3 1500N,0W(0-15)	15A-15
F3 1500N,0W(15-30)	15A-30
F3 1500N, 50W(0-15)	15B-15
F3 1500N,50W(15-30)	15B-30
F3 1500N,100W(0-15)	15C-15
F3 1500N,100W(15-30)	15C-30
F3 1500N,150W(0-15)	15D-15
F3 1500N,150W (15-30)	15D-30
F3 1500N,250W(0-15)	15-E-15
F3 1500N,250W(15-30)	15-E-30
F3 1500N,500W(0-15)	15F-15
F3 1500N,500W(15-30)	15-F-30
F3 1500N,750W(0-15)	15G-15
F3 1500N,750W(15-30)	15G-30
F3 1500N,1000W(0-15)	15H-15
F3 1500N,1000W(15-30)	15H-30
F3 1500N,1250W(0-15)	15-I-15
F3 1500N,1250W(15-30)	15-I-30
F3 1500N,1500W(0-15)	15J-15
F3 1500N, 1500W(15-30)	15J-30
F3 1500N,1750W(0-15)	15K-15
F3 1500N,1750W(15-30)	15K-30
F3 1500N,2000W(0-15)	15L-15
F3 1500N,2000W(15-30)	15L-30
F3 1500N,-250W(0-15)	15M-15
F3 1500N,-250W(15-30)	15M-30
F3 1500N,-423W(0-15)	15N-15
F3 1500N,-423W(15-30)	15-N-30
F3 1600N,0W(0-15)	16A-15
F3 1600N,0W(15-30)	16A-30
F3 1600N,50W(0-15)	16B-15
F3 1600N, 50W(15-30)	16B-30
F3 1600N,100W(0-15)	16C-15
F3 1600N,100W(15-30)	16C-30
F3 1600N,150W(0-15)	16D-15
F3 1600N,150W(15-30)	16-E-15
F3 1600N,250W(0-15)	16-E-30
F3 1600N,250W(15-30)	16F-15

Table D.3. (continued)

F3 1700N,0W(0-15)	17A-15
F3 1700N,0W(15-30)	17A-30
F3 1700N,250W(0-15)	17B-15
F3 1700N,250W(15-30)	17B-30
F3 1700N,500W(0-15)	17C-15
F3 1700N,500W(15-30)	17C-30
F3 1700N,750W(0-15)	17D-15
F3 1700N 750W(15-30)	17D-30
F3 1700N,1000W(0-15)	17-E-15
F3 1700N,1000W(15-30)	17-E-30
F3 1700N,1250W(0-15)	17F-15
F3 1700N,1250W(15-30)	17F-30
F3 1700N,1500W(0-15)	17G-15
F3 1700N,1500W(15-30)	17G-30
F3 1700N,1750W(0-15)	17H-15
F3 1700N,1750W(15-30)	17H-30
F3 1700N,1983W(0-15)	17-I-15
F3 1700N,1983W(15-30)	17-I-30
F3 1700N,-250W(0-15)	17J-15
F3 1700N,-250W(15-30)	17J-30
F3 1700N,-500W(0-15)	17K-15
F3 1700N,-500W(15-30)	17K-30
F3 1700N,-604W(0-15)	17L-15
F3 1700N,-604W(15-30)	17L-30
F3 1900N 0W(0-15)	19A-15
F3 1900N,0W(15-30)	19A-30
F3 1900N,250W(0-15)	19-B-15
F3 1900N,250W(15-30)	19-B-15
F3 1900N,500W(0-15)	19C-15
F3 1900N,500W(15-30)	19C-30
F3 1900N,750W(0-15)	19D-15
F3 1900N,750W(15-30)	19D-30
F3 1900N,1000W(0-15)	19-E-15
F3 1900N,1000W(15-30)	19-E-30
F3 1900N,1250W(0-15)	19F-15
F3 1900N,1250W(15-30)	19F-30
F3 1900N,1500W(0-15)	19G-15
F3 1900N,1500W(15-30)	19G-30
F3 1900N,1750W(0-15)	19H-15

Table D.3. (continued)

F3 1900N,1750W(15-30)	19H-30
F3 1900N,2000W(0-15)	19-I-15
F3 1900N,2000W(15-30)	19-I-30
F3 1900N-250W(0-15)	19J-15
F3 1900N,-250W(15-30)	19J-30
F3 1900N,-500W(0-15)	19K-15
F3 1900N,-500W(15-30)	19K-30
F3 1900N,-665W(0-15)	19L-15
F3 1900N,-665W(15-30)	19L-30
F3 1500N 0W(0-15)	15-C-0
F3 1500N 0W(15-30)	15-C-15
F3 1500N 0W(30-45)	15-C-30
F3 1500N 0W(45-60)	15-C-45
F3 1500N 0W(60-75)	15-C-60
F3 1500N 0W(75-90)	15-C-75
F3 1500N 0W(90-105)	15-C-90
F3 1500N 0W(105-120)	15-C-105
F3 1500N 0W(120-135)	15-C-120
F3 1500N 0W(135-150)	15-C-135
F3 1500N 0W(150-165)	15-C-150
F3 1500N 0W(165-180)	15-C-165
F3 1500N, 0W (180-195)	15-C-180
F3 1500N 0W(195-210)	15-C-195
F3 1500N 0W(210-225)	15-C-210
F3 1500N 0W(225-236)	15-C-225
F3 1900N 1250W(0-15)	19-AC-0
F3 1900N 1250W(15-30)	19-AC-15
F3 1900N 1250W(30-45)	19-AC-30
F3 1900N, 1250W(45-60)	19-AC-45
F3 1900N 1250W(60-75)	19-AC-60
F3 1900N 1250W(75-90)	19-AC-75
F3 1900N 1250W(90-105)	19-AC-90
F3 1900N 1250W(105-120)	19-AC-105
F3 1900N 1250W(123-135)	19-AC-120
F3 1900N 1250W(135-150)	19-AC-135
F3 1900N 1250W(150-165)	19-AC-150
F3 1900N 1250W(165-180)	19-AC-165
F3 1900N 1250W(180-195)	19-AC-180
F3 1900N 1250W(195-210)	19-AC-195

Table D.3. (continued)

F3 1900N 1250W(210-225)	19-AC-210
F3 1900N 1250W(225-240)	19-AC-225
F3 1900N 1250W(226-232)	19-AC-226
F3 1900N 1500W(0-15)	19BC-0
F3 1900N 1500W(15-30)	19-BC-15
F3 1900N 1500W(30-45)	19BC-30
F3 1900N 1500W(45-60)	19BC-45
F3 1900N 1500W(60-75)	19BC-60
F3 1900N 1500W(75-90)	19BC-75
F3 1900N 1500W(90-105)	19BC-90
F3 1900N 1500W(105-117)	19BC-105
F3 1900N 1500W(117-135)	19BC-117
F3 1900N 1500W(135-150)	19BC-135
F3 1900N 1500W(150-165)	19BC-150
F3 1900N 1500W(165-180)	19BC-165
F3 1900N, 1500W(180-195)	19BC-180
F3 1900N 1500W(195-210)	19BC-195
F3 1900N 1500W(210-233)	19BC-210
F3 1500N,250W(0-15)	15-AC-0
F3 1500N,250W(15-30)	15AC-15
F3 1500N,250W(30-45)	15AC-30
F3 1500N,250W(45-60)	15AC-45
F3 1500N,250W(60-75)	15AC-60
F3 1500N,250W(75-90)	15AC-75
F3 1500N,250W(90-105)	15AC-90
F3 1500N,250W(105-120)	15AC-105
F3 1500N,250W(120-135)	15AC-120
F3 1500N,250W(135-150)	15AC-135
F3 1500N,250W(150-165)	15AC-150
F3 1500N,250W(165-180)	15AC-165
F3 1500N,250W(180-195)	15AC-180
F3 1500N,250W(195-210)	15AC-195
F3 1500N,250W(210-225)	15AC-210
F3 1500N,250W(225-233)	15AC-225
F3 1500N, 500W(0-15)	15BC-0
F3 1500N, 500W(15-30)	15BC-15
F3 1500N, 500W(30-45)	15BC-30
F3 1500N, 500W(45-60)	15BC-45
F3 1500N, 500W(60-75)	15BC-60

Table D.3. (continued)

F3 1500N, 500W(75-90)	15BC-75
F3 1500N, 500W(90-105)	15BC-90
F3 1500N, 500W(105-120)	15BC-105
F3 1500N, 500W(120-135)	15BC-120
F3 1500N, 500W(135-150)	15BC-135
F3 1500N, 500W(150-165)	15BC-150
F3 1500N, 500W(165-180)	15BC-165
F3 1500N, 500W(180-195)	15BC-180
F3 1500N, 500W(195-210)	15BC-195
F3 1500N, 500W(210-225)	15BC-210
F3 1500N, 500W(225-239)	15BC-225
F3 1500N, 750W(0-15)	15CC-0
F3 1500N, 750W(15-30)	15CC-15
F3 1500N, 750W(30-45)	15CC-30
F3 1500N, 750W(45-60)	15CC-45
F3 1500N, 750W(60-75)	15CC-60
F3 1500N, 750W(75-90)	15CC-75
F3 1500N, 750W(90-105)	15CC-90
F3 1500N, 750W(105-120)	15CC-105
F3 1500N, 750W(120-135)	15CC-120
F3 1500N, 750W(135-150)	15CC-135
F3 1500N, 750W(150-165)	15CC-150
F3 1500N, 750W(165-180)	15CC-165
F3 1500N, 750W(180-195)	15CC-180
F3 1500N, 750W(195-210)	15CC-195
F3 1500N, 750W(210-225)	15CC-210
F3 1500N, 750W(225-240)	15CC-225
F3 1500N, 750W(240-255)	15CC-240
F3 1500N, 750W(255-270)	15CC-255
F3 1500N, 750W(270-285)	15CC-270
F3 1500N, 750W(285-300)	15CC-285
F3 1500N, 750W(300-315)	15CC-300
F3 1500N, 750W(315-330)	15CC-315
F3 1500N, 750W(330-345)	15CC-330
F3 1500N, 750W(340-357)	15CC-340
1500N, 1000W (0-15)	15DC-0
1500N, 1000W (15-30)	15DC-15
1500N, 1000W (30-45)	15DC-30
1500N, 1000W (45-60)	15DC-45

Table D.3. (continued)

1500N,1000W (60-75)	15DC-60
1500N, 1000W (75-90)	15DC-75
1500N, 1000W (90-105)	15DC-90
1500N, 1000W (105-120)	15DC-105
1500N, 1000W(120-135)	15DC-120
1500N, 1000W(135-150)	15DC-135
1500N, 1000W (150-165)	15DC-150
1500N, 1000W (165-180)	15DC-165
1500N, 1000W (180-195)	15DC-180
1500N, 1000W (195-210)	15DC-195
1500N, 1000W (210-225)	15DC-210
1500N, 1000W (225-238)	15DC-225
1500N, 1250W (0-15)	15EC-0
1500N, 1250W (15-30)	15EC-15
1500N, 1250W (30-45)	15EC-30
1500N, 1250W (45-60)	15EC-45
1500N, 1250W (60-75)	15EC-60
1500N, 1250W (75-90)	15EC-75
1500N, 1250W (90-105)	15EC-90
1500N, 1250W (105-120)	15EC-105
1500N, 1250W (120-135)	15EC-120
1500N, 1250W (135-150)	15EC-135
1500N, 1250W (150-165)	15EC-150
1500N, 1250W (165-180)	15EC-165
1500N, 1250W (180-195)	15EC-180
1500N, 1250W (195-210)	15EC-195
1500N,1250W (210-225)	15EC-210
1500N, 1250W (225-238)	15EC-225
1500N, 1500W (0-15)	15FC-0
1500N, 1500W (15-30)	15FC-15
1500N, 1500W (30-45)	15FC-30
1500N, 1500W (45-60)	15FC-45
1500N, 1500W (60-75)	15FC-60
1500N, 1500W (75-90)	15FC-75
1500N, 1500W (90-105)	15FC-90
1500N, 1500W (105-120)	15FC-105
1500N, 1500W (120-135)	15FC-120
1500N,1500W (135-150)	15FC-135
1500N, 1500W (150-165)	15FC-150

Table D.3. (continued)

1500N, 1500W (165-180)	15FC-165
1500N, 1500W (180-195)	15FC-180
1500N, 1500W (195-210)	15FC-195
1500N, 1500W (210-225)	15FC-210
1500N, 1500W (225-239)	15FC-225
1500N, 1750W (0-15)	15GC-0
1500N, 1750W (15-30)	15GC-15
1500N, 1750W (30-45)	15GC-30
1500N, 1750W (45-60)	15GC-45
1500N, 1750W (60-75)	15GC-60
1500N, 1750W (75-90)	15GC-75
1500N, 1750W (90-105)	15GC-90
1500N, 1750W (105-120)	15GC-105
1500N, 1750W (120-135)	15GC-120
1500N, 1750W (135-150)	15GC-135
1500N, 1750W (150-165)	15GC-150
1500N, 1750W (165-180)	15GC-165
1500N, 1750W (180-195)	15GC-180
1500N, 1750W (195-210)	15GC-195
1500N, 1750W (210-225)	15GC-210
1500N, 1750W (225-236)	15GC-225
1700N, 1250W (0-15)	17AC-0
1700N, 1250W (15-30)	17AC-15
1700N, 1250W (30-45)	17AC-30
1700N, 1250W (45-60)	17AC-45
1700N, 1250W (60-75)	17AC-60
1700N, 1250W (75-90)	17AC-75
1700N, 1250W (90-105)	17AC-90
1700N, 1250W (105-120)	17AC-105
1700N, 1250W (120-135)	17AC-120
1700N, 1250W (135-150)	17AC-135
1700N, 1250W (150-165)	17AC-150
1700N, 1250W (165-180)	17AC-165
1700N, 1250W (180-195)	17AC-180
1700N, 1250W (195-210)	17AC-195
1700N, 1250W (210-225)	17AC-210
1700N, 1250W (225-236)	17AC-225
1700N, 1500W (0-15)	17BC-0
1700N, 1500W (15-30)	17BC-15

Table D.3. (continued)

1700N, 1500W (30-45)	17BC-30
1700N, 1500W (45-60)	17BC-45
1700N, 1500W (60-75)	17BC-60
1700N, 1500W (75-90)	17BC-75
1700N, 1500W (90-105)	17BC-90
1700N, 1500W (105-120)	17BC-105
1700N, 1500W (120-135)	17BC-120
1700N, 1500W (135-150)	17BC-135
1700N, 1500W (150-165)	17BC-150
1700N, 1500W (165-180)	17BC-165
1700N, 1500W (180-195)	17BC-180
1700N, 1500W (195-210)	17BC-195
1700N, 1500W (210-225)	17BC-210
1700N, 1500W (225-236)	17BC-225

APPENDIX E. MULTI-ELEMENT ANALYSIS

Table E.1. Results of elements analyzed for surface samples through ICP-OES.

Sample ID	Cd (mg/kg)
2A-15	0.99
2A-30	1.17
2B-15	1.09
2B-30	0.91
2C-15	1.67
2C-30	0.62
2D-15	0.91
2D-30	BDL
2-E-15	1.17
2-E-30	0.96
2F-15	0.76
2F-30	BDL
2G-15	1.36
2G-30	0.49
2H-15	0.65
2H-30	0.44
2I-15	1.09
2I-30	BDL
2J-15	0.91
2J-30	0.78
6K-15	1.07
6K-30	1.25
6L-15	1.01
6L-30	0.96
6M-15	1.09
6M-30	6.93
	*2nd: 0.68
6N-15	0.81
6N-30	0.91
6O-15	1.01
6O-30	1.17
6P-15	1.75
	*2nd: 0.13
6P-30	0.91
6Q-15	1.35
6Q-30	0.96
6R-15	7.43
6R-30	1.20
	*2nd: 5.36
6S-30	0.91

Table E.1. (continued)

11A-15	0.73
11A-30	0.70
11B-15	1.35
11B-30	BDL
11C-15	BDL
11C-30	1.12
11-D-15	1.12
11-D-30	BDL
11-E-15	1.20
11-E-30	0.63
11-F-15	1.69
11-F-30	BDL
11-G-15	0.99
11-G-30	BDL
11-H-15	2.45
	*2nd: 1.88
11-H-30	2.32
	*2nd: 1.56
11-I-15	BDL
11-I-30	0.73
15-A-15	1.33
	*2nd: 1.04
15-A-30	1.07
	*2nd: 0.81
15-B-15	1.28
15-B-30	0.96
15-C-15	1.17
15-C-30	1.14
15-D-15	1.35
15-D-30	1.43
15-E-15	1.15
	*2nd: 0.39
15-E-30	0.65
	*2nd: 0.18
15-F-15	1.51
15-F-30	0.62
15-G-15	1.72
	*2nd: 1.09
	*3rd: 0.18
15-G-30	0.70
15-H-15	1.25
15-H-30	BDL
15-I-15	1.14
15-J-15	1.69

Table E.1. (continued)

15-J-30	0.61
15-K-15	1.04
15-K-30	0.94
15-L-15	1.67
15-L-30	0.73
15-M-15	0.83
15-M-30	BDL
15-N-15	1.15
15-N-30	0.81
16-A-15	1.72
16-A-30	1.25
16-B-15	1.33
16-B-30	1.07
16-C-15	1.25
16-C-30	1.17
16-D-15	1.35
16-E-15	1.04
16-E-30	1.48
16-F-15	0.65
17-A-15	1.75
	*2nd: 0.83
17-A-30	1.28
17-B-15	1.69
17-B-30	1.46
17-C-15	1.09
17-C-30	BDL
17-D-15	1.33
17-D-30	0.47
17-E-15	1.43
17-E-30	BDL
17-F-15	1.12
17-F-30	BDL
17-G-15	1.23
17-G-30	BDL
17-H-15	0.96
17-H-30	BDL
17-I-15	1.17
17-I-30	1.04
17-J-15	1.62
17-J-30	1.25
17-K-15	1.33
17-K-30	BDL
17-L-15	1.04
19-A-15	1.17

Table E.1. (continued)

19-A-30	1.51
19-B-15	1.35
19-B-30	1.15
19-C-15	1.43
19-C-30	0.94
19-D-15	1.17
19-D-30	1.17
19-E-15	0.86
19-E-30	0.76
19-F-15	1.02
	*2nd 0.81
19-F-30	0.47
19-G-15	BDL
	*2nd 1.25
19-G-30	0.26
	*2nd: 0.99
19-H-15	2.16
19-H-30	0.68
19-I-15	1.43
19-I-30	1.98
19-J-15	1.56
19-J-30	1.66
19-K-15	0.99
19-K-30	0.75
19-L-15	0.99
19-L-30	1.20
RF	13.73
RF	13.78
RF	14.03
RF	14.06
RF	13.36
RF	13.78
RF	13.94
RF	13.38
RF	13.95
RF	13.82
RF	14.08
RF	14.22
RF	14.45

*2nd, *3rd- Samples reanalyzed
*NA - Not analyzed
BDL- Below detection limit of the instrument
RF- Reference material

Table E.2. Results of multi elements analyzed for core samples through ICP-OES

Sample ID	Metal Concentration (mg/kg)												
	Al	**As**	**Be**	**Ca**	**Co**	**Cr**	**Cu**	**Fe**	**Mn**	**Mo**	**Ni**	**Cd**	**Zn**
F3 1500N 0W													
15-C-0	1.75	4.01	0.83	0.36	10.21	21.99	20.48	1.30	3913.89	0.10	49.19	1.04	99.55
15-C-15	1.59	4.16	0.70	0.26	10.07	19.30	19.48	1.12	2513.39	0.13	36.67	0.81	74.10
15-C-30	1.46	4.17	0.60	0.21	7.17	18.84	20.20	1.09	792.54	0.03	18.22	0.16	58.02
15-C-45	1.43	3.62	0.65	0.21	12.39	18.33	20.52	1.12	2666.60	BDL	28.17	0.47	60.98
15-C-60	1.44	4.51	0.76	0.21	9.26	18.45	20.41	1.30	2601.10	BDL	29.56	0.25	68.60
15-C-75	1.23	4.35	0.73	0.21	13.42	15.28	24.09	1.04	4198.71	BDL	49.19	0.23	78.02
15-C-90	1.33	4.97	0.73	0.21	10.08	16.93	19.32	1.02	3048.36	BDL	45.49	0.18	63.96
15-C-105	1.33	6.40	0.73	0.26	14.28	17.56	25.23	1.17	4266.75	BDL	60.89	0.52	83.96
15-C-120	1.25	4.84	0.68	0.23	11.82	16.38	20.99	1.07	3127.16	BDL	41.81	0.21	68.79
15-C-135	1.46	4.25	0.70	0.26	11.67	18.11	24.38	1.02	2634.36	0.03	39.52	0.52	67.40
15-C-150	1.15	3.20	0.60	0.21	7.68	13.88	24.41	0.83	1797.63	0.08	29.72	0.21	56.50
15-C-165	1.12	4.17	0.62	0.26	10.23	14.84	22.03	1.02	2312.51	0.18	34.03	0.20	67.10
15-C-180	1.41	2.92	0.99	0.44	10.57	22.65	20.25	1.30	2438.58	BDL	44.85	BDL	76.01
15-C-195	1.12	1.48	0.60	0.23	5.88	14.48	17.52	0.78	1066.79	BDL	25.98	0.14	56.50
15-C-210	1.48	2.01	0.70	0.29	6.36	19.02	18.18	1.02	1032.50	BDL	26.47	0.16	60.47
15-C-225	1.38	1.93	0.65	0.26	5.96	16.72	18.15	0.86	927.11	BDL	24.68	0.14	52.70
F3 1500N 250W													
15-AC-0	1.95	11.23	2.58	0.52	15.09	26.73	29.47	674.82	5251.18	0.76	68.32	0.39	128.02
15-AC-15	1.85	9.97	2.39	0.36	13.72	22.67	26.81	615.90	2782.06	0.60	47.56	0.18	73.36
15-AC-30	2.19	10.37	2.34	0.31	12.01	26.76	30.30	719.59	2638.45	0.49	32.75	0.04	83.91
15-AC-45	1.59	10.41	2.26	0.29	10.07	20.68	25.11	575.12	2267.05	0.57	32.65	0.01	72.71
15-AC-60	1.77	10.65	2.42	0.29	12.57	22.41	25.95	617.92	3195.80	0.44	39.46	0.05	73.43
15-AC-75	1.77	9.27	2.34	0.31	15.80	22.57	28.92	515.13	4042.57	0.52	41.57	0.13	63.78
15-AC-90	1.74	8.85	2.32	0.31	11.86	21.28	25.68	484.03	2641.62	0.44	32.18	0.04	59.21
15-AC-105	1.93	8.39	2.37	0.31	10.24	22.99	25.23	511.57	2188.18	0.39	30.34	BDL	60.09

Table E.2. (continued)

15-AC-120	1.67	9.17	2.34	0.31	14.35	21.41	29.39	525.33	3620.33	0.57	40.90	0.04	67.16
15-AC-135	1.51	8.80	2.29	0.34	11.56	19.44	27.33	481.04	2473.75	0.55	32.12	0.01	60.20
15-AC-150	1.56	9.21	2.37	0.34	11.87	21.42	24.23	484.67	3842.25	0.47	57.99	0.09	70.66
15-AC-165	1.28	10.52	2.32	0.31	11.85	17.55	26.32	515.35	4189.81	0.39	51.01	0.16	74.23
15-AC-180	1.46	9.43	2.29	0.31	15.96	20.13	28.13	472.77	4830.86	0.55	70.44	0.16	81.90
15-AC-195	1.41	8.32	2.22	0.31	9.59	19.61	19.14	414.26	2635.22	0.60	33.24	BDL	59.37
15-AC-210	1.22	8.33	2.19	0.34	10.21	17.42	19.27	410.16	2666.28	0.55	30.91	BDL	60.39
15-AC-225	1.30	9.96	2.24	0.34	10.61	18.65	23.54	477.53	4760.57	0.49	38.50	BDL	73.81
F3 1500N 500W													
15-BC-0	2.11	9.65	2.56	0.60	12.91	26.32	29.97	617.98	5060.06	0.76	56.97	0.12	121.05
15-BC-15	2.06	10.98	2.55	0.39	14.13	25.45	28.91	666.24	2744.68	0.62	50.80	BDL	83.26
15-BC-30	2.53	11.27	2.50	0.39	10.72	31.72	33.62	817.71	788.22	0.63	32.32	BDL	91.94
15-BC-45	1.77	12.67	2.50	0.31	16.56	22.89	33.32	1009.38	2673.03	0.42	42.55	BDL	89.82
15-BC-60	1.95	9.40	2.40	0.31	11.62	24.98	24.17	567.37	2585.13	0.70	28.94	BDL	69.55
15-BC-75	0.47	7.52	1.77	0.08	3.69	7.52	6.24	118.36	603.42	0.81	8.64	0.08	18.76
15-BC-90	2.01	9.90	2.48	0.34	14.10	24.55	27.00	523.93	3980.17	0.57	39.62	BDL	71.44
15-BC-105	2.09	10.37	2.55	0.36	14.99	25.78	29.30	561.72	4228.48	0.60	44.29	BDL	73.28
15-BC-120	1.77	8.73	2.42	0.36	14.35	22.45	28.10	498.49	3690.53	0.65	46.36	BDL	72.91
15-BC-135	1.88	9.25	2.45	0.36	13.03	24.29	26.09	517.61	3925.98	0.65	45.87	BDL	69.74
15-BC-150	1.62	9.12	2.40	0.42	15.50	21.52	33.61	444.16	5451.59	0.70	84.23	0.03	112.75
15-BC-165	1.54	10.21	2.34	0.39	11.72	20.92	24.36	477.05	4258.61	0.68	42.96	BDL	74.38
15-BC-180	1.70	9.96	2.48	0.44	14.06	23.34	25.27	535.97	4697.53	0.70	52.56	BDL	83.81
15-BC-195	1.95	7.42	2.45	0.42	7.21	24.28	28.91	445.60	865.73	0.57	20.43	BDL	57.26
15-BC-210	1.35	9.60	2.34	0.44	11.68	17.85	25.34	431.07	4534.93	0.62	71.74	0.01	111.63
15-BC-225	1.49	11.18	2.40	0.42	13.87	19.66	29.67	501.93	4827.73	0.65	58.00	BDL	91.99
F3 1500N 750W													
15-CC-0	2.32	10.59	2.71	0.55	14.58	28.46	32.68	721.77	4679.30	0.70	58.43	0.18	105.95
15-CC-15	1.88	10.24	2.63	0.39	13.52	21.68	29.70	669.12	3797.80	0.70	49.06	BDL	83.05

Table E.2. (continued)

15-CC-30	1.69	10.62	2.03	0.23	7.16	18.95	19.75	505.44	364.49	0.65	21.13	0.16	52.52
15-CC-45	2.24	9.92	2.53	0.36	14.84	26.90	33.04	681.64	2541.70	0.60	39.65	BDL	80.37
15-CC-60	1.82	8.75	2.34	0.39	11.61	23.45	27.78	623.85	2818.56	0.10	46.96	0.62	74.58
15-CC-75	2.06	8.35	2.30	0.44	12.91	25.12	28.75	615.33	2791.02	BDL	60.66	0.44	74.20
15-CC-90	1.43	7.90	2.03	0.47	11.93	18.58	23.58	478.28	3022.96	0.16	38.90	0.36	63.94
15-CC-105	1.62	7.25	2.06	0.44	11.94	20.95	22.65	482.10	3162.59	0.10	42.59	0.39	62.78
15-CC-120	1.72	6.66	2.08	0.44	11.19	21.65	21.78	490.42	2798.25	0.00	40.72	0.36	69.42
15-CC-135	1.20	6.46	1.93	0.42	9.61	16.70	19.82	378.62	2567.08	0.13	33.03	0.39	58.92
15-CC-150	1.36	7.51	2.01	0.44	12.70	18.30	23.38	457.27	4206.74	0.10	47.94	0.44	72.89
15-CC-165	1.46	6.03	2.00	0.36	9.31	19.74	18.52	427.83	2362.24	0.05	28.12	0.36	55.51
15-CC-180	0.73	6.49	1.75	0.23	7.40	11.72	13.16	284.17	2532.81	0.36	24.88	0.42	41.21
15-CC-195	1.25	8.89	1.98	0.36	11.65	17.75	22.28	495.56	3144.99	0.13	38.28	0.44	66.39
15-CC-210	1.49	6.62	2.03	0.39	11.11	20.52	24.70	469.31	3568.36	0.03	35.81	0.42	71.22
15-CC-225	1.28	7.06	2.01	0.44	10.08	18.08	21.15	419.40	4042.40	0.13	39.57	0.26	70.51
15-CC-240	1.46	7.82	2.08	0.39	10.48	20.66	23.84	476.31	3814.58	0.18	38.75	0.31	67.49
15-CC-255	1.56	6.85	2.09	0.39	11.39	20.59	24.47	457.13	3817.43	0.08	42.85	0.29	70.66
15-CC-270	1.30	8.38	2.00	0.39	10.98	18.01	24.88	459.50	4376.15	0.18	48.46	0.34	78.03
15-CC-285	1.70	8.79	2.17	0.44	14.64	22.44	24.34	547.01	4607.03	0.00	37.70	0.26	68.74
15-CC-300	1.23	10.44	2.01	0.42	12.45	17.87	23.09	504.90	2987.36	0.26	39.25	0.04	69.98
15-CC-315	1.41	8.77	2.06	0.42	16.39	19.16	29.99	488.65	5118.15	0.08	61.67	0.37	89.10
15-CC-330	1.51	8.36	2.11	0.44	16.44	21.13	28.22	536.15	4987.92	0.08	59.62	0.05	89.09
15-CC-340	1.28	7.17	1.98	0.39	10.48	17.96	21.35	417.48	3156.91	0.10	44.55	0.29	70.98
F3 1500N 1000W													
15-DC-0	2.16	10.69	3.81	0.47	14.65	24.19	28.20	16131.15	1.93	45.35	45.35	0.76	90.72
15-DC-15	2.40	9.95	3.60	0.39	10.87	30.10	31.48	17895.78	1.75	26.66	26.66	0.36	84.17
15-DC-30	2.63	9.39	3.93	0.42	13.78	31.75	33.05	18371.95	1.90	40.49	40.49	0.47	88.29
15-DC-45	2.26	9.50	3.98	0.52	12.44	27.79	30.65	17029.38	1.72	60.11	60.11	0.49	86.08
15-DC-60	2.40	10.71	3.85	0.83	14.61	30.79	29.80	18052.89	1.88	53.73	53.73	0.03	88.74
15-DC-75	1.80	10.36	3.57	1.82	14.21	22.67	28.08	14057.52	1.85	45.55	45.55	0.44	77.69

Table E.2. (continued)

15-DC-90	1.46	9.34	3.50	1.93	12.89	19.20	27.03	11743.07	2.01	47.64	47.64	0.44	75.53
15-DC-105	1.41	9.34	3.46	2.00	14.50	19.21	27.04	12824.43	2.03	49.09	49.09	0.49	78.75
15-DC-120	1.85	9.42	3.82	1.14	15.06	23.93	28.33	14421.05	1.85	51.85	51.85	0.47	79.53
15-DC-135	2.03	7.48	3.88	1.15	11.64	25.08	25.27	13946.31	1.93	41.21	41.21	0.44	76.50
15-DC-150	2.19	7.33	3.94	0.55	11.24	27.32	23.46	13977.93	1.80	38.45	38.45	0.29	82.17
15-DC-165	1.88	6.99	3.83	0.42	11.47	24.30	21.51	12439.12	1.93	34.49	34.49	0.39	82.49
15-DC-180	1.87	6.19	3.64	0.44	10.95	24.53	20.01	12325.05	1.82	33.79	33.79	0.44	125.53
15-DC-195	1.64	8.69	3.83	0.39	17.15	22.59	19.18	12301.73	1.95	53.16	53.16	0.36	69.63
15-DC-210	1.64	6.89	3.59	0.39	11.73	22.82	15.61	10523.83	2.03	33.90	33.90	0.29	53.90
15-DC-225	1.51	8.02	3.77	0.39	12.96	21.63	17.46	10697.30	2.06	47.81	47.81	0.29	71.08
F3 1500N 1250W													
15-EC-0	2.14	12.93	3.94	0.34	13.34	27.55	32.42	17526.83	2.16	31.41	31.41	0.60	87.21
15-EC-15	1.98	11.21	3.59	0.29	9.78	23.70	32.68	17911.80	1.90	30.75	30.75	0.44	85.20
15-EC-30	2.29	11.58	4.11	0.34	12.73	29.73	38.42	21597.65	1.87	40.17	40.17	0.60	101.83
15-EC-45	2.00	13.58	4.01	0.34	14.46	27.68	43.05	15393.56	1.90	33.45	33.45	0.52	87.63
15-EC-60	1.95	12.32	4.09	0.31	9.77	27.95	44.60	13565.36	1.85	22.07	22.07	0.42	63.02
15-EC-75	1.90	11.39	3.93	0.34	8.87	26.53	47.26	10939.09	2.11	21.56	21.56	0.47	60.81
15-EC-90	1.93	18.63	3.91	0.26	8.23	35.25	49.58	11044.16	2.11	14.09	14.09	0.37	58.75
15-EC-105	1.48	13.38	3.88	0.23	8.35	25.97	40.24	9393.83	2.13	12.44	12.44	0.29	58.87
15-EC-120	1.36	15.94	3.60	0.31	8.95	26.68	48.96	9376.46	2.37	11.95	11.95	0.29	65.52
15-EC-135	1.59	17.14	3.63	0.37	9.49	26.94	41.26	8443.58	2.01	10.98	10.98	0.29	70.69
15-EC-150	1.66	24.43	3.72	0.42	9.99	31.06	49.87	10152.33	2.19	11.11	11.11	0.31	82.26
15-EC-165	1.46	18.89	3.62	0.26	9.47	28.06	46.74	8437.53	2.19	10.12	10.12	0.31	75.48
15-EC-180	1.51	37.44	3.88	0.21	10.12	30.41	48.99	11127.86	2.19	10.74	10.74	0.31	81.38
15-EC-195	1.36	17.61	3.89	0.16	9.05	39.03	60.92	11001.19	2.63	9.70	9.70	0.07	69.14
15-EC-210	1.82	14.20	3.64	0.70	6.71	34.24	49.43	20645.39	4.27	8.74	8.74	0.13	42.38
15-EC-225	1.41	37.11	3.62	0.60	5.83	39.84	62.14	26536.20	7.99	8.28	8.28	0.65	38.20
F3 1500N 1500W													

Table E.2. (continued)

15-FC-0	2.29	12.85	4.02	0.44	14.03	22.61	29.23	20803.86	503.70	3.02	37.52	0.63	113.68
15-FC-15	2.06	15.15	3.62	0.39	9.16	20.75	26.01	19227.71	64.30	3.67	23.27	0.26	95.90
15-FC-30	2.03	14.31	3.64	0.29	8.93	22.20	34.15	18647.99	52.31	2.94	19.96	0.42	88.28
15-FC-45	1.64	15.74	3.57	0.29	7.90	24.39	39.48	17304.41	34.79	2.84	14.77	0.31	68.87
15-FC-60	1.66	17.74	3.75	0.23	8.09	30.15	46.27	14629.60	34.46	3.07	13.29	0.26	75.40
15-FC-75	1.61	13.01	3.83	0.23	9.29	30.92	52.55	15376.75	58.17	3.54	14.57	0.26	85.08
15-FC-90	1.59	7.69	3.65	0.29	7.77	22.62	49.86	16312.73	34.38	2.11	13.29	0.34	64.66
15-FC-105	1.53	19.90	3.56	0.34	9.78	22.50	53.18	27140.78	88.40	2.99	15.06	0.57	98.16
15-FC-120	1.69	17.04	3.80	0.26	7.63	39.89	65.47	12062.80	31.21	2.29	10.45	0.23	77.87
15-FC-135	1.46	18.69	3.75	0.29	8.25	40.50	65.25	15230.64	29.70	2.08	11.09	0.08	84.82
15-FC-150	1.69	14.73	3.83	0.29	10.20	30.16	58.52	18134.38	43.69	2.06	12.05	0.31	123.26
15-FC-165	1.75	12.11	3.88	0.26	9.59	34.52	49.97	15210.21	46.89	2.01	11.07	0.26	109.97
15-FC-180	2.03	14.88	3.93	0.29	9.21	40.10	54.07	13692.21	53.47	1.93	10.46	0.23	101.06
15-FC-195	1.72	24.74	4.18	0.26	9.68	33.58	54.75	20914.29	46.76	1.83	11.04	0.34	109.33
15-FC-210	1.72	18.14	3.75	0.23	8.04	38.28	54.59	10048.93	23.26	2.21	9.32	0.26	70.98
15-FC-225	1.28	22.17	3.49	0.21	7.70	33.47	54.29	9889.01	18.27	2.26	9.32	0.21	59.78
F3 1500N 1750W													
15-GC-0	2.27	13.45	4.09	0.37	19.35	25.03	31.86	21196.02	2053	2.87	51.34	0.89	115.29
15-GC-15	2.14	16.81	3.67	0.31	9.96	24.81	38.03	19936.81	122	2.95	21.48	0.36	89.68
15-GC-30	1.90	15.77	3.93	0.26	9.06	26.62	41.62	22152.65	55.57	2.91	15.90	0.49	83.36
15-GC-45	1.72	14.64	3.41	0.29	7.14	18.21	38.02	22271.54	35.10	2.87	10.74	0.31	58.92
15-GC-60	1.46	15.99	3.57	0.18	8.10	27.55	51.35	21313.62	37.73	2.27	10.89	0.34	77.40
15-GC-75	1.38	19.66	3.59	0.16	7.67	34.12	54.90	15323.67	27.85	2.26	10.58	0.23	70.21
15-GC-90	1.59	22.01	3.70	0.18	8.26	38.34	58.84	16574.93	39.30	2.19	10.94	0.31	78.61
15-GC-105	1.69	13.28	3.77	0.18	8.90	39.02	54.67	12615.21	29.62	1.95	12.00	0.26	83.46
15-GC-120	1.54	17.04	3.80	0.21	11.42	29.56	49.23	20788.03	74.81	1.95	15.09	0.31	108.92
15-GC-135	1.43	22.08	3.83	0.21	10.48	32.25	57.09	17946.80	36.78	2.01	12.77	0.29	98.69
15-GC-150	1.25	25.03	3.62	0.21	9.04	28.18	49.27	14442.63	24.32	1.93	10.13	0.23	79.14
15-GC-165	1.48	20.17	3.69	0.23	8.22	35.49	53.45	13632.96	27.84	1.98	10.17	0.26	73.01

Table E.2. (continued)

15-GC-180	1.48	24.29	3.67	0.21	7.81	35.70	54.73	24171.62	24.47	2.08	9.61	0.36	72.15
15-GC-195	1.51	29.10	3.72	0.21	8.32	34.85	64.13	27350.45	27.20	2.13	10.12	0.39	83.74
15-GC-210	1.54	17.13	3.88	0.23	9.65	35.82	51.07	17043.95	30.21	2.09	11.13	0.08	93.64
15-GC-225	1.49	16.97	3.75	0.21	8.76	34.69	59.40	12203.79	28.28	2.09	10.27	0.23	79.20
F3 1700N 1250W													
17-AC-0	2.40	11.94	2.79	0.26	12.18	32.02	38.69	20115.82	345	0.70	35.02	0.57	107.71
17-AC-15	2.32	11.84	2.47	0.29	8.61	35.83	43.90	17476.99	61.28	0.49	21.00	0.47	88.21
17-AC-30	1.82	13.18	2.29	0.16	7.27	35.23	53.83	19699.11	49.14	0.57	13.91	0.34	73.28
17-AC-45	1.85	19.42	2.42	0.16	7.59	38.01	56.88	18303.25	58.34	0.63	12.41	0.44	77.47
17-AC-60	1.56	22.07	2.27	0.16	6.54	31.89	48.22	24312.11	50.98	0.31	10.19	0.36	69.35
17-AC-75	1.30	34.78	2.24	0.16	7.93	30.12	51.89	19731.28	67.63	0.60	10.56	0.10	81.49
17-AC-90	1.20	11.48	2.11	0.16	6.83	27.70	50.50	7774.33	32.94	0.57	8.45	0.29	72.38
17-AC-105	1.48	20.82	2.60	0.18	7.39	32.33	48.99	15720.81	60.52	0.81	9.03	0.83	79.47
17-AC-120	1.43	16.63	2.24	0.16	6.84	29.85	56.23	14416.29	57.17	0.62	7.65	0.52	79.31
17-AC-135	1.69	13.32	2.37	0.21	8.51	30.12	49.81	13331.76	53.61	0.52	8.64	0.31	100.63
17-AC-150	1.36	7.30	1.96	0.37	6.47	12.57	29.10	12683.29	48.73	0.83	7.38	0.31	75.14
17-AC-165	1.67	11.74	2.37	0.23	8.41	34.86	54.23	12416.03	38.98	0.70	9.30	0.44	90.63
17-AC-180	1.64	13.43	2.37	0.21	8.21	35.85	49.04	11162.09	42.92	0.55	8.27	0.29	95.87
17-AC-195	1.30	28.78	3.62	0.21	9.00	31.15	51.99	17076.34	38.64	2.00	8.85	0.29	85.87
17-AC-210	2.03	22.98	2.56	0.23	8.92	40.46	51.15	16442.39	53.31	0.29	8.89	0.34	103.47
17-AC-225	1.61	15.80	2.37	0.21	8.77	34.57	51.00	12832.15	49.36	0.55	9.24	0.29	92.44
F3 1700N 1500W													
17-BC-0	2.11	7.47	2.99	0.44	22.02	30.35	34.54	20506.97	794.50	0.73	64.10	0.62	137.78
17-BC-15	1.93	6.80	2.55	0.26	16.42	31.48	43.49	17110.75	194.96	0.55	62.51	0.39	130.18
17-BC-30	1.93	7.40	2.45	0.23	14.84	24.30	45.13	20619.95	101.48	0.81	46.51	0.42	130.05
17-BC-45	1.56	7.59	2.35	0.23	10.41	22.82	43.65	21449.71	80.09	1.62	28.37	0.50	111.61
17-BC-60	1.83	9.31	2.56	0.26	12.65	23.00	47.31	20649.74	87.15	2.03	32.34	0.50	140.43
17-BC-75	1.69	8.49	2.06	0.42	6.74	12.53	24.51	15480.29	47.01	2.06	16.46	0.47	72.40

Table E.2. (continued)

17-BC-90	0.78	9.32	2.04	0.23	8.14	17.15	54.65	21888.39	57.55	1.54	12.32	0.60	99.26
17-BC-105	1.22	13.46	2.24	0.26	10.57	21.94	42.73	18109.61	71.16	1.09	23.35	0.47	106.24
17-BC-120	1.70	14.86	2.45	0.31	8.01	25.14	48.27	19192.56	73.91	1.83	15.23	0.44	93.67
17-BC-135	0.97	15.06	2.17	0.23	9.63	22.81	53.08	14760.87	62.60	0.44	14.14	0.34	101.64
17-BC-150	1.64	9.84	2.45	0.34	9.03	22.59	57.84	20790.35	62.89	1.17	14.57	0.14	106.97
17-BC-165	1.33	19.46	2.24	0.26	8.22	25.07	55.39	23508.42	62.22	0.97	12.65	0.50	81.48
17-BC-180	1.49	13.93	2.40	0.23	8.06	28.70	52.54	21287.68	49.52	0.78	12.81	0.42	93.16
17-BC-195	1.51	13.79	2.42	0.23	7.51	39.02	61.36	11103.15	45.67	0.68	11.60	0.31	74.35
17-BC-210	2.58	13.66	2.65	0.36	11.27	32.34	43.38	17528.38	502.85	1.80	40.49	0.39	100.52
17-BC-225	1.35	10.94	2.47	0.23	10.23	25.59	46.06	15580.32	58.09	0.52	16.77	BDL	108.83
F3 1900N 1250W													
19-AC-0	1.82	8.07	0.96	0.21	7.16	27.15	29.21	1.48	250.94	0.03	15.75	0.81	81.92
19-AC-15	1.38	6.80	0.68	0.16	4.51	27.33	33.11	1.02	5.73	0.03	10.89	0.17	68.73
19-AC-30	1.54	10.23	0.83	0.18	5.41	28.50	36.72	1.20	7.34	BDL	11.37	0.17	76.26
19-AC-45	3.12	34.60	2.58	0.44	17.55	73.47	73.74	3.36	92.56	BDL	35.93	BDL	ADL
19-AC-60	1.51	7.60	0.91	0.16	5.93	26.87	40.43	1.09	1.09	BDL	8.43	0.2	72.04
19-AC-75	1.64	8.57	0.78	0.26	4.66	15.69	30.51	1.35	5.32	0.03	8.42	0.60	65.12
19-AC-90	1.46	7.38	0.86	0.18	5.37	29.14	43.53	0.86	1.04	BDL	6.44	0.12	67.93
19-AC-105	1.41	11.54	0.81	0.68	5.35	25.89	37.40	1.36	11.46	BDL	6.03	0.63	72.27
19-AC-120	1.54	11.71	0.81	0.83	4.98	26.19	34.67	1.25	54.73	0.47	6.60	0.55	70.54
19-AC-135	1.20	12.58	0.73	0.18	6.55	23.80	38.89	1.23	7.78	0.31	6.84	0.20	93.72
19-AC-150	1.38	6.54	0.76	0.16	5.68	26.59	37.12	0.65	0.26	0.05	6.10	BDL	69.47
19-AC-165	1.46	12.83	0.86	0.16	6.09	27.68	37.38	0.99	9.91	0.00	7.21	0.07	72.87
19-AC-180	1.02	9.39	0.68	0.13	3.89	26.40	42.89	0.60	BDL	0.18	5.61	BDL	49.02
19-AC-195	1.36	6.83	0.81	0.18	3.76	34.32	53.85	0.65	BDL	0.23	6.34	BDL	48.48
19-AC-210	1.12	48.38	0.83	0.26	3.25	28.16	48.80	3.51	BDL	4.03	5.54	1.85	55.70
19-AC-225	1.09	18.34	0.70	0.16	2.58	29.61	58.82	2.99	BDL	4.16	6.19	1.33	35.20
19-AC-226	1.33	12.89	0.34	0.47	0.86	3.67	3.88	0.83	0.26	2.34	5.34	0.13	11.70

Table E.2. (continued)

F3 1900N 1500W													
19-BC-0	1.77	6.33	1.12	0.29	16.21	23.27	24.34	1.72	586.12	0.52	37.43	1.05	106.99
19-BC-15	1.46	6.72	0.94	0.18	11.99	19.65	25.93	1.62	200.32	0.65	29.79	0.99	94.09
19-BC-30	1.61	9.97	0.81	0.21	6.17	18.53	23.65	1.77	18.03	2.13	19.28	1.01	74.94
19-BC-45	1.51	9.37	0.88	0.18	8.32	21.70	34.60	2.24	36.63	4.29	26.69	0.94	119.44
19-BC-60	1.30	11.72	0.83	0.16	9.46	18.34	36.44	2.14	31.15	3.49	25.66	1.12	132.42
19-BC-75	1.67	8.01	0.78	0.26	6.94	15.41	28.45	1.83	20.65	1.54	17.58	0.78	96.67
19-BC-90	1.41	5.24	0.78	0.18	4.74	22.73	30.79	0.91	BDL	0.70	9.78	0.09	69.26
19-BC-105	1.35	15.66	0.88	0.18	6.17	19.69	40.09	1.90	18.78	1.53	13.11	0.86	78.80
19-BC-120	1.10	5.27	0.81	0.18	4.64	22.32	44.90	1.12	4.82	0.44	7.40	0.16	73.42
19-BC-135	1.25	7.70	0.75	0.29	5.28	16.34	47.86	2.08	25.71	0.44	8.51	1.20	77.92
19-BC-150	1.69	11.91	1.12	0.23	6.98	29.65	54.79	1.67	15.87	0.10	9.90	0.70	111.42
19-BC-165	0.99	13.23	0.76	0.18	4.20	27.12	51.13	1.36	2.71	0.55	6.60	0.21	79.21
19-BC-180	1.90	11.23	1.69	0.47	8.44	61.01	55.93	1.51	19.21	BDL	12.46	BDL	111.44
19-BC-195	1.33	5.83	0.83	0.21	4.92	27.73	40.98	0.70	BDL	0.08	6.33	0.01	67.64
19-BC-210	1.33	5.26	0.78	0.18	5.52	26.13	37.30	0.83	BDL	0.10	7.06	0.04	75.30

Table E.3. Simple statistical results for core samples.

Sample ID	**Metal Statistics (mg/Kg)**												
	Al	**As**	**Be**	**Ca**	**Co**	**Cr**	**Cu**	**Fe**	**Mn**	**Mo**	**Ni**	**Cd**	**Zn**
F3 1500N, 0W													
Mean	1.37	3.81	0.70	0.26	9.82	17.67	20.98	1.07	2458.62	0.09	36.53	0.35	68.29
Median	1.39	4.16	0.70	0.25	10.15	17.83	20.44	1.06	2557.24	0.09	35.35	0.21	67.25
Min	1.12	1.48	0.60	0.21	5.88	13.88	17.52	0.78	792.54	0.03	18.22	0.09	52.70
Max	1.75	6.40	0.99	0.44	14.28	22.65	25.23	1.30	4266.75	0.18	60.89	1.04	99.55
F3 1500N 250W													

Table E.3. (Continued)

Mean	1.64	9.55	2.33	0.33	12.34	21.36	25.93	530.95	3376.62	0.52	42.50	0.11	72.64
Median	1.63	9.35	2.33	0.31	11.87	21.35	26.14	513.35	2988.93	0.53	38.98	0.07	71.69
Min	1.22	8.32	2.19	0.29	9.59	17.42	19.14	410.16	2188.18	0.39	30.34	0.01	59.21
Max	2.19	11.23	2.58	0.52	15.96	26.76	30.30	719.59	5251.18	0.76	70.44	0.39	128.02
F3 1500N, 500W													
Mean	1.77	9.83	2.41	0.38	12.51	22.72	27.12	545.91	3432.24	0.65	45.39	0.05	80.85
Median	1.82	9.78	2.45	0.39	13.45	23.81	28.51	520.77	3953.08	0.65	45.08	0.03	78.82
Min	0.47	7.42	1.77	0.08	3.69	7.52	6.24	118.36	603.42	0.42	8.64	0.01	18.76
Max	2.53	12.67	2.56	0.60	16.56	31.72	33.62	1009.38	5451.59	0.81	84.23	0.12	121.05
F3 1500N, 750W													
Mean	1.54	8.16	2.12	0.40	11.87	20.27	24.29	503.63	3386.12	0.21	42.44	0.30	71.15
Median	1.47	8.12	2.05	0.40	11.63	20.13	23.71	485.37	3159.75	0.13	40.19	0.35	70.58
Min	0.73	6.03	1.75	0.23	7.16	11.72	13.16	284.17	364.49	0.00	21.13	0.04	41.21
Max	2.32	10.62	2.71	0.55	16.44	28.46	33.04	721.77	5118.15	0.70	61.67	0.62	105.95
F3 1500N,1000W													
Mean	1.94	8.77	3.75	0.83	13.13	24.87	25.38	14171.16	1.90	43.95	43.95	0.40	81.92
Median	1.88	9.34	3.81	0.49	12.92	24.24	27.03	13962.12	1.91	45.45	45.45	0.44	80.85
Min	1.41	6.19	3.46	0.39	10.87	19.20	15.61	10523.83	1.72	26.66	26.66	0.03	53.90
Max	2.63	10.71	3.98	2.00	17.15	31.75	33.05	18371.95	2.06	60.11	60.11	0.76	125.53
F3 1500N, 1250W													
Mean	1.74	17.99	3.81	0.34	9.70	30.04	46.03	13943.30	2.62	17.97	17.97	0.38	70.52
Median	1.74	15.07	3.88	0.33	9.48	28.00	47.00	11086.01	2.15	12.19	12.19	0.34	69.91
Min	1.36	11.21	3.59	0.16	5.83	23.70	32.42	8437.53	1.85	8.28	8.28	0.07	38.20
Max	2.29	37.44	4.11	0.70	14.46	39.84	62.14	26536.20	7.99	40.17	40.17	0.65	101.83
F3 1500N, 1500W													

Table E.3. (Continued)

Mean	1.73	16.18	3.76	0.29	9.08	30.41	49.23	16539.14	72.74	2.55	14.78	0.31	89.19
Median	1.69	15.44	3.75	0.29	9.04	30.54	52.86	15844.74	45.22	2.28	12.67	0.26	86.68
Min	1.28	7.69	3.49	0.21	7.63	20.75	26.01	9889.01	18.27	1.83	9.32	0.08	59.78
Max	2.29	24.74	4.18	0.44	14.03	40.50	65.47	27140.78	503.70	3.67	37.52	0.63	123.26
F3 1500N, 1750W													
Mean	1.62	18.96	3.73	0.23	9.51	31.26	50.48	18685.29	167.16	2.28	14.57	0.34	84.09
Median	1.52	17.09	3.71	0.21	8.83	33.18	52.40	18941.81	32.66	2.11	10.91	0.31	81.28
Min	1.25	13.28	3.41	0.16	7.14	18.21	31.86	12203.79	24.32	1.93	9.61	0.08	58.92
Max	2.27	29.10	4.09	0.37	19.35	39.02	64.13	27350.45	2053.41	2.95	51.34	0.89	115.29
F3 1700N, 1250W													
Mean	1.67	17.22	2.44	0.21	8.09	32.03	49.09	15843.38	69.27	0.67	11.80	0.39	85.80
Median	1.63	14.61	2.37	0.21	8.07	32.17	50.75	16081.60	52.15	0.59	9.14	0.34	83.68
Min	1.20	7.30	1.96	0.16	6.47	12.57	29.10	7774.33	32.94	0.29	7.38	0.10	69.35
Max	2.40	34.78	3.62	0.37	12.18	40.46	56.88	24312.11	344.76	2.00	35.02	0.83	107.71
F3 1700N, 1500W													
Mean	1.60	11.34	2.41	0.28	10.86	25.30	47.12	18722.95	146.98	1.16	26.51	0.43	105.54
Median	1.60	10.39	2.44	0.26	9.93	24.68	46.68	19849.77	67.02	1.03	16.61	0.44	103.94
Min	0.78	6.80	2.04	0.23	6.74	12.53	24.51	11103.15	45.67	0.44	11.60	0.14	72.40
Max	2.58	19.46	2.99	0.44	22.02	39.02	61.36	23508.42	794.50	2.06	64.10	0.62	140.43
F3 1900N 1250W													
Mean	1.49	13.78	0.88	0.28	5.50	28.26	40.06	1.44	34.49	0.99	9.35	0.52	63.18
Median	1.41	10.23	0.81	0.18	5.35	27.15	37.40	1.20	7.34	0.21	6.60	0.20	69.10
Min	1.02	6.54	0.34	0.13	0.86	3.67	3.88	0.60	0.26	0.00	5.34	0.07	11.70
Max	3.12	48.38	2.58	0.83	17.55	73.47	73.74	3.51	250.94	4.16	35.93	1.85	93.72
F3 1900N 1500W													

Table E.3. (Continued)

Mean	1.44	8.90	0.92	0.23	7.33	24.64	38.48	1.56	81.67	1.18	15.84	0.67	91.26
Median	1.41	8.01	0.83	0.18	6.17	22.32	37.30	1.67	19.93	0.60	12.46	0.82	79.21
Min	0.99	5.24	0.75	0.16	4.20	15.41	23.65	0.70	2.71	0.08	6.33	0.01	67.64
Max	1.90	15.66	1.69	0.47	16.21	61.01	55.93	2.24	586.12	4.29	37.43	1.25	132.42

*BDL- Below detection limit

*ADL- Above detection limit